Characterization of the Futsch/MAP1B Rescue of Locomotion Defects in a Drosophila Model of Amyotrophic Lateral Sclerosis

Thesis

Characterization of the Futsch/MAP1B Rescue of Locomotion Defects in a Drosophila Model of Amyotrophic Lateral Sclerosis

Monsurat Titi Gbadamosi

A dissertation submitted to The Open University, United Kingdom in fulfilment of the requirements for the award of the degree of Doctor of Philosophy in Life sciences

Neurobiology Group, International Centre for Genetic Engineering and Biotechnology (ICGEB), Trieste, Italy

Director of Studies: Fabian Feiguin, MD, PhD

External Supervisor: Marco Baralle, PhD

July, 2021

To my Dad, Alhaji Y.A. Gbadamosi. May your reign be long and healthy.

ABSTRACT

The most abundant pathological protein in the debilitating neurodegenerative disease, Amyotrophic Lateral Sclerosis (ALS) is TDP-43. Knock-down of its *Drosophila* homologue TBPH, recapitulates the disease in fly, with mutants showing reduced life span and locomotion impairment among other features. These can be restored by expressing human TDP-43 both in neurons and glial cells. It has been observed in TBPH mutants a reduction of the Futsch protein, the homologue of the human MAP1B responsible for the stabilization of the synaptic microtubule cytoskeleton during growth at the neuromuscular junction. We used our *Drosophila* model of ALS to investigate the role of Futsch in the rescue of locomotion defects observed in the disease using the UAS-GAL4 system. Futsch expression in TBPH mutants using both pan-neuronal and motor neuron-specific drivers show a significant rescue of larval motility. The synaptic organization defect observed in the mutants was recovered through the restoration of the synaptic branches, boutons and shape. Also some synaptic and vesicle proteins such as Dlg, Synapsin, Syntaxin, Csp and acetylated tubulin were recovered. The defect in the cycling of synaptic vesicles and the level of the BMP signal transducer, pMad were ameliorated by the expression of Futsch in TBPH mutants. It is interesting to note that TBPH mutants expressing the

GTPases Rab4 and Rab5, which are vesicle proteins associated with endosomal trafficking and recycling, were able to recover the levels of Futsch, acetylated tubulin and synaptic pMad. However, only Rab4 gave also a functional recovery of improved locomotion despite its reduced expression level compared to Rab5. We conclude that improved synaptic vesicle recycling system and enhanced BMP growth signalling are parts of the mechanisms involved in the recovery of locomotion defects observed in TBPH mutants expressing Futsch. We speculate that this recovery may be achieved through the functional anatomical recovery of the synaptic organization at the neuromuscular junction via the enhanced BMP growth signalling. Also included in the speculation is improved neurotransmission at the synaptic terminals resulting from the recovered vesicle recycling system.

ACKNOWLEDGEMENTS

I couldn't have achieved the feat of completing this dissertation alone especially during this time when the world is in a pandemic! Indeed, I am indebted to a lot of people who has contributed to the success of this endeavour in one way or another. First on the list is Dr Fabian Feiguin, my supervisor. I am sincerely grateful to him. Fabian gave me a chance when I really needed one. For this, I am eternally grateful. Thank you Fabian.

ICGEB, Trieste as an organization made all of these possible and as a staunch believer in the goals of the institute, I am grateful for being awarded the prestigious Arturo Falaschi PhD fellowship and I am a proud Alumnus. Thank you for judging me worthy of the award and giving me the opportunity to take a right step in the direction of my amazing but scary life goals.

Dr Marta Vicente-Crespo and Prof Ahmed Adedeji deserve a paragraph here. Marta and Prof gave me the necessary "push" that I needed during my application phase. The hunt for a PhD fellowship was a tough one for me and they both had confidence in me when I had none in myself. They kept me going and at last, I got into ICGEB, Italy. Thank you Marta and thank you prof. I appreciate you both.

My Lab members are next on the list. Raffaella Klima was not just the research associate in neurobiology lab, she was like a mother to me and

us all. Thank you Raffa for everything. Both research-wise and otherwise. Your contributions to this success story were immense and I appreciate your help. I do hope I have incorporated all that you taught me. Dr Giulia Romano was also of great help while she was in our lab. Thank you Giulia for showing me how things are done. I am indebted to Dr Nina Strah who was the last PhD student to graduate before me. Even though she left, Nina maintained contact and helped me through the process. I dare say we have become good friends. Thank you Nina for not just being there but also for understanding. This paragraph will not be complete without the mention of our graduate students, Noura Banani and Matea Mihelcic. They were fellow lab members turned friends. Thank you girls for being there with me and sharing in my experience. I appreciate you both.

My family back home has been a great pillar of support through all of this. I love and miss them always. My Dad is my number one fan on this journey. So yes daddy, you got your Dr Gbadamosi in the family now. Your only daughter did it and you have earned the bragging rights. So, brag away sir!. Thank you for not killing this dream of mine because you could have. I could always count on my Mom to come through for me no matter the situation I put or find myself. Thanks Mom for your support always. It gave me strength when I was lonely and homesick. My brothers are just that. Mine! Thanks guys for cheering me on when I got tired. It meant and

still means a lot to me. Thank you. My sister-in-law and Rashidat AbdulAzeez have also been of great help. I appreciate your constant vote of confidence. Thank you both. Aunty Remi and Family, Thanks for your moral support too. A senior colleague that has turned good friend is Dr Olayemi J. Olajide. Thank you Joseph for all your words of encouragement. They most times came when I needed to hear them. Thank you.

My beautiful daughter, Manal came when things were a bit complicated. Her arrival into this world showed me that I can truly handle more than I thought I could. Thank you Manal for changing and putting my life into what I call the “right perspective”. Let’s go there girl.

To my Nigerian friends in Trieste, I am sincerely grateful to you all and indebted to your kindness. Borire’s family and Muri-Saibu’s family including Jamiu Adeniran Thank you. Without you all, I couldn’t have arrived here. Thank you for babysitting Manal and for giving me moral support. I appreciate your kindness.

To myself, Monsurat Titi Gbadamosi, I say Good job! Remember to celebrate because you have done this against all odds. You did not quit when the going got tough. So, congratulations! We are in such a hurry to achieve our life goals that we forget to enjoy the process, so, take a pause today and appreciate yourself. Tomorrow is another day to proceed.

Last but most definitely not the least, my sincere gratitude to God for making all of this possible. Alhamdulilah.

TABLE OF CONTENTS

LIST OF FIGURES

LIST OF TABLES

LIST OF PUBLICATIONS

Klima, R, Romano, G., Gbadamosi, M., Megighian, A., & Feiguin, F. (2021). Immuno-electrophysiology on Neuromuscular Junctions of Drosophila Third Instar Larva. *Bio-protocol*, *11*(3). https://doi.org/10.21769/bioprotoc.3913

LIST OF ABBREVIATIONS

3′-UTR 3′-untranslated region

AD Alzheimer’s disease

AEL After egg laying

ALS Amyotrophic Lateral Sclerosis

ALS2 Alsin 2

ANOVA Analysis of variance

AP Adaptor proteins

ATP Adenosine triphosphate

ATXN2 Ataxin 2

BMP Bone morphogenetic protein

C9orf72 chromosome 9 open reading frame 72

CAS9 CRISPR associated protein 9

CDK5 Cyclin dependent kinase 5

CFTR Cystic fibrosis transmembrane conductance regulator

CLIP Cross-linking immunoprecipitation

CRISPR Clustered regularly interspaced short palindromic repeats

CSP Cysteine string protein

Cyo-GFP Curly-O/ Green fluorescent protein

Dfmrp Drosophila fragile X mental retardation protein

dFXR *Drosophila* fragile x mental retardation

Dlg Disc large

EAAT Excitatory amino acid transporter

eEJC evoked Excitatory junctional currents

eIF2a Eukaryotic initiation factor 2a

ESCRT Endosomal sorting complexes required for transport

fALS Familial amyotrophic lateral sclerosis

FMR Fragile x mental retardation

FTLD Fronto-Temporal Lobar Degeneration

FUS fused in sarcoma

gbb Glass boat bottom

GEF Guanine nucleotide exchange factor

GluRIIA Glutamate receptors IIA

GTP Guanosine triphosphate

HD Huntington’s disease

HL3 Hemolymph-like solution

HRP Horseradish peroxidase

HSP Hereditary spastic paraplegia

hTDP-43 Human Tar-DNA-binding protein-43

IPSC Induced pluripotent stem cells

ISN Intersegmental nerve

KIF5A Kinesin heavy chain isoform 5A

lncRNA Long non-coding Ribonucleic acid

Mad Mothers against dpp

MALAT1 Metastasis associated in lung adenocarcinoma transcript 1

MAP Microtubule associated protein

MAP1B Microtubule associated protein 1b

MATR3 Matrin 3

mEJC miniature Excitatory junctional currents

miRNA micro Ribonucleic acid

mRNA messenger Ribonucleic acid

NEAT1 Nuclear enriched abundant transcript 1

NEK1 NEMA-like kinase 1

NES Nuclear export signal

NIPA1 Non-imprinted in Prade-Willi/Angelman syndrome region protein 1

NLS Nuclear localization signal

NMJ Neuromuscular junction

OPTN Optineurin

OXPHOS Oxidative phosphorylation

PABP poly-(A)-binding protein

PBS Phosphate buffered saline

PBST Phosphate buffered saline with 0.1% Tween 20

PD Parkinson’s disease

PFA Paraformaldehyde

PFN1 Profilin 1

PHB2 Prohibitin 2

pMad Phosphorylated *mothers against dpp*

RNA Ribonucleic acid

RNAi interference Ribonucleic acids

ROS Reactive oxygen species

RRP Readily releasable pool

sALS Sporadic amyotrophic lateal sclerosis

sax saxophone

SETX Senataxin

SNa Segmental nerve a

SNAP-25 Synaptosomal nerve-associated protein 25

SNAREs soluble N-ethylmaleimide-sensitive factor attachment protein receptors

SNb Segmental nerve b

SNc Segmental nerve c

SNd Segmental nerve d

SOD1 Superoxide dismutase 1

TARDBP Tar DNA-binding protein

TBK1 TANK-binding kinase 1

TBPH Tar binding protein homologue

TDP-43 Tar DNA-binding protein-43

TIA-1 T cell-restricted intracellular antigen-1

tkv thickvein

TN Transverse nerve

TUBA4A Tubulin A4A

UAS/GAL4 Upstream activating sequence/ Galactose 4

UBQLN2 & UBQLN4 Ubiquilin 2 & 4

VABP Valosin-binding potein

VAMP Vesicle-associated membrane protein

VAPB Vesicle associated protein B

VCP Valosin-containing protein

VDAC1 voltage-gated anion channel 1

VEGF Vascular endothelial growth factor

VNC Ventral nerve cord

wit wishful thinking

1.0 INTRODUCTION

1.1 Amyotrophic Lateral Sclerosis (ALS)

ALS is a fatal, rapidly progressing neurodegenerative disease that is specific to the motor neurons. It has an incidence spanning from about 0.43 to 2.35 per 100,000 people in Asia and western Europe respectively. Statistically, men are more affected than women and peak disease is reached at 60-70 years (Palese *et al.,* 2019). While in 90-95% of cases it appears as sporadic starting around 60 years of age, there are also familial cases in 5-10% of all patients with an earlier onset starting around 50 years (Al-Chalabi *et al.,* 2017).

The late French Neurologist, Jean-Martin Charcot was credited to be the first person to use the term *Amyotrophic lateral sclerosis* to refer to the set of neurological symptoms of the disease in 1874 but they have been described earlier in 1824 by Charles Bells (Rowland & Shneider, 2001). The prognosis is 2-4 years from diagnosis and the majority die of respiratory failure, which is a consequence of the disease that is preceded by muscle stiffness, paralysis, deformed joints with pain, difficulties in eating, swallowing, talking, walking and also breathing (Hobson & McDermott, 2016). Although, there are some reported cases of cognitive decline in sporadic ALS (Chiang *et al.,* 2010) Usually, the cognitive

function is preserved being the hallmark that differentiates ALS from Fronto-Temporal Lobar Degeneration (FTLD).

About 75% of patients present a limb-onset with symptoms typically starting from the arms, beginning with loss of manual dexterity and weakness of the limbs, and ending with foot drop and difficulty in walking. Cases of bulbar onset of ALS have been reported in older women with a consequent worse prognosis of the disease. The symptoms include dysarthria to anarthria, twitching of the tongue which is a classic characteristic, head drop and poor balance (Chiò *et al.,* 2009; Gordon, 2013).

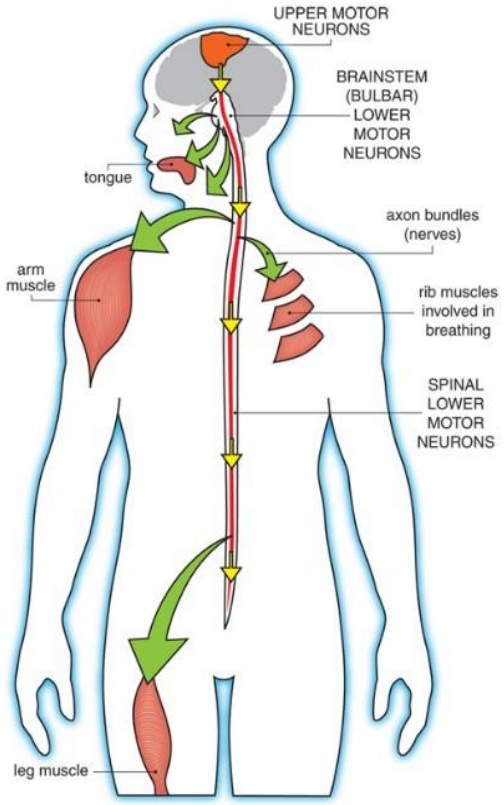

Figure 1: ALS progress showing affected nerve and muscle areas. It is thought to start in the upper motor neurons in the motor cortex and brainstem and reaches the voluntary muscles of the tongue, ribs, arms and legs via the lower motor neurons through the spinal cord (figure adapted from www.mda.org)

Why both upper and lower motor neurons (Figure 1) are particularly susceptible to the disease is not clear but it could be that defects in microtubule structure and presumably axonal transport result in a devastating insult to these kind of cells. Some motor neurons have the longest axonal projections in the body with most lacking buffering capacity (Poulain & Sobel, 2010). Also, they are comparatively large excitable cells with high energy demands in close association with non-neuronal cells (Robberecht & Philips, 2013).

1.1.2 Pathogenesis of ALS

Several gene mutations have been linked with ALS and they include: *C9orf72* (which encodes chromosome 9 open reading frame 72)*, Sod1* (Superoxide dismutase 1) (Kunst *et al.,* 1997)*, Fus* (fused in sarcoma) (Vance *et al.,* 2009), *Tbk1* (TANK-binding kinase 1)*,* (Oakes *et al.,* 2017), *Vcp* (Valosin-containing protein) (Koppers *et al.,* 2012)*, Ubqln2 & Ubqln4* (Ubiquilin 2 & 4) (H. X. Deng *et al.,* 2011; Edens *et al.,* 2017), *Nek1* (NEMA-like kinase 1) (Brenner *et al.,* 2016), *Optn* (Optineurin) (Maruyama *et al.,* 2010), *Pfn1* (Profilin 1) (Tanaka *et al.,* 2016), *Matr3* (Matrin 3) (Johnson *et al.,* 2014), *Kif5a* (Kinesin heavy chain isoform 5A) (Nicolas *et al.,* 2018), *Setx* (Senataxin) (M. Hirano et al., 2011) and the TDP-43 gene (*Tardp)*, among others (Van Damme *et al.,* 2017). Of all these genes, the most frequently occurring mutations are in *C9orf72, Sod1, Fus* and *Tdp-*

43 (Figure 2) (Vijayakumar *et al.,* 2019). Only TDP-43 is within the scope of this study.

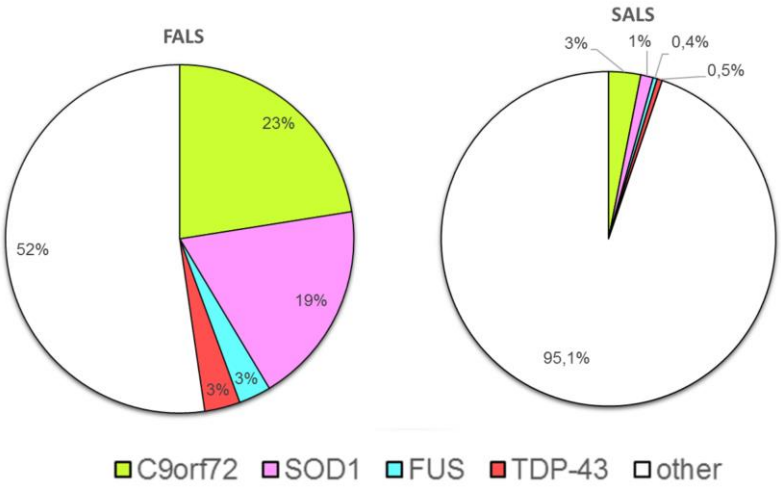

Figure 2 Schematic representation of the most frequently occurring gene mutations in familial and sporadic amyotrophic lateral sclerosis (Adapted from Zou *et al.*, 2017).

1.1.3 Treatment and Management of ALS

Till date, ALS has no known cure so, care is palliative. Riluzole (2-aminotrifluoromethoxybenzotiazole) is used to slow down the progression of the disease and it prolongs survival for approximately three months. Riluzole acts by blocking sodium channels preventing the release of glutamate, excess of which leads to excitotoxicity (Figure 3). Glutamate-induced excitotoxicity leads to neuronal injury causing death of the neuron through excessive stimulation of glutamate receptors and induction of calcium influxes.

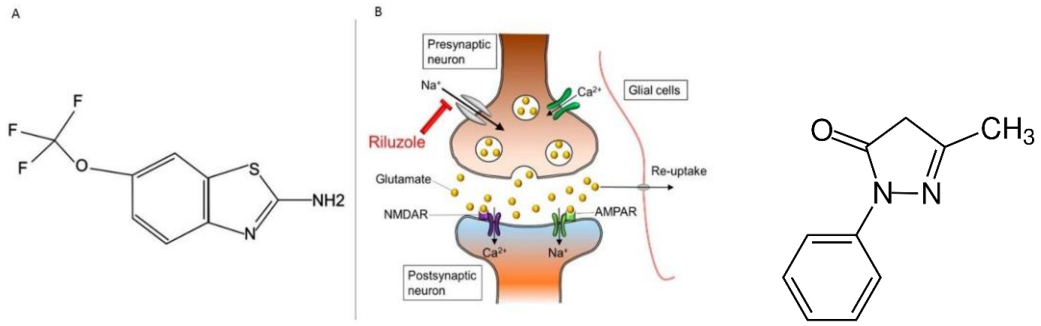

Figure 3 The structure and mode of action of riluzole. A) The chemical structure of riluzole. B) Riluzole is able to prevent glutamate excitotoxicity by blocking its release from the neurons and promoting its uptake by glial cells. Thus, its action is neuroprotective. C) Structure of Edaravone, it exerts both antioxidant and neuroprotective effects. Adapted from www.mdpi.com

The drug Edaravone (2,4-dihydro-3H-pyrazol-3-one) is a potent antioxidant and has recently come in use. Not only does it scavenges free radicals in neurons, it is also able to slow down the disease progression by limiting the extent of lipid peroxidation via free radical generation and the cell membrane damage from oxidative stress (Janke & Montagnac, 2017). While research into ALS cure is on-going, the management of ALS patients is based on prolonging patients' life and also maintaining certain qualities of life by a specialized care team. This team is composed of cross-disciplinary clinics, medications that are neuroprotective, therapeutic symptomatic relieve and respiratory support (Gordon, 2013).

1.1.4 Molecular mechanisms of ALS

ALS is cellularly characterized by loss of motor neurons' cell bodies, axonal retraction and gliosis (proliferation of glial cells forming scar tissue

in response to an insult or injury in the brain). Surviving neurons contain inclusions that are ubiquitin and p62 positive. Figure 4 summarizes the proposed mechanisms involved in ALS, which is truly a heterogenic disease with numerous contributing factors and associating mechanisms. Among the several mechanisms, alterations in nucleocytoplasmic transport of RNA molecules and RNA-binding proteins are suggested as disease-causing. This is because several mutations have been identified in many nucleo-cytoplasmic shuttling RNA-DNA binding proteins such as TDP-43 and FUS proteins that are implicated in the disease among others. Also a mis-localization of proteins from nucleus to cytoplasm, inducing nuclear depletion and cytoplasmic aggregation is a further mechanism proposed. The resulting loss of function in the nucleus and gain of function in the cytoplasm are thought to be detrimental to the cell especially for TDP-43, FUS, ATXN2 and hnRNPA1/A2 proteins. Increase in oxidative stress and reactive oxygen species contribute to the pathology of ALS. Several ALS-related proteins (SOD1, TDP-43, C9orf72) are able to move into the mitochondria altering its functions and resulting in impairment (Lezi & Swerdlow, 2012). Axonal transport defects are also implicated and are caused by disruption in axonal structure and function as a result of functional disorganization of cytoskeletal proteins. (Van damme *et al.,* 2017). Also alterations in the transport of vesicles have been suggested since many ALS-related proteins such as vesicle

associated membrane protein (VABP) and Alsin 2 (ALS2) are involved in vesicular transport. The downregulation of the glutamate transporter EAAT, responsible for removal of excess glutamate from the synaptic cleft leading to excitotoxicity, is an obvious and deeply researched mechanism (Shaw & Eggett, 2000). Neuroinflammation as a result of activation of astrocytes and microglial with oligodendrocytes dysfunction may be a contributing mechanism (Van damme *et al.,* 2017).

Of the several proposed mechanisms of ALS progression, which include RNA metabolism, mitochondrial function impairment, endocytic impairment, oxidative stress, problems with misfolded proteins and autophagy, glutamate signalling and excitotoxicity, (Alami *et al.,* 2014; Bowling *et al.,* 1993; Hirano *et al.,* 1984; Kawahara *et al.,* 2004; Niwa *et al.,* 2002; Prasad *et al.,* 2019; Swerdlow *et al.,* 1998; Takuma *et al.,* 1999; Wiedemann *et al.,* 2002; Zhang *et al.,* 2018), only the axonal transport irregularities underline the important contribution of microtubules and the cytoskeleton in the neurodegenerative process while also taking into account the intracellular transport (Cueille *et al.,* 2007; Robberecht & Philips, 2013).

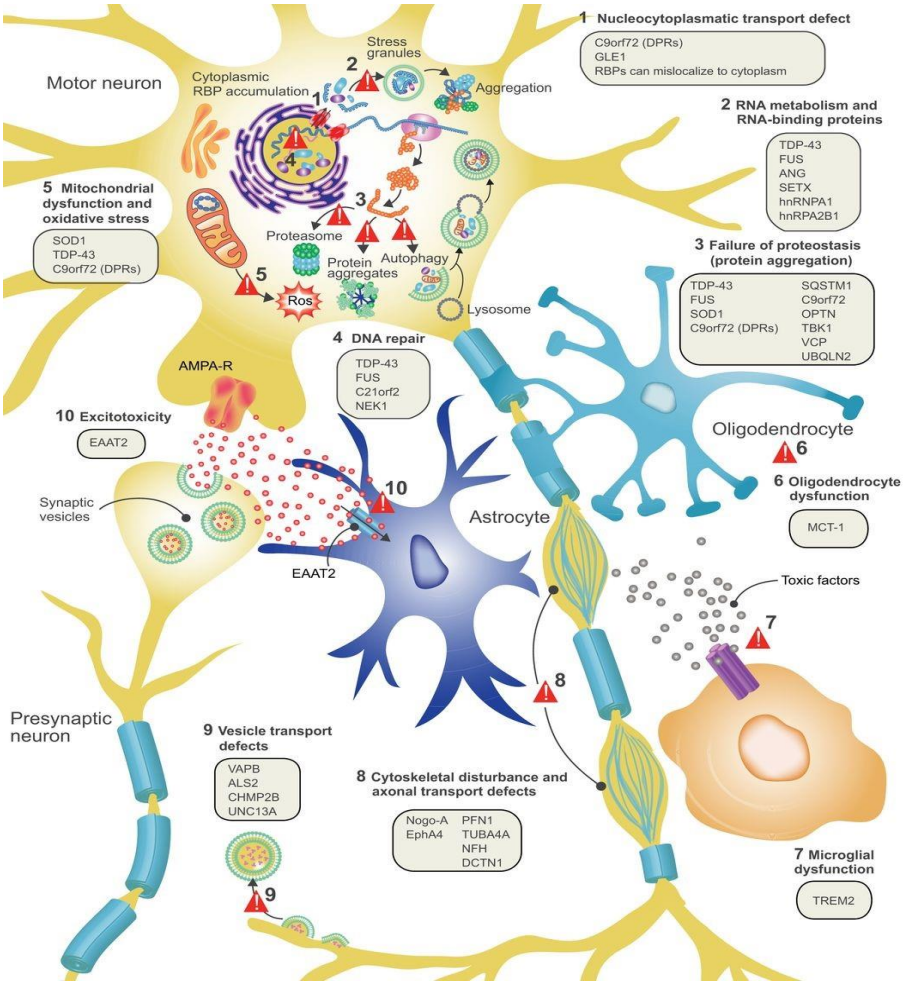

Figure 4 Schematic representation of proposed mechanisms of ALS disease. (1) Alterations in nucleocytoplasmic transport of RNA molecules and RNA-binding proteins. (2) Altered RNA metabolism: several important RNA-binding proteins become mis-localized in ALS, with cytosolic accumulation and nuclear depletion which causes defects in transcription and splicing. Altered dynamics of stress granule formation or disassembly can propagate cytoplasmic aggregate formation. (3) Impaired proteostasis with accumulation of aggregating proteins causing overload of the proteasome system and reduced autophagy may contribute and/or cause this accumulation. (4) Impaired DNA repair could also contribute to ALS pathogenesis. (5) Mitochondrial dysfunction and oxidative stress: many ALS-related proteins can enter mitochondria and disrupt normal functioning causing increased formation of reactive oxygen species (ROS). (6) Oligodendrocyte dysfunction and degeneration, leading to reduced support for motor neurons. (7) Neuroinflammation: activated astrocytes and microglia secrete fewer neuroprotective factors and more toxic factors. (8) Defective axonal transport: many ALS-related mutations cause disorganization of the cytoskeletal proteins and disrupt axonal transport. (9) Defective vesicular transport: Many ALS-related proteins are involved in vesicular transport, suggesting that impaired vesicular transport contributes to ALS pathogenesis. (10) Excitotoxicity: loss of the astroglia glutamate transporter EAAT2 causes accumulation of extracellular glutamate, which causes excessive stimulation of glutamate receptors and calcium influx. (adapted from van-damme *et al.,* 2017 figure inclusive).

1.1.5 Models of Amyotrophic Lateral Sclerosis

Several models have been developed based on molecular and genetic analysis of ALS to study specific aspects of the disease because a single model cannot recapitulate the exact human disease with its multifactorial and multidimensional features. They vary from cell culture systems to *Drosophila*, to rodents and recently human patient-derived stem cell models (Van Damme *et al.,* 2017) (Figure 5). Each model presents peculiar merits and demerits all of which contribute to our understanding of the disease (Figure 5). Most probably, a combination of the systems will allow us achieve a successful translation from laboratories to the patients in the clinics.

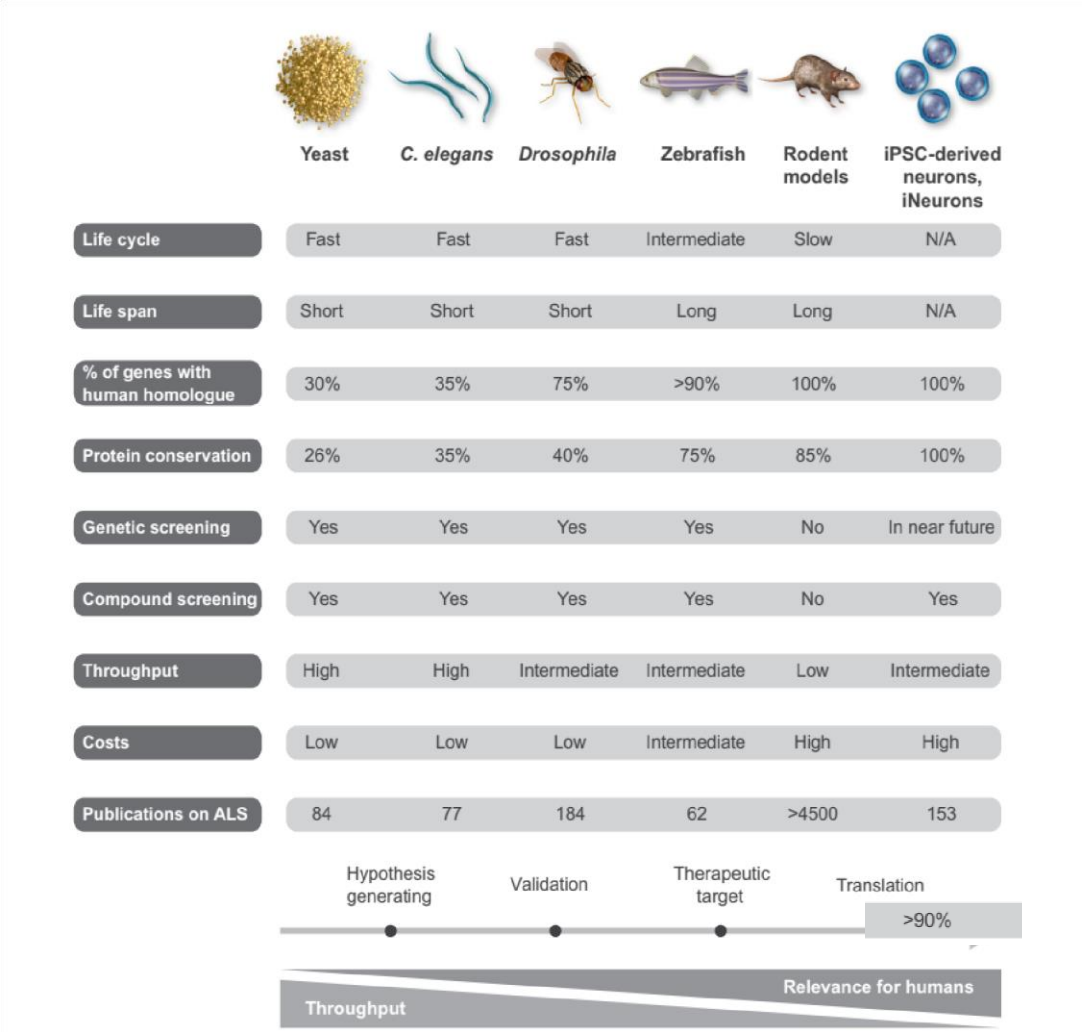

Figure 5 Models currently in use for research in ALS. Merits and demerits of each system is summarized from yeast to IPSC-derived neurons. Adapted from (Van Damme et al., 2017).

Many cell lines are used to test and screen the biological functions of ALS-associated genes and proteins. Even if such simple models cannot recapitulate the complex human disease, they do contribute significantly to the understanding of the pathology of the disease. One of such models uncovered the role of C9orf72 in autophagy (Webster *et al.,* 2016). The discovery of RNA-binding protein ATAXIN 2 (ATXN2) as a genetic risk factor for ALS resulted from analysis performed on a single cell organism

like yeast (*Saccharomyces cerevisiae*), also for the identification of molecules modifier of TDP-43.

Yeast, that present about 30% homology between its genes and that of humans, is a quite suitable organism for cytotoxic screening since a simple growth assay could indicate toxicity manifested as reduced growth rate (Elden *et al.,* 2010; Jovičič *et al.,* 2015). Primary cultures of motor neurons of mice and rats are useful to study the exposure and vulnerability of motor neurons to various factors and insults. They are also useful in understanding the factors that improve their survival in unbiased screens in an effort to study the cellular effects of gene mutations and protein aggregations (Bordet *et al.,* 2007; Van Damme *et al.,* 2017).

Coming to multicellular organisms, *C. elegans* (*Caenorhabditis elegans*) is a transparent nematode with about 35% gene homology with humans has contributed significantly to ALS research. The four main ALS-associated genes (*SOD1, C9orf72, TARDBP and FUS*) have been created in this model system (Therrien & Parker, 2014). A TDP-43 proteinopathy model using *C. elegans* revealed Calcineurin as an important phosphatase that is involved in the removal of pathological C-terminal phosphorylation of TDP-43 (Liachko *et al.,* 2016).

Zebrafish (*Danio rerio*) with approximately 90% gene homology with humans is famous in embryology research for its transparent embryos and

is gaining tract as a model in ALS study (Phillips & Westerfield, 2014). There are Zebra fish models of ALS in which interactions and similarities in TDP-43 and FUS proteins related to motor neuron toxicity have been discovered. With this model, it was discovered that the expression of the wild-type genes of TDP-43 and FUS could rescue the motor neuron toxicity induced by the knockdown of their respective genes, but not the toxicity induced by a mutant SOD1 expression (Kabashi *et al.,* 2011). Additionally, progranulin, a neurotrophic factor was found to improve the motor neuron toxicity induced by mutant TDP-43 and FUS, but not of mutant SOD1 (Kabashi *et al.,* 2011; Laird *et al.,* 2010).

Drosophila melanogaster, the fruit fly, with a 75% gene homology with humans is the most common small animal model in ALS research for several good reasons such as an array of genetic tools available for various screenings and manipulations (Ugur *et al.,* 2016). There are numerous fly models of ALS linked to mutations in SOD1 (Watson *et al.,* 2008), in TARDBP (Estes *et al.,* 2011; Feiguin *et al.,* 2009; Vanden Broeck *et al.,* 2013) in FUS (Lanson *et al.,* 2011), in C9orf72 (Mizielinska *et al.,* 2014; Xu *et al.,* 2013), in ALS2 (Takayama *et al.,* 2014), in VAPB (Ratnaparkhi *et al.,* 2008; Tsuda *et al.,* 2008), in VCP (Johnson *et al.,* 2015) and in SETX (Mushtaq *et al.,* 2016). Several validation and confirmation experiments have been carried out using the fly, such as the

role of stress granule factors poly-(A)-binding protein (PABP) and eIF2a phosphorylation as modifiers of TDP-43 toxicity (Kim *et al.,* 2014). The *Drosophila* model of ALS shed more light on the physiological role of TDP-43 with respect to its interactions with synaptic proteins such as Syntaxin, Synapsin and CSP (Romano *et al.,* 2014) and the control of the growth of the neuromuscular junction by mediating the action of the microtubule binding protein, Futsch (Godena *et al.,* 2011) (Figure 22).

Rodent models with >90% gene homology with humans are the most desirable in modelling human diseases. Gurney *et al.,* 1994 provided the first transgenic mice overexpressing the human genomic mutant SOD1. Since then, several other rodent models involving many of the ALS-associated proteins have been generated, all of which have contributed significantly to our understanding of the disease pathogenesis. This includes uncovering links between protein misfolding and aggregation, autophagy, vesicular and axonal transport, mitochondrial dysfunction and cytoskeletal alterations (Fischer *et al*., 2004; Shi *et al.,* 2010; Staats *et al.,* 2013) Although, the mammalian rodent systems are similar to the humans and offer great advantages providing good insights into the disease, they possess peculiar problems such as inbreeding which may become unreliable when crossbreeding with another transgenic line is required. This does not model the exact human condition and restrict the testing of

hypotheses to one at a time eventually becoming extremely expensive and time-consuming (Van Damme *et al.,* 2017).

Patient induced stem cell models are a boost to ALS research as they obliterate the requirement of overexpressing a particular pathogenic transgene associated with ALS since they already contain an endogenous mutation with respect to the patient's own genetic makeup, thus they are a better model for ALS (Van Damme *et al.,* 2017). Many aspects of the disease such as protein aggregation/mis-localization and functional read-outs like neuro-filamentous disorganization, inefficient nucleocytoplasmic transport, increased motor neuron death and excitotoxicity have been modelled successfully using iPSC-derived spinal neurons (Bilican *et al.,* 2012; Chen *et al.,* 2014; Kiskinis *et al.,* 2018; Matus *et al.,* 2014; Zhang *et al.,* 2015). There is hope that future use of gene editing techniques such as CRISPR/CAS9 for genetic screens in patient-derived stem cells phenotypic read-outs can possibly be more successful in ALS direct translational research since they already have the genetic background of an individual that is afflicted with ALS (Qi *et al.,* 2017).

1.2 Transactive response DNA binding protein 43 kDa (TDP-43)

The 43kDa RNA-binding protein, TDP- 43 contains 414 amino acids. It is central to ALS pathophysiology because its mis-localization from the

nucleus where it is predominantly located to the cytoplasm in the form of insoluble ubiquitinated aggregates is found in most patients. The presence of these aggregates is considered one of the hallmarks of the disease (Barber *et al.,* 2006; Coyne *et al.,* 2014; Neumann *et al.,* 2006; Saberi *et al.,* 2015). Dominant mutations of this protein are enough to cause the familial ALS reiterating the unrivalled role of TDP-43 in the pathogenesis of the disease (Al-Chalabi *et al.,* 2012). Together with ALS, Frontotemporal lobal degeneration, Primary lateral sclerosis and Progressive muscular dystrophy are collectively known as TDP-43 proteinopathies. They are all related with mutations and aggregation of this protein (Dugger & Dickson, 2017). Only TDP-43 associated with ALS is within the scope of this study.

TDP-43 encoded by the *TARDP* gene located on chromosome 1 has an N-terminal domain which contains 2 RNA recognition motifs for binding RNAs and DNAs, a nuclear localization and export signals for presence in the nucleus and shuttling to the cytoplasm respectively, a C-terminal domain that contains a Q/N (glutamine/asparagine) and a glycine-rich regions (Figure 6). It also contains mitochondrial localization motifs M1, M3, and M5. (Prasad *et al.,* 2019). There is considerable overlap in TDP-43 mutations in sALS & fALS and also between them and FTLD.

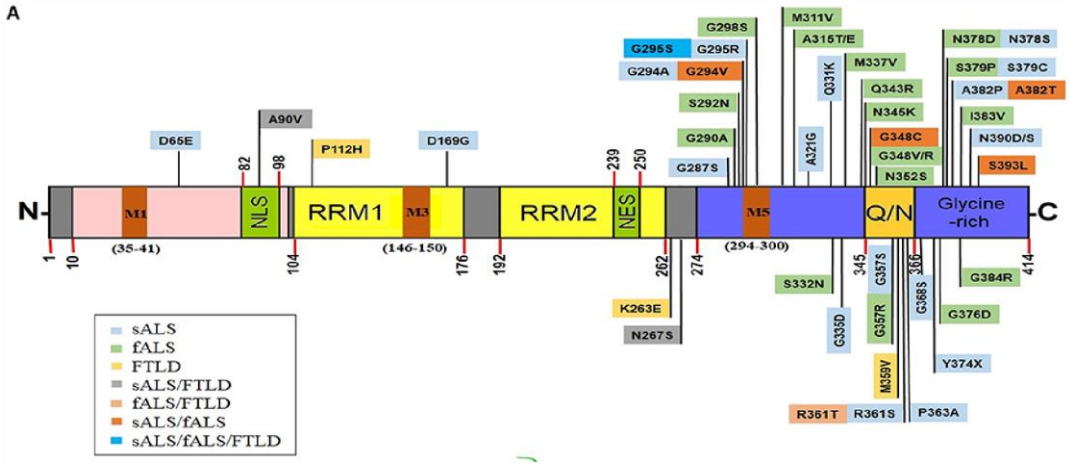

Figure 6 Schematic representation of TDP-43 structure comprising an NT domain, two RRM domains, a nuclear export signal (NES), a nuclear localization signal (NLS), a prionlike disordered C-terminal domain (with glutamine/asparagine-rich (Q/N) and Glycine-rich regions) and mitochondrial localization motifs (M1−35–41; M3−146–150; M5−294–300). Figure adapted from (Prasad *et al.,* 2019).

1.2.1 Functions of TDP-43

TDP-43 function is vital to the development of mammals, zebra fish and invertebrates (Diaper *et al.,* 2013; Estes *et al.,* 2011; Feiguin *et al.,* 2009; Kabashi *et al.,* 2009; Kraemer *et al.,* 2010; Rowland & Shneider, 2001; Yang *et al.,* 2014; Zhang *et al.,* 2003). Its role includes, but is not limited to splicing, mRNA stability, transport, and translation. Also, microRNA biogenesis and long non-coding RNA (lncRNA) processing. All of these processes are related to RNA metabolism (Buratti & Baralle, 2009; Godena *et al.,* 2011) (Figure 7).

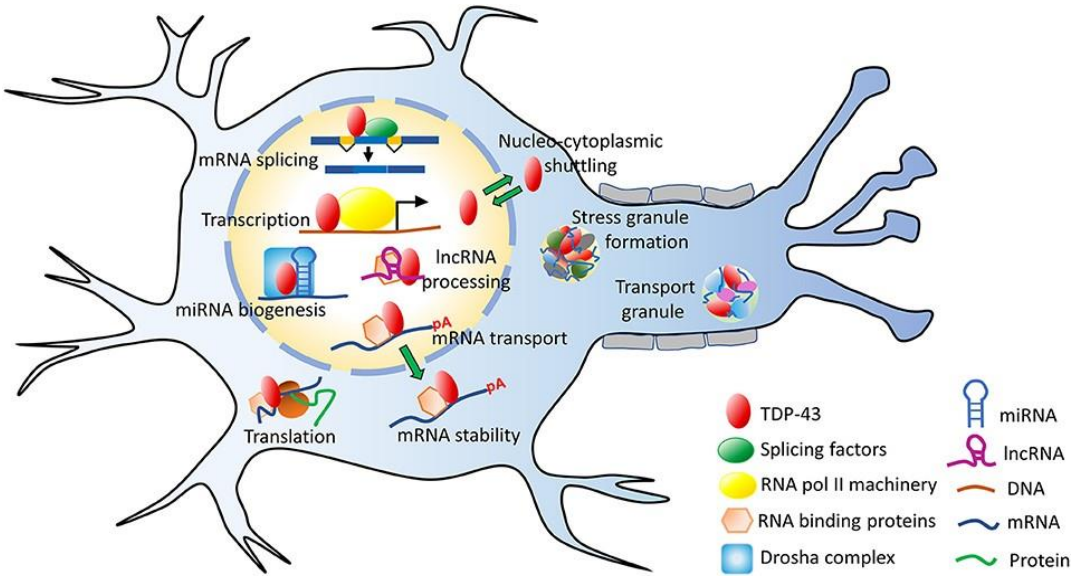

Figure 7 Schematic representation of TDP-43 functions. It is a constitutively expressed protein that is involved in many processes and exerts its function through mediation of other proteins, RNAs and recently discovered miRNAs. Figure adapted from (Prasad *et al.,* 2019).

mRNA transcription and splicing.

TDP-43 localizes to the euchromatin regions of the nucleus where transcription and splicing occur in the physiological state. It is involved in the regulation of transcripts of several genes such as *CFTR, FUS* and of itself, *TARDP* gene, among others (Buratti & Baralle, 2010). Alterations in the presence or absence of TDP-43 is detrimental. Nuclear depletion causes splicing aberrations also in the motor neurons. While overexpression leads to the formation of complexes that makes it unavailable for binding other proteins (Highley *et al.,* 2014; Yang *et al.,* 2014).

mRNA Maturation and Stability

TDP-43 binds to the transcripts of many mRNAs including its own through their 3′-untranslated regions (3′-UTR) altering their half-lives and consequently stabilizing them. Its own transcript, the human low molecular weight neurofilament mRNA and the vascular endothelial growth factor are classical examples (Prasad *et al.,* 2019).

mRNA Translation

TDP-43 was reported to bind more than 6000 RNA sequences by a high throughput sequencing of CLIP RNA derivatives which give credence to the importance of this protein to viability (Tollervey *et al.,* 2011). It can negatively affect the translation of many mRNAs by seclusion of factors involved in translation into stress granules (Aulas *et al.,* 2015). TDP-43 regulates the translation of Futsch which is the *Drosophila* homologue of the mammalian MAP1B at the neuromuscular junctions (Coyne *et al.,* 2014).

mRNA Transport

mRNAs are transported to far locations by ribonucleoprotein (RNP) granules on microtubules in some instances. TDP-43 interacts with RNAs to produce these RNPs whose transportation has been found to be

negatively affected in an ALS-associated TDP-43 mutation (Alami *et al.,* 2014).

miRNA and lncRNAs Processing

TDP-43 is involved in the biogenesis, maturation and processing of micro RNAs (miRNAs) and long non-coding RNAs (lncRNAs). This is through interactions with drosha and dicer complexes (Buratti & Baralle, 2010). Nuclear enriched abundant transcript 1 (NEAT1) and Metastasis associated in lung adenocarcinoma transcript 1 (MALAT1) are lncRNAs that bind with TDP-43 and are also found at elevated levels in FTLD of TDP-43 origin (Tollervey *et al.,* 2011). Although lncRNAs (>200 nucleotides) do not encode for proteins, they are believed to be involved in various mechanisms associated with regulation of gene expression (Prasad *et al.,* 2019).

Stress Granule Formation

Stress granules are formed quickly and usually in a reversible manner upon exposure to conditions such as oxidative stress, infections among others (Anderson & Kedersha, 2008). So, formation of stress granules are a protective reaction in the cell upon exposure to insults and injury. They can become pathological inclusion bodies as seen in the brains of ALS and FTLD patients (Van Damme *et al.,* 2008). TDP-43 is involved in the assembly and maintenance of stress granules. It regulates the expression

of rasGAP SH3 domain binding protein 1 (G3BP) and T cell-restricted intracellular antigen-1 (TIA-1) which are key stress granule nucleating proteins (McDonald *et al.*, 2011).

TDP-43 regulates itself by binding to the 3′ untranslated region (UTR) of its own mRNA transcript thereby keeping its cellular level, and possibly solubility constant, an action it also performs for several other transcripts which is the basis for its mRNA regulatory function (Ayala *et al.,* 2011). A change in this level either by increase (overexpression leading to a gain of function) or decrease, associated with a loss of function, is the rationale of several animal model studies recapitulating many aspects of ALS phenotype and pathology such as reduced lifespan, locomotion defects, uncoordinated movements and progressive neurodegeneration leading to paralysis (Chiang *et al.,* 2010).

One of such models was generated and in use in our laboratory where *Drosophila* that lacks *TBPH* (by gene deletion), the fly homologue of human *TDP-43*, recapitulate phenotypes of ALS (Feiguin *et al.,* 2009). Moreover, in null alleles of TBPH, alterations in the organization of the synaptic microtubules in the terminal boutons of the neuromuscular junctions were observed, due to the fact that TBPH mediates the Futsch function, a microtubule associated protein (Feiguin *et al.,* 2009; Godena *et al.,* 2011).

1.3 Microtubules and their associated proteins

Microtubules are hollow polymers of alpha and beta tubulin dimers. The dimers are arranged to form a polarized structure having plus (beta tubulin) and minus (alpha tubulin) ends. Their general functions in different animals and cell types are conserved as regards motility and cell division (Clark *et al.,* 2016) (Figure 8). They are an important component of the neuronal cytoskeleton and play a key role in the development, growth and maintenance of neuronal functions (De Vos & Hafezparast, 2017). They provide the structural framework for distinct axonal and dendritic compartments and many neurodegenerative diseases are characterized by changes in specific cytoskeletal components (Brandt, 2001; McMurray, 2000). Neuronal microtubules play an essential role in the transport and subsequent regulation of synaptic vesicle dynamics underlying neurotransmission (Rodesch & Broadie, 2000). They are also important in facilitating activity-dependent axonal transport of varying structures (Clark *et al.,* 2016). The dynamic nature of microtubules and the strict regulation of their stability allow them perform their dynamic functions in all cell types (Brunden *et al.,* 2017). They are constantly required to be in a state of dynamic instability, an energy-intensive process where they are able to switch between a growing state, which requires addition of subunits to their end (assembly), and a shortening state, where

protofilaments are able to break off to release single units of dimers into the cytoplasm (disassembly) (Cassimeris, 2010).

Neuronal polarity is conferred by microtubules by virtue of the slow-growing minus end composed of alpha tubulin and a fast-growing plus end with beta tubulin forming different neuronal compartments. The axonal compartment is entirely composed of microtubules oriented with their plus end distally located while the somato-dendritic compartment contains an equal amount of plus and minus ends microtubules distally implying a mixed orientation (Yau *et al.,* 2016). Although yet to be fully understood, numerous post translational modifications of tubulin such as acetylation, tyrosination, glutamylation, polyamination, glycylation and glutathyonilation are chemical modifications sought as potential therapeutic targets for neurodegenerative disorders. They are thought to aid the functions of microtubules by improving stability and affecting specific binding domains of their associated proteins (Taes *et al.,* 2013).

Microtubule associated proteins (MAPs) are a large group of 'structural' proteins that have the ability to interact with the microtubule assembly promoting their instability or stability. This is achieved by cutting microtubules or preventing them from depolymerization respectively (Cassimeris, 2010; De Vos & Hafezparast, 2017). MAPs improve the functions of microtubules by facilitating intracellular signalling,

cytoskeletal interactions and altering microtubule stability and dynamics (Sayas *et al.,* 2015). The classical MAPs expressed only in neurons are MAP1a and 1b, MAP2 and tau, of which the last two are the most characterized (De Vos & Hafezparast, 2017; Halpain & Dehmelt, 2006; Villarroel-Campos & Gonzalez-Billault, 2014). This study will focus on Futsch, the *Drosophila* orthologue of the MAP1B.

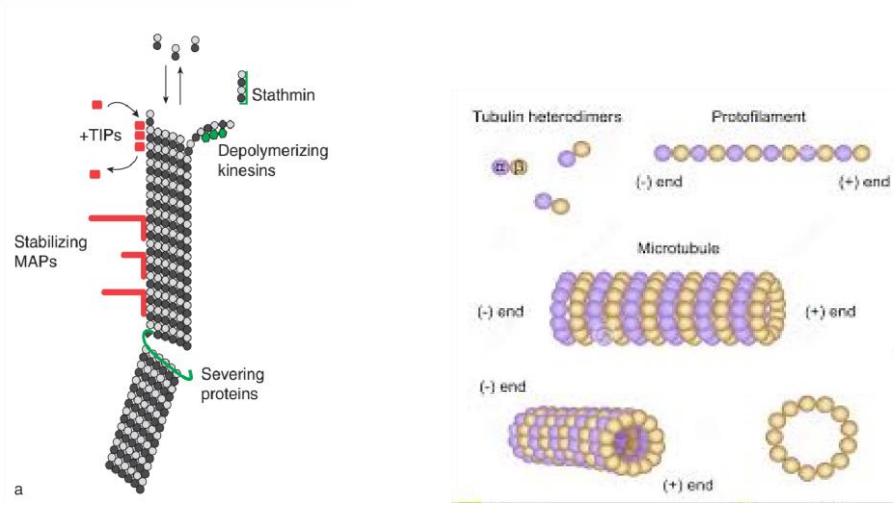

Figure 8 Schematic structure of a microtubule: Typically contains about 13 protofilaments in parallel binding in a head-tail fashion and the external and internal dimensions are about 24nm and 12nm respectively. MAPs can be stabilizing, destabilizing or severing proteins depending on their actions on microtubules inferable from their names.

MAPs bind to microtubules to influence their structure and behaviour which invariably control their functions (Figure 9). Some MAPs prevent bundling of microtubules by keeping them apart (Figure 9A), others control the numbers of microtubule protofilaments through their connections to specific number of tubulin molecules (Figure 9E). Most MAPs act as

cellular crosslinkers between microtubules and the filaments (actin and intermediate filaments) (Figure 9D) while others guard against breaking of the microtubules influencing their dynamics (Figure 9C). Some MAPs have been implicated in intracellular transport (Figure 9F) while a few others are thought to have roles in neuronal membrane trafficking (Figure 9B) (Bodakuntla *et al.,* 2019).

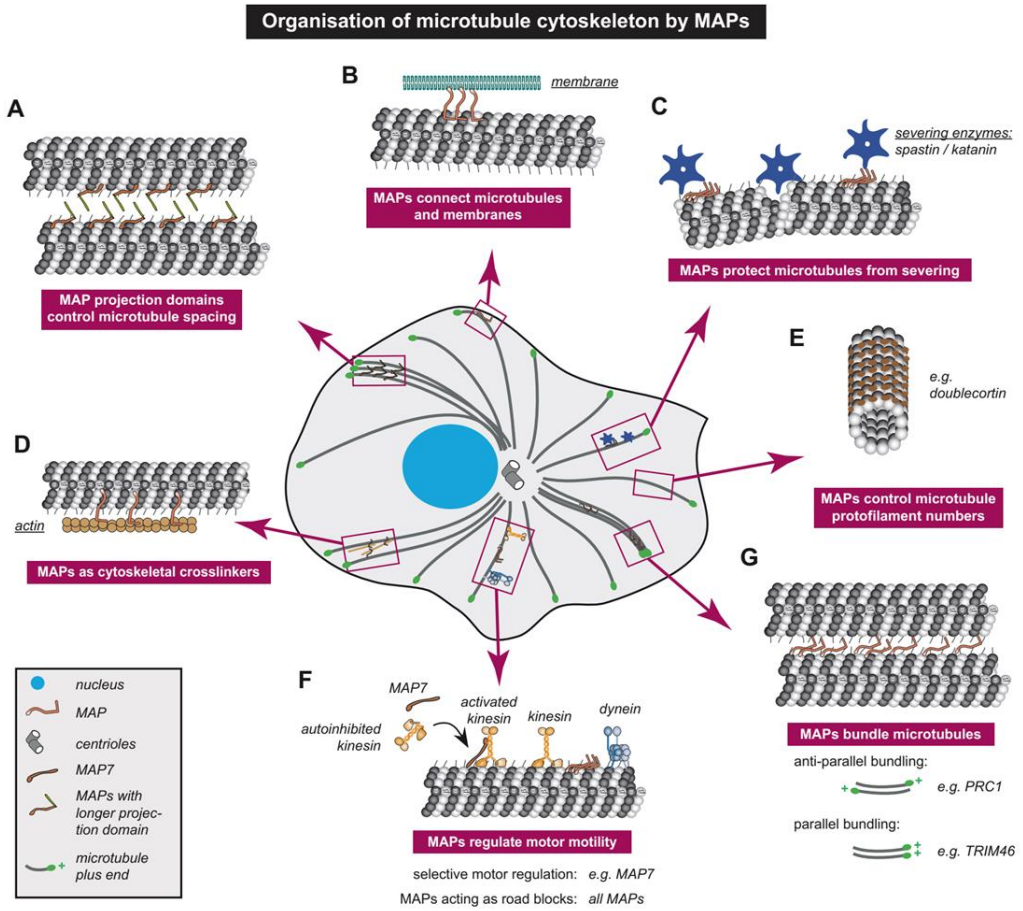

Figure 9 : Schematic representation of ways MAPs bind to microtubules to influence their functions: (A) binding and spacing microtubules with long MAP projection domains, (B) connecting microtubules to membranes, (C) protecting microtubules from cutting enzymes thus, preventing disassembly, (D) crosslinking different cytoskeletal elements, (E) controlling the protofilament numbers of microtubules, (F) affecting the binding and motility of motor proteins by either forming a complex with the motor, or by occupying the motor path at the microtubule surface, (G) promoting microtubule bundling, by neutralising acidic tubulin carboxy-terminal tails. (adapted from Bodakuntla *et al.,* 2019 figure inclusive)

Alterations in microtubule-associated proteins (MAPs) are associated with several congenital and sporadic age-related neurological disorders such as tauopathies, characterized by filamentous inclusions of hyperphosphorylated Tau (Johnson & Bailey, 2002). Mutated Tau in FTLD with parkinsonism linked to chromosome 17 (Spillantini & Goedert, 1998) presents neurofibrillary tangles and neurodegeneration caused by an abnormal increase in the number of microtubule binding domains in Tau. (Hutton *et al.,* 1998). Although, the classical MAPs differ in their structures and major functions, they all bind to tubulin, stabilize microtubules and are able to connect to other components of the cytoskeleton such as actin thus, there is a functional redundancy in the MAPs (da Cruz, 2005).

MAP1B is crucial to the formation and maintenance of a functional nervous system as suggested by the embryonic lethality recorded in its hypomorphic murine mutant (Gonzalez-Billault *et al.,* 2001). Takei *et al.,* 1997) reported a noticeable delay in the development of the nervous system in a MAP1B mutant in which the first 571 amino acids were preserved. MAP1B is localized to areas rich in “unstable” microtubules such as dendritic spines and axonal growth cones where it has an important function in mediating their dynamics through direct physical interactions and probably signalling (Ketschek *et al.,* 2015; Tortosa *et al.,* 2013; Tymanskyj *et al.,* 2012; Villarroel-Campos & Gonzalez-Billault,

2014). It has also been implicated in membrane trafficking in neurons through its regulatory action on Rab35, a protein involved in vesicle recycling. (Villarroel-Campos *et al.,* 2016).

1.4 Microtubules in Amyotrophic Lateral Sclerosis (ALS)

Mutations in microtubule proteins, as precise cause of ALS and other neurodegenerative disorders, are yet to be defined as either direct or indirect effect (Clark *et al.,* 2016), but problems involving microtubules and their associated proteins have been linked to several neurodegenerative diseases such as Amyotrophic Lateral Sclerosis (ALS, (Smith *et al.,* 2014), Parkinson's disease (PD, (Cartelli *et al.,* 2010), Alzheimer's disease (AD, (Matsuyama & Jarvik, 1989), Schizophrenia (Andrieux et al., 2006), Huntington's disease (HD) and various congenital developmental disorders (Tischfield & Engle, 2010). Recent literature suggests that the disruption of microtubule stability and its dynamics, possibly as a result of alterations in their associated proteins, may be the initial propeller behind several sporadic and familial ALS disease. This presupposes that microtubule-mediated deficits in axonal transport are the threshold point for motor neuron viability (Clark *et al.,* 2016). Mutations in TUBA4A, a microtubule protein of tubulin isoform is sufficient to cause a very rare form of familial ALS (Smith *et al.,* 2014) (Figure10D).

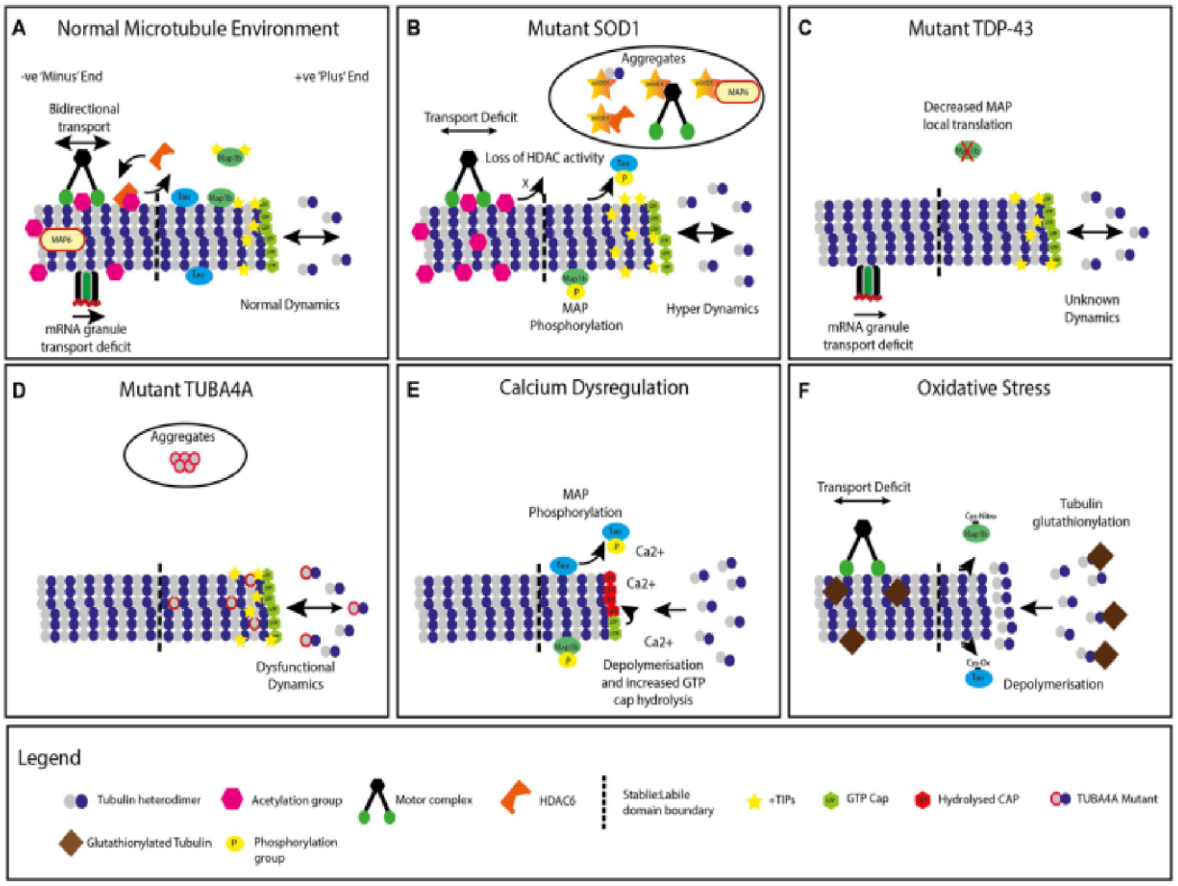

Figure 10 Modifications to neuronal microtubules (MT) in amyotrophic lateral sclerosis (ALS). (A) Normal microtubule +TIP dynamics and kinesin/dynein transport, mRNA granule transport and chemical modifications. (B) Mutant superoxide dismutase 1 (SOD1) expression leading to microtubule hyperdynamics, increased +TIP protein density, decreased transport, increased acetylation, phosphorylation of microtubule associated proteins (MAPs) and accumulation of microtubule protein containing aggregates. (C) Mutant TDP-43 expression causes dysfunction in mRNA granule transport. Decreased local translation of MAP1B mRNA is also observed in TDP-43 mutants. (D) Mutant TUBA4A expression alters microtubule dynamics and network stability, with unknown impact on +TIP proteins, transport or chemical modifications. Select mutations are incorporated into intracellular aggregates. (E) Energy depletion and calcium dysregulation generates increased microtubule depolymerization, tubulin guanosine triphosphate (GTP) cap hydrolysis, and increased MAP phosphorylation. (F) Neuronal oxidative stress leads to tubulin glutathionylation, increased microtubule depolymerization, decreased axonal transport and alterations to MAPs, with unknown impact on classical chemical modifications or +TIP proteins. (adapted from Clark *et al.,* 2016. Figure inclusive).

TDP-43 is involved in mRNA transport through interactions with the microtubule-dependent transport of mRNP granules (Alami *et al.,* 2014). This is of significance because TDP-43 is involved in mRNA translation of proteins locally, especially at the neuromuscular junction and other synapses, which suggests that alteration in this transport event is

implicated in the reduction of important proteins necessary for axonal and synaptic growth. (Fallini *et al.,* 2012; Lagier-Tourenne *et al.,* 2012; Polymenidou *et al.,* 2011) (Figure 10C).

SOD1 mutations account for approximately 20% of all familial ALS cases (Robberecht and Philips, 2013) and several mice models are available. These mice were found to have significant alterations in axonal transport which presuppose a connection with the microtubules and indeed change in their dynamics have been reported to be causal for the motor neuron malfunctions seen in these mice (Kleele *et al.,* 2014) (Figure 10B). A mutation that occurs more frequently than other previously known mutations in FTLD and both sALS and fALS called the hexanucleotide repeat expansion of the non-coding region of open reading frame 72 on chromosome 9 (C9ORF72) was identified in 2009 (DeJesus-Hernandez *et al.,* 2011; Renton *et al.,* 2011). Although, the mechanism of its pathogenesis is still obscure, a link with the microtubules has been suggested based on the homology of the C9ORF72 to a guanine nucleotide exchange factor (GEF) which is a signalling factor for the Rab-GTPases involved in vesicular trafficking of proteins (Droppelmann *et al.,* 2014).

Brockington *et al.,* 2010 reported a decreased expression of the microtubule associated proteins Tau, MAP1B, and MAP6 in a vascular

endothelial growth factor (VEGF) mice model of ALS predicting a possible dysfunction in the stability of microtubules in ALS. (Park *et al.,* 2013) reported a cause for microtubule depolymerization as a result of energy depletion which in a vicious cycle subsequently promote the inability of the microtubules to facilitate movement of mitochondria (Figure 10). This leads to an accumulation of these organelles as observed in SOD1 mutant mice (Park *et al.,* 2013). Inhibition of kinesin bindings on microtubules has been suggested as part of the toxic mechanism in ALS.

Excitotoxicity leading to motor neuron death which can be by excessive intracellular calcium levels, overstimulation by glutamate, damaged mitochondria or lack of calcium ion buffers has been reported to be a primary mechanism in ALS (Blizzard *et al.,* 2015). Direct alteration of microtubule dynamics by calcium is possible (Figure 10E) (O'Brien *et al.,* 1997) and increased levels of calcium can cause depolymerization of microtubules containing MAPs causing destabilization which can lead to caspase activation and subsequent collapse of the cytoskeleton (King *et al.,* 2014). Also, abnormal activity of cyclin dependent kinase 5 (CDK5) which is reported in the SOD1 mouse model of ALS can be caused by excessive intracellular calcium levels (Patzke & Tsai, 2002). Damaged mitochondria producing excessive and aberrant reactive oxygen species increase the oxidative stress environment which can lead to the oxidation

of tubulin and some microtubule associated proteins thus having a destabilization effect on the microtubules. Glutathionylation of tubulin also occur particularly in the motor neurons changing the structure of microtubules and their dynamics (Carletti *et al.,* 2011) (Figure 10F).

1.5 Mitochondria Dysfunction in Amyotrophic Lateral Sclerosis

Mitochondria, often referred to as the ‘power house’ of a cell, are double membrane-bound organelles involved in several important processes necessary for survival of the cell. Such processes include ATP and reactive oxygen species (ROS) generation, synthesis of metabolites and calcium homeostasis (Benard *et al.,* 2007). Motor neurons with very long axons and dendrites possess limited glycolytic abilities. They rely mostly on mitochondria to provide energy required for the maintenance of synaptic transmission and activities in the ion channels. Thus, mitochondria are needed to be efficiently transported to regions of high energy demands such as the neuromuscular junctions (Sheng, 2014) (Figure 11).

It is perhaps pertinent to recall and note, that the first mutation identified in association with fALS, is the one of the SOD1 gene that is localized to the mitochondria and is involved in the regulation of its functions. This presupposes a role for mitochondrial dysfunction in the biogenesis of the disease (Deng *et al.,* 2006; Israelson *et al.,* 2010; Kawamata & Manfredi,

2010). Reduced respiration rate and ATP synthesis are symptoms of mitochondria dysfunction observed in ALS patients, symptoms that precede rather than follow behavioural deficits (Mattiazzi *et al.,* 2002). Similarly, experimental models of ALS both in vitro and in vivo have recorded impaired activities of oxidative phosphorylation (OXPHOS) complexes, elevated mitochondria calcium levels and increased production of reactive oxygen species leading to loss of anti-oxidant activities. These were also recorded as increase oxidative stress in the spinal cords of ALS patients (Ikawa *et al.,* 2015; Wiedemann *et al.,* 2002).

TDP-43, an important protein in ALS pathogenesis, that can localize to the mitochondria, has been found to be accumulated in the mitochondria of subjects with ALS and FTLD activating its unfolded protein response and thereby causing damage (Wang *et al.,* 2019). The inhibition of TDP-43 mitochondria localization blocks its neuronal toxicity, linking mitochondria bioenergetics to TDP-43 neuronal toxicity (Wang *et al.,* 2016). Also, there is evidence that TDP-43 interacts with key mitochondria proteins such as voltage-gated anion channel 1 (VDAC1), Prohibitin 2 (PHB2), a crucial mitophagy receptor and mitochondria protease LonP1 (Davis *et al.,* 2018; Wang *et al.,* 2019) implicating mitochondria dysfunction in TDP-43 associated toxicity.

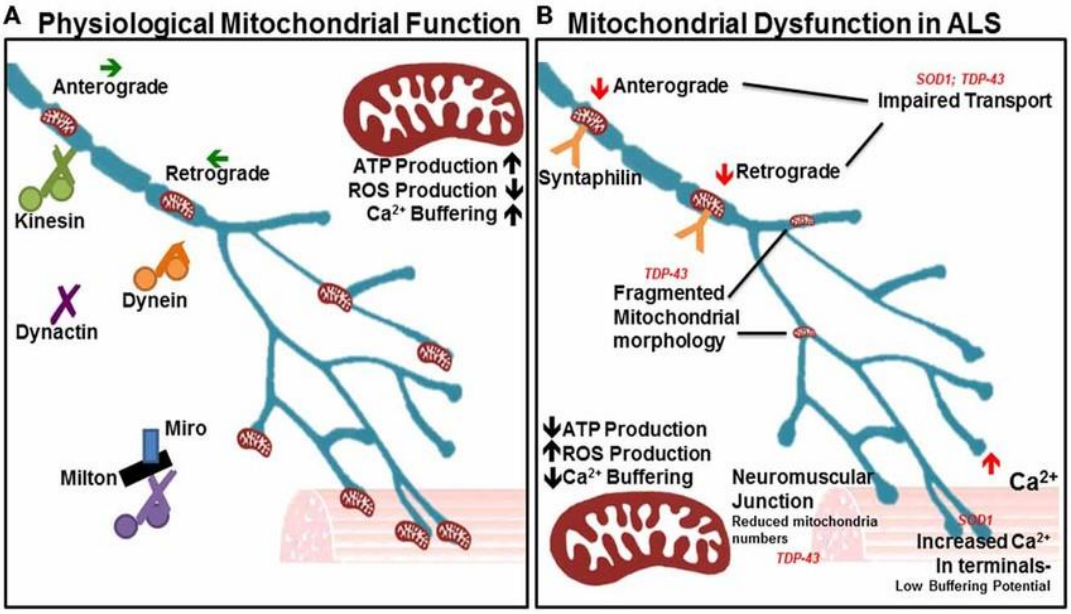

Figure 11 Schematic showing several aspects of mitochondria functions affected in ALS. (A) Normal mitochondrial functions in the physiologic state with a balanced dynamic of fission/fusion reactions, efficient trafficking as required in different compartments and regulated bioenergetics. (B) Impaired mitochondrial functioning in ALS with fragmentation, altered bioenergetics causing increase production of ROS, reduced ATP and inefficient transport (figure adapted from www.researchgate.net).

Abnormal mitochondria morphology or fragmentation has also been reported in TDP-43 associated models in mice, cell lines and biopsied human spinal cords tissues (Hirano *et al.,* 1984; Magrané *et al.,* 2014; Song *et al.,* 2013; Velde *et al.,* 2011; Vinsant *et al.,* 2013). This possibly results from more fission than fusion of the mitochondria that are constantly required to be in a dynamic state of fission/fusion (McBride *et al.,* 2006; Wang *et al.,* 2013). Mitochondria fusion and fission proteins have been implicated directly in mitochondria bioenergetics as they regulate respiratory complex assemblies and are vital to the maintenance of mitochondria functions (Cogliati *et al.,* 2013; Liu *et al.,* 2012) So,

alterations in mitochondria structural dynamics possibly have a contributory role in the mechanism of ALS pathogenesis (Jiang *et al.,* 2015).

Altered mitochondria distribution is becoming recognized as an important factor contributing to many neurodegenerative diseases not only to ALS. Mitochondria are distributed in different compartments of the neurons according to their energy demands so that, areas around synapses with great energy requirements have more mitochondria than other regions with less energy requirements (Jiang *et al.,* 2015). Significant mitochondria clusters in the soma and proximal axonal hillock have been reported in the lumbar spinal cords of ALS patients and similarly in the motor neurons of SOD1 and TDP-43 cell and animal models (De vos *et al.,* 2007; Igaz *et al.,* 2011; Janssens *et al.,* 2013; Sasaki & Iwata, 2007; Sotelo-Silveira *et al.,* 2009). This implies that efficient trafficking of mitochondria is extremely important in order to successfully fulfil all energy requirements of the neuron to maintain its functions (Figure 11).

Newly formed mitochondria must be able to move to the synapses and dendrites where they are required and conversely, damaged mitochondria must also be able to move back to the soma for degradation. So, movement of mitochondria is bidirectional utilizing both retrograde and anterograde transport which are respectively regulated by dynein and

kinesin motor proteins (Sasaki & Iwata, 2007; Schwarz, 2013). Microtubules are the highway for fast transport while actin filaments are the ones used for slow movement (Frederick & Shaw, 2007). The role of mitochondria dynamics in the pathogenesis of neurodegenerative diseases is becoming more pronounced though the exact mechanism of progression is still obscure and thus, is a viable research path worth pursuing. It is definitely a common pathology that could be insightful (Jiang *et al.,* 2015).

1.6 Drosophila melanogaster

D. melanogaster is a Dipteran commonly known as the fruit fly. Thomas Morgan and his colleagues are known as the pioneers of using the fly for biological research since the 1900s. This small but useful invertebrate model has proven to be a good one for studying neurodegeneration since 1972 when Hotta and Benzer identified the first neurodegenerative mutant, *dropdead*, in a fly phototaxis gene screen (Zhang *et al.,* 2018). The fly is particularly favoured over other animal models because it is easier, faster and cheaper to maintain. It has a short life span of about 50 days. It has approximately 14000 genes distributed on 4 chromosomes and 75% of human genes has a functional fly orthologue with a general 40% homology (McGurk *et al.,* 2015).

1.6.1 Life cycle of *Drosophila*

At 25 degrees Celsius, the life cycle of *Drosophila* is completed in about 10-14 days (Figure 12), and being temperature sensitive, at higher temperature, the cycle shortens while it slightly lengthens at lower ones. Egg laying marks the beginning of embryogenesis and is completed in about 22 hours. Development into first instar larva occurs approximately 24 hours after egg laying (AEL) and is followed respectively by the second and third instar larva 48 and 72 hours after AEL. The larva becomes pupa in about 2-3 days and metamorphosis is completed when the adult fly eclose from the pupa case, a process that takes about 4-5days (Figure 12). Newly born flies are distinct for their light body pigmentation and closed wings which opens few hours after eclosion.

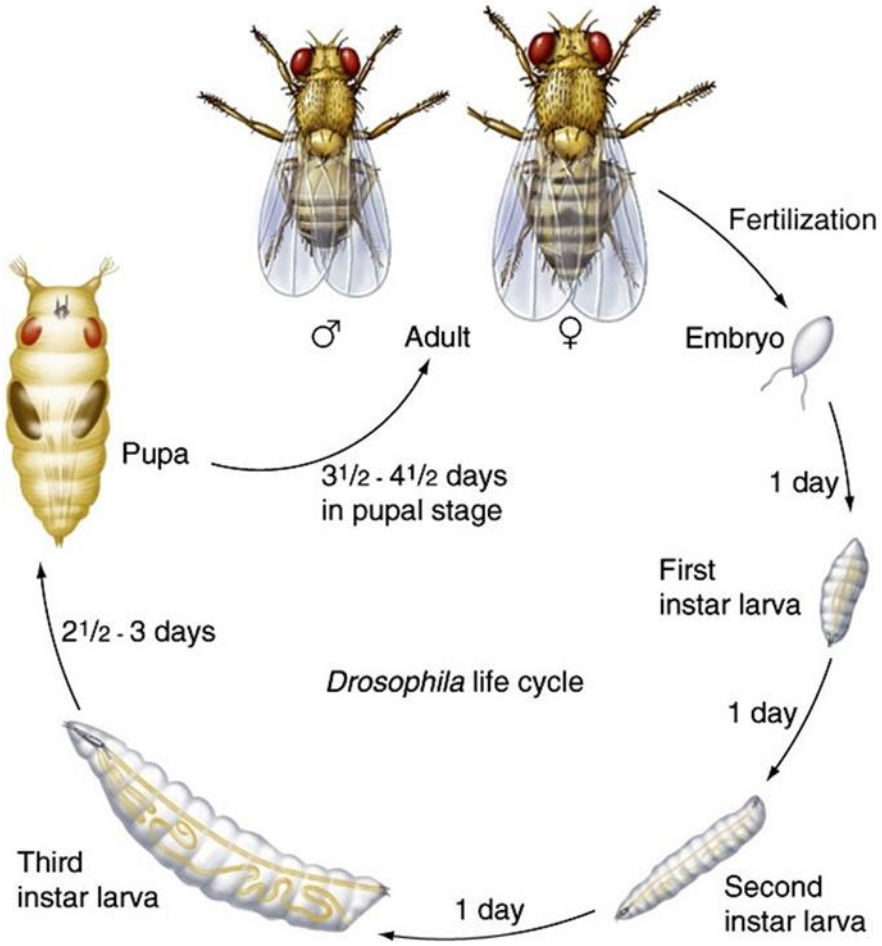

Figure 12 Life cycle of D. melanogaster. The cycle is completed in 10-14 days at 25degrees Celsius and sexual maturity is attained by 4-8hours after Eclosion. Young female flies can lay up to 100 eggs in a day and virgin females lay few sterile eggs (figure adapted from www.researchgate.net).

Drosophila are sexually dimorphic with males and females looking different yet similar (Figure 13). The males have a pair of sex combs on the forelegs and a black pair of claspers at the tip of the abdomen. The females, generally bigger, become sexually active about 8 hours after eclosion. Wildtype flies have red eyes and segmented abdomen.

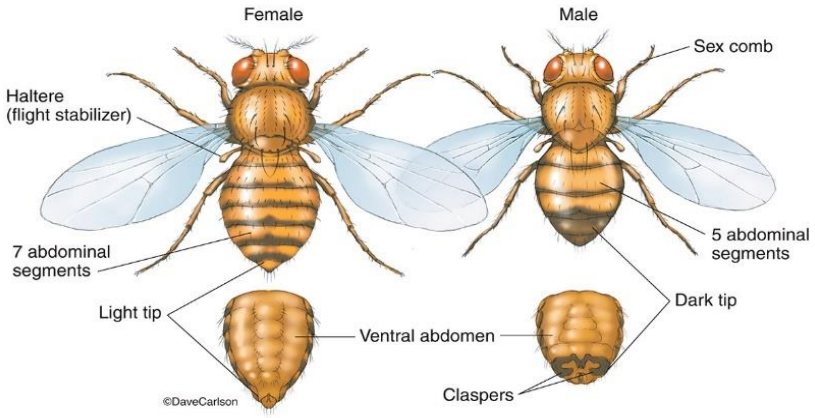

Figure 13 Illustrations of male and female D. melanogaster. Females are slightly bigger than the males with seven abdominal segments while the males have five. They are visibly distinguishable by the tip of their abdomen. It is light and pointed in the females while it is dark and round in the males. (figure adapted from www.carlsonstockart.com).

1.6.2 Modelling Human Diseases in *Drosophila*

The fly brain is quite complex, yet it is simpler than the mammalian counterpart. It is able to handle high-tasking motor functions such as climbing, flying and walking. It consists of about 100,000 neurons as compared with the more than a billion present in the human brain (Pandey & Nichols, 2011). Importantly, a wide range of tools and methods including the famous UAS/GAL4 system (Brand & Perrimon, 1993) are available for genetic manipulations and various studies of human diseases (Ugur *et al.,* 2016).

While the fly embryo is particularly favoured in developmental studies such as organogenesis, cell fate patterning and determination, and neuronal development, the third instar larva is mostly used to study physiological processes since innate tasks like crawling, can provide important phenotypic insights. Significant contributions has been made to the study of human biology by the examination of certain molecular and genetic mechanisms of the developmental processes in the pupa using the imaginal discs which are composed of undifferentiated cells that will eventually form all the adult structures. The adult fly, although significantly different from humans has an appreciable degree of conserved biology. It possesses a brain that can mediate complex behaviours such as learning and memory, sleep, aggression, circadian rhythm, courtship, walking and climbing among others. So, the adult fly is used to study quite a wide range of processes genetically including neurodegeneration (Pandey and Nichols, 2011).

Forward genetics approach involves expressing in flies, human genes with specific mutations linked with the disease in question and screening in vivo the function of these proteins. While reverse genetics involves studying the function of the conserved gene of endogenous proteins with the strongest homology linked with the human disease in the fly. Both approaches are used to study the molecular function of human genes in

Drosophila employing the UAS/GAL4 system (Galactose-4, upstream activating sequence). This allows the possibility of having different phenotypes by increasing, decreasing or eliminating gene expression in a tissue specific manner (Brand and Perrimon, 1993). Numerous neurodegenerative disease models in flies have been created using this system. With the UAS/GAl4 system it is possible to allow the expression of any transgene in a tissue-specific manner. Any gene, also a human disease-linked transgene, can be cloned downstream of UAS sequences, to which GAL-4, a yeast transcriptional activator, specifically binds to activate gene transcription. The GAL-4 gene is generally fused to a selected promoter, tissue specific, so that only when the fly harbouring the GAL-4 is crossed with the one harbouring the UAS fused to the gene of interest, is the gene expressed thanks to the transcriptional activity of GAL-4 in a tissue specific manner in the progeny of the flies crossed (Figure 14).

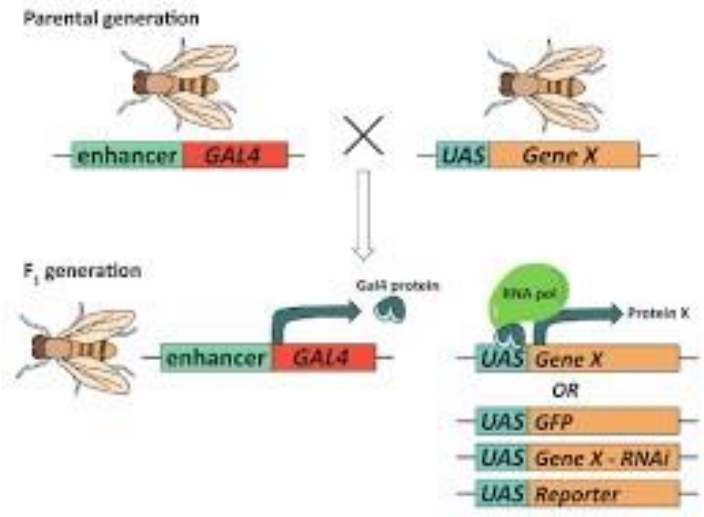

Figure 14 UAS/GAL-4 system. In a fly line, a transgene is placed downstream a UAS activation domain containing the binding sites of GAL-4 and in another fly line, GAL-4 is placed with a tissue specific enhancer. This allows the expression of the said gene in the the specific tissue of the offspring. Figure adapted from (Kelly *et al.,* 2017).

Genome wide screening to identify possible influencers can be performed once the fly model of neurodegenerative disease reproduces specific phenotypes linked with the disease. Hypomorphic alleles can also be created using the UAS/GAL4 system by inducing the expression of interference RNAs, known as RNAi, cloned under UAS control, against specific genes (Figure 14). Large screening of mutations of genes that affect a neurodegenerative phenotype is also another way of searching for possible modifiers of a disease with an unbiased approach that can lead to the discovery and identification of new pathways and proteins involved in the disease mechanism (Muqit & Feany, 2002).

1.6.3 *Drosophila* Neuromuscular Junction

The neuromuscular junction of the fly larva is an excellent model to study synaptic development, organization, function and transmission. This is because it is large, easily seen, singularly specified and the whole system is relatively simple (Keshishian, 1996). It is similar to human synaptic plaques and central glutamatergic synapses in the brain. It can also be easily manipulated both anatomically and physiologically (Menon *et al.,* 2013). It is a model of choice as many of the proteins involved in synapses are conserved in *Drosophila* and vertebrates so, their development at the molecular and cellular level are very similar (Keshishian, 1996) (Figure 15C).

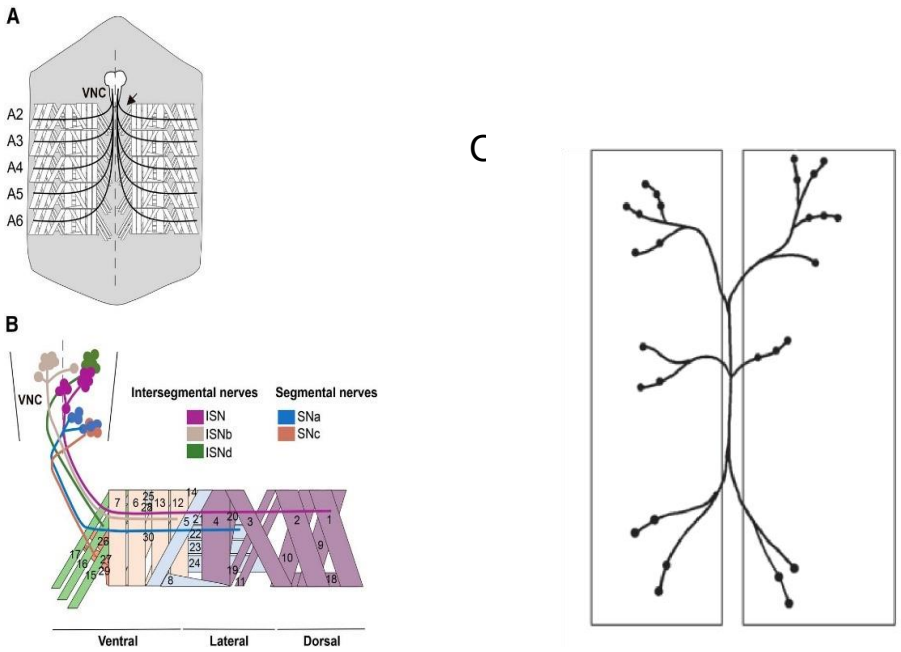

Figure 15 Schematic representation of (A) Abdominal segments A2-A6 of a dissected third instar larva showing the NMJ. (B) Innervation of one abdominal hemi-segments shown in (C)The NMJ of the 6 and 7 muscles of the same segment showing the nerves. Larvae are bilaterally symmetrical from abdominal segment 2-7. Figure adapted from (Pérez-Moreno & O'Kane, 2018).

There are 30 muscles in each hemi-segment of the larva innervated by specific motor neurons whose axons project together as a peripheral nerve from a ventral nerve cord neuromere (Figure 15B). Cell bodies located in the ventral nerve cord (VNC) project their axons through six main nerves consisting of ISN (intersegmental nerve, SNa (segmental nerve a), SNb (segmental nerve b), SNc (segmental nerve c), SNd (segmental nerve d) and a transverse nerve (TN) that projects to very few motor neurons (Pérez-Moreno & O'Kane, 2018). The neuromuscular junction or synapse is formed when the axons of the motor neurons reach the muscle surface via differentiation of specialised structures known as synaptic boutons. They are well studied and categorized into four types based on size namely :

- Type Ib. They are glutamatergic, present in all muscles and are the largest measuring about 3-6µm.
- Type Is. They are similar to 1b but smaller with a dimension of 2-4 µm.
- Type II boutons use as neurotransmitters glutamate and octopamine. They are not present in all muscles like the type I boutons and are the smallest with a size of 1-2 µm (Monastirioti *et al.,* 1995).

- Type III boutons have glutamate and insulin as putative hormone transmitters and are present only on muscle 12. Their size is medium with 2-3µm dimension (Gorczyca *et al.,* 1993).

1.6.4 *Drosophila* Futsch

The MAP1B homologue is encoded by the *futsch* gene in *Drosophila*. MAP1B is the first MAP to be expressed in neurons and is required for axonal and dendritic growth. It regulates microtubules at the neuromuscular junction in *Drosophila*. Futsch is a 575kDa protein containing predicted 5327 amino acids (Figure 16A). It presents a strong homology to the mammalian MAP1B and is recognized by the monoclonal antibody mAB 22c10 (Roos *et al.,* 2000). The central domain is highly repetitive with an homology to the vertebrate neurofilaments while the N and C terminals are homologous to the vertebrate MAP1B (Figure 16C) (Hummel *et al.,* 2000). It is found in all parts of the neuron with the axon having the highest concentration (Bush, 1996; Robberecht & Philips, 2013). It is composed of a heavy chain HC (300kDa) and two light chains LC-1 (32kDa) and LC-3 (18kDa). It has a microtubule binding domain and an actin binding domain both of which are found in the heavy chain (Cueille *et al.,* 2007) presupposing that it could be a link between microtubules and microfilaments as reported by SatoYoshitake and colleagues in 1989.

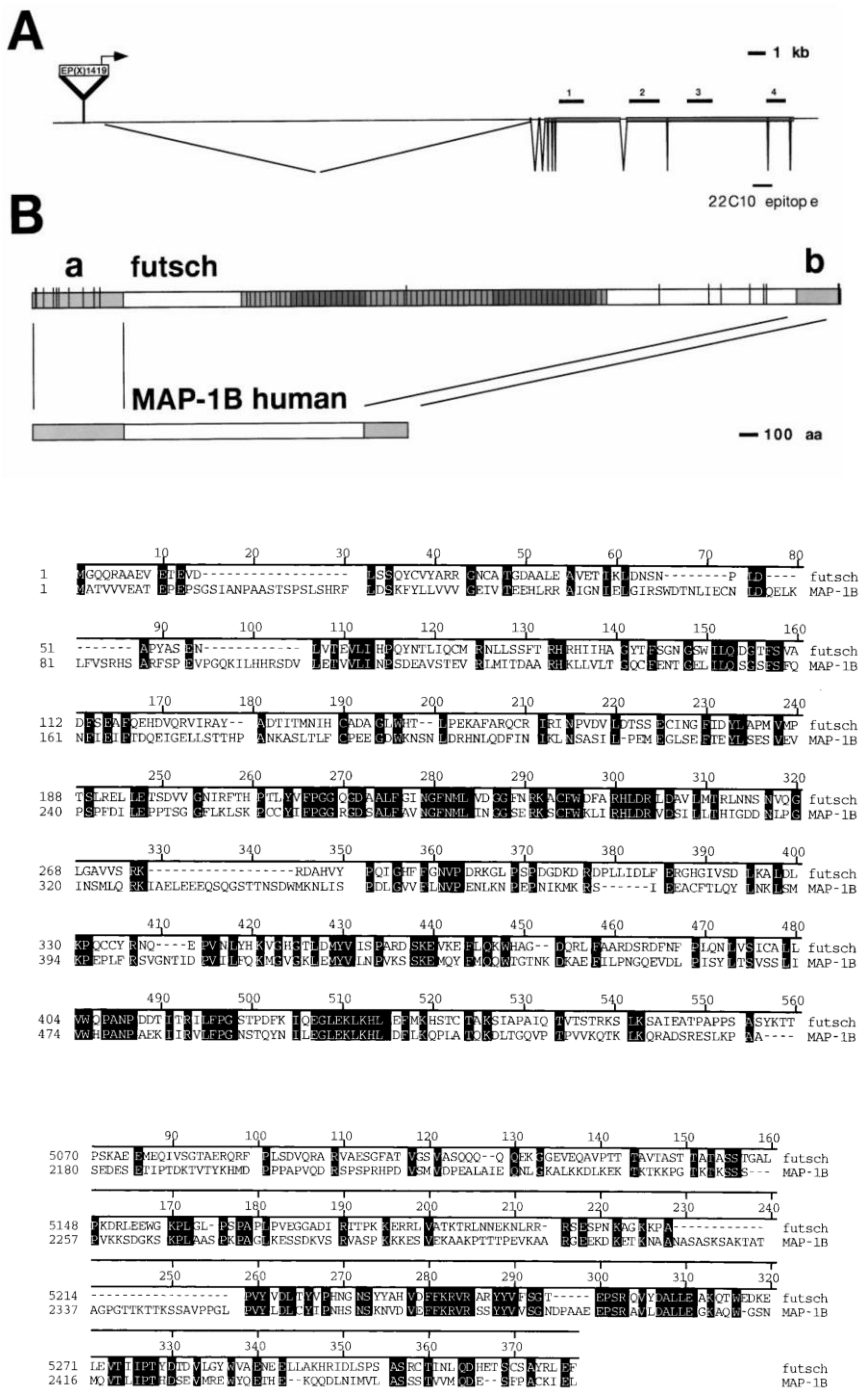

Figure 16 The *futsch* Locus Encodes a MAP1B homolog Protein (A) The genomic organization of futsch and the location of the 22C10 epitope are indicated. B) The deduced Futsch protein is 5327 amino acids in length; N- and C-terminal domains share similarity to the vertebrate MAP1B protein. The middle part of the Futsch protein is composed of 60 direct repeats of a 37 amino acid–long domain. The level of shading indicates the degree of sequence identity. A sequence comparison of regions designated (a) and (b) is shown in more detail is shown in C) Sequence Comparison of Futsch and Human MAP1B N- and C-Terminal Protein Sequences (a) shows the N-terminal 600 amino acids, and (b) shows the C-terminal 295 amino acids. Identical amino acids are shaded in black. (Adapted from Hummel *et al.,* 2000).

Phosphorylation is the most important post translational modification of MAP1B and is important in maintaining its function as a microtubule stabilizer (Cassimeris, 2010). The embryonic nervous system presents defects in axonal and dendritic growth in the loss-of function allele of *futsch* (Hummel *et al.,* 2000), while hypomorphic alleles that are viable present alterations in microtubule organization at the synapse. Also at the neuromuscular junction, a reduction in bouton number and an increase in bouton size were observed (Roos *et al.,* 2000). *Futsch* is negatively regulated by the *Drosophila* fragile x mental retardation (*dFXR*) gene which acts as its translational repressor to regulate microtubule-dependent synaptic growth and function (Zhang *et al.,* 2001). The 3-related genes for FMR present in mammals are represented by a single dFXR in *Drosophila*. FMR and dFXR proteins show considerable similarities in their molecular characteristics, expression patterns and functions (Figure 17). Importantly, the features observed in dFXR mutants are consistent with synaptic defects found in human fragile X patients and *FMR1* knock-out mice. These observations reiterate *Drosophila* as an attractive genetic model to study many diseases including Fragile X syndrome (Zhang *et al.,* 2001).

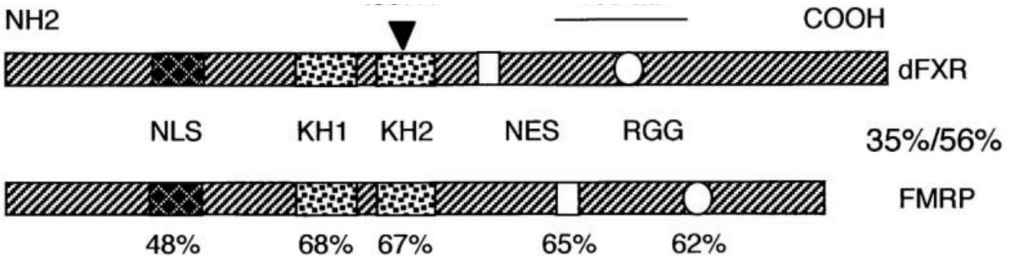

Figure 17 Protein domains in dFXR and human FMRP. The percentage similarities in amino acids between the homologs are indicated. Abbreviations are as follows: KH, K homology domain; NLS, nuclear localization signal; NES, nuclear export signal; and RGG, a motif rich in arginine and glycine (Adapted from Hummel *et al.,* 2000).

We have observed that the protein levels of Futsch is reduced in TBPH mutant flies and mutations in this protein recapitulates many phenotypes of the mutant flies including locomotion defects (Godena *et al.,* 2011; Roos *et al.,* 2000). Overexpression of Futsch was found to be neuroprotective implying disrupted cytoskeletal arrangement as part of the disease mechanism of ALS caused by TDP-43 dysfunction (Coyne *et al.,* 2014).

1.6.5 The synaptic vesicle cycle in *Drosophila*

The synaptic vesicle cycle is composed of both exocytosis and endocytosis. Neurotransmission is effectively achieved by regulated exocytosis of neurotransmitters encapsulated in synaptic vesicles at the active zones of the nerve terminals. This is a highly specialized event that shares many molecular components and characteristics with the less specialized membrane fusion in other cells. So, the soluble N-

ethylmaleimide-sensitive factor attachment protein receptors (SNAREs), the ATPase N-ethylmaleimide-sensitive factor and the Rab-GTPases, which are all proteins involved in the membrane fusion complex, are found to be highly conserved in the animal kingdom from yeast to humans. They are also needed for normal vesicular trafficking and synaptic activities (Rothman, 1994).

Repeated rapid rounds of neurotransmission are maintained aand sustainable as a result of the continuous formation and fusion of the synaptic vesicles from and with the synaptic membranes. At the presynaptic terminal, activation of the SNARE protein complex is achieved in response to the initial influx of calcium. These proteins involved in the fusion of the lipid bilayers are present on both the surface of the presynaptic membrane and the synaptic vesicle membranes (Figure 18) (Jahn *et al.,* 2003).

SNARE proteins are classified as R-SNARE and Q-SNARE based on the composition of the conserved arginine or glutamine residues in the core of their SNARE motifs as opposed to the previous classification into v-SNARE and t-SNARE as a result of their presence on the vesicles or target membranes (Fasshauer *et al.,*1998).

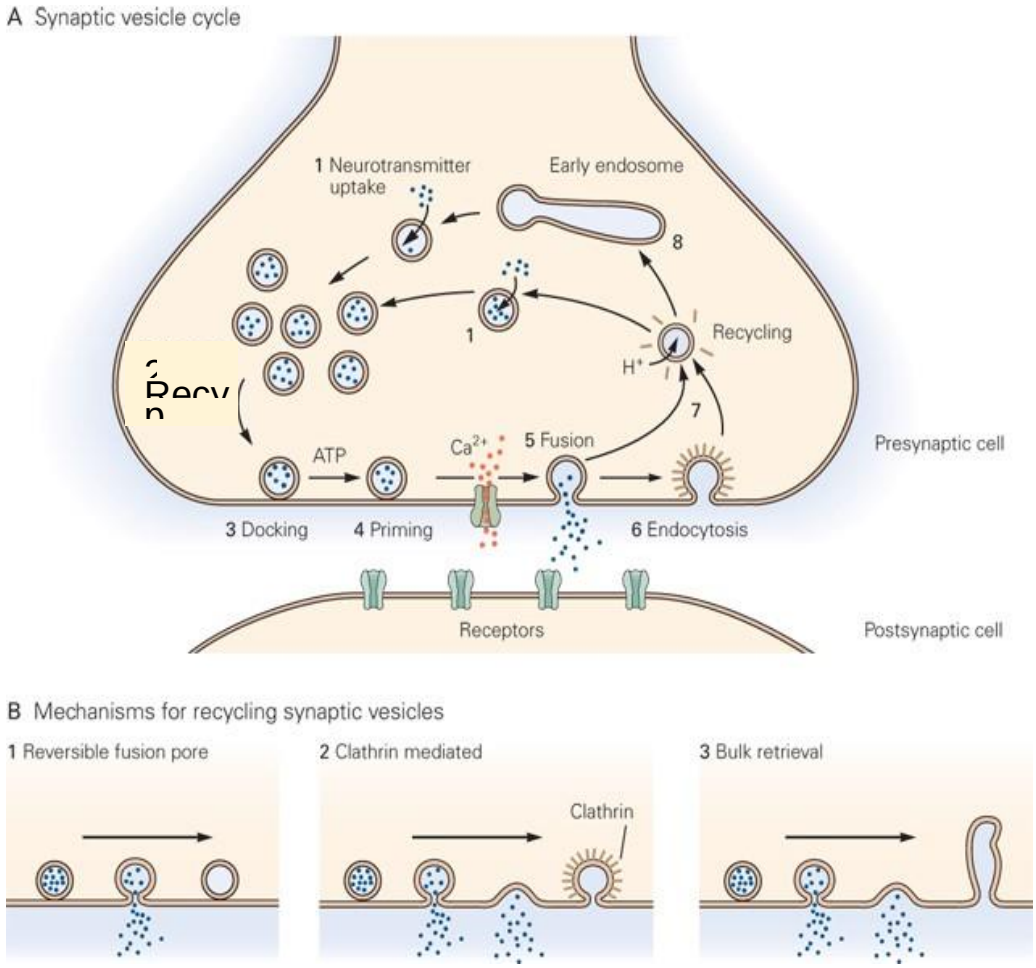

Figure 18 The synaptic vesicle cycle and mechanism of recycling. (1). Formed vesicles are filled with neurotransmitters. (2) a synaptic vesicle pool ready for exocytosis. (3) vesicles move to the synaptic membrane where they dock and are (4) primed after which a burst of calcium ions trigger (5) the fusion and opening of a pore. (6) Empty vesicles are endocytosed via the clathrin-mediated pathway (7) Vesicles are uncoated and filled with neurotransmitters to be returned to the pool or (8) recycled via endosomes for sorting and subsequent actions. Figure adapted from neurology.mhmedical.com

Majorly, three proteins are responsible for mediating the exocytosis cycle of the synaptic vesicles in *Drosophila*. Syntaxin 1A is present in plasma membrane at the synaptic terminal and is involved in docking of synaptic vesicles. Synaptobrevin or vesicle-associated membrane protein (VAMP) is a protein localized in the synaptic vesicles. It aids their fusion to the

plasma membrane. Synaptosomal nerve-associated protein 25 (SNAP-25) is a protein responsible for the formation of tight complexes. It clusters the synaptic vesicles to the plasma membranes (Südhof, 2004).

At the active zone, the interaction of Synaptobrevin, an R-SNARE protein with the domains of the Q-SNARE proteins Syntaxin 1 and SNAP-25 leads to the formation of the synaptic 'SNARE core complex' which drives the docking process of the synaptic vesicles leading to fusion with the presynaptic membranes (McMahon & Gallop, 2005). The SNARE core complex is a four helix structure formed by 2 helices of SNAP-25 and one each from Syntaxin 1A and Synaptobrevin. Syntaxin and Synaptobrevin are anchored by their C-terminal domains in their respective membranes while SNAP-25 is tethered to the plasma membrane via several cysteine-linked palmitoyl chains (Martens & McMahon, 2008).

Fused vesicles release their cargoes and the recycling process begins through endocytosis via different pathways of which the most used and studied is the clathrin-mediated endocytosis (Figure 18B2). Here, adaptor proteins (AP) recruit clathrin to the plasma membrane inducing invaginations. Subsequent fission of the synaptic vesicles from the plasma membranes is mediated by dynamin and endophilin. Synaptojanin uncoats the vesicles that are directed back to the functional pool thereby

allowing the empty vesicles to be recycled (Murthy & Camilli, 2003; Richmond & Broadie, 2002).

The bulk endocytic pathway involving the transport and recycling of vesicles via specialized endosomes is less characterized (Hoopmann *et al.,* 2010) (Figure 18B3). There is some evidence of a transient fusion pore also known as the 'kiss and run' recycling pathway involving closure of the pore immediately after cargo release into the synaptic cleft (Figure 18B1) (Verstreken *et al.,* 2002, 2003). Newly endocytosed vesicles are either recycled to the functional pool or internalized into multivesicular bodies through ESCRT (endosomal sorting complexes required for transport) machinery and are targets for degradation (Stenmark, 2009) (Figure 18A).

The Rab proteins are a family of small GTPases responsible for regulation of intracellular trafficking which includes the above described process by virtue of their ability to interact with the synaptic vesicles. They affect their specific binding to endosomes, their relations with the SNARE proteins and also mediate the interactions of the endosomes with the microtubules (Baetz & Goldenring, 2013; Ito-Ishida *et al.,* 2012).

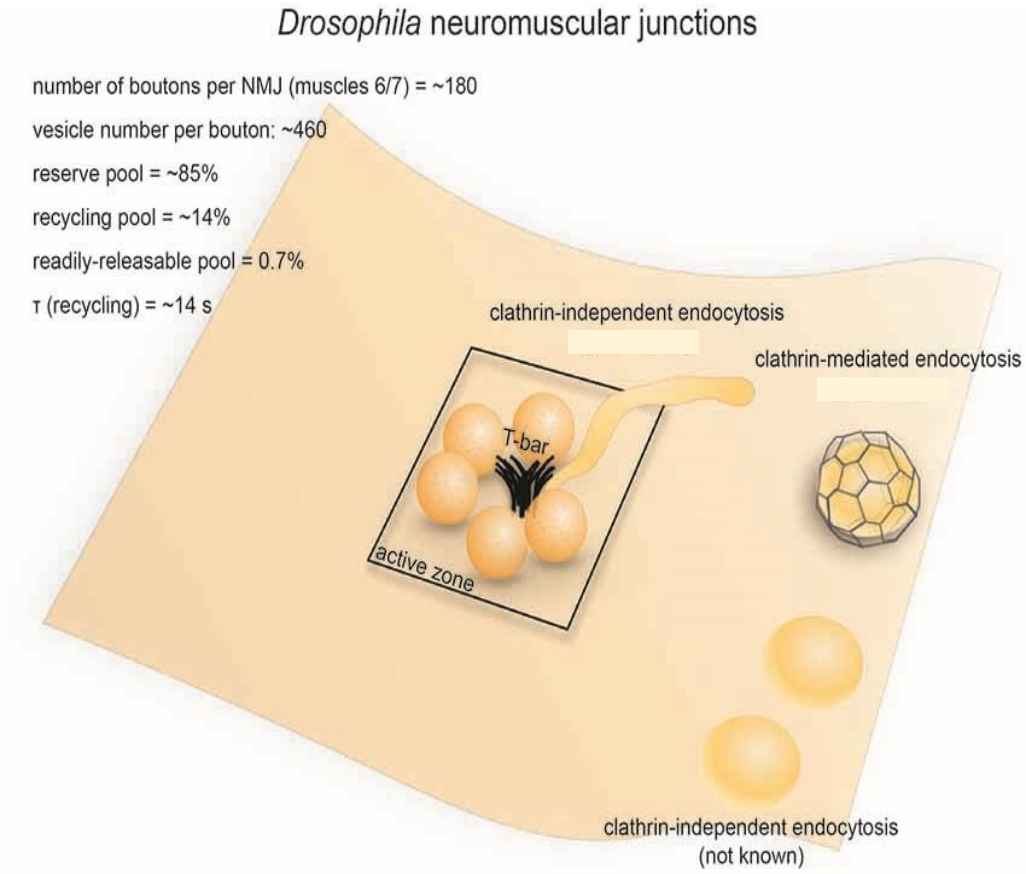

Figure 19 The vesicle pools in *Drosophila* neuromuscular junction and endocytic pathways. A typical NMJ in *Drosophila* has 200-300 active zones where endo and exocytosis occur. Both clathrin-mediated and clathrin-independent endocytosis occur at Drosophila NMJs. The exact time courses of these endocytic pathways have not been determined. (adapted from (Gan & Watanabe, 2018) figure inclusive).

Each NMJ in *Drosophila* contains ~180 boutons (Schuster *et al.,* 1996) with each bouton having 7–41 active zones (Atwood *et al.,* 1993). A dense T shaped projection called the T-bar seen on electron microscopy of fixed samples is the center of the active zone which is surrounded by a synaptic vesicle-rich area (Figure 19). Approximately 460 synaptic vesicles are present in a single bouton bringing the total number of vesicles to about 83000 in the neuromuscular junction between muscles 6 and 7 as roughly

180 boutons are present in this specialized synapse (Delgado *et al.,* 2000; Schuster *et al.,* 1996). The recycling pool of vesicles can be completely turned over in approximately 10-14s as the maximum rate of synaptic vesicle recycling at a normal NMJ averages about 1000 vesicles per second (Delgado *et al.,* 2000; Poskanzer *et al.,* 2006). 14% of the total number of vesicles constitute the recycling pool which are located at the periphery of the bouton, the readily releasable pool has about 0.7% while the rest of the vesicles, about 85% are the reserve pool found in the core of the bouton (Figure 19) (Delgado *et al.,* 2000; Kuromi & Kidokoro, 1998; Muller *et al.,* 2012; Ramaswami *et al.,* 1994).

1.7 Our *Drosophila* model of Amyotrophic Lateral Sclerosis (TBPH null flies).

In Feiguin *et al.,* 2009, it was described the generation of a *Drosophila* model of ALS with the deletion of the TPBH gene, which is the orthologue of the human TDP-43 in flies (Figure 20). Endogenous expression of the protein was completely abolished in these null mutants and the flies recapitulate many of the ALS phenotypes such as reduced life span, and significant locomotion impairment as a result of structural defects of the neuromuscular junction. Both phenotypes and NMJ structural defects

were recovered by the expression of both TBPH and hTDP-43 in the neurons of these flies (Figure 21).

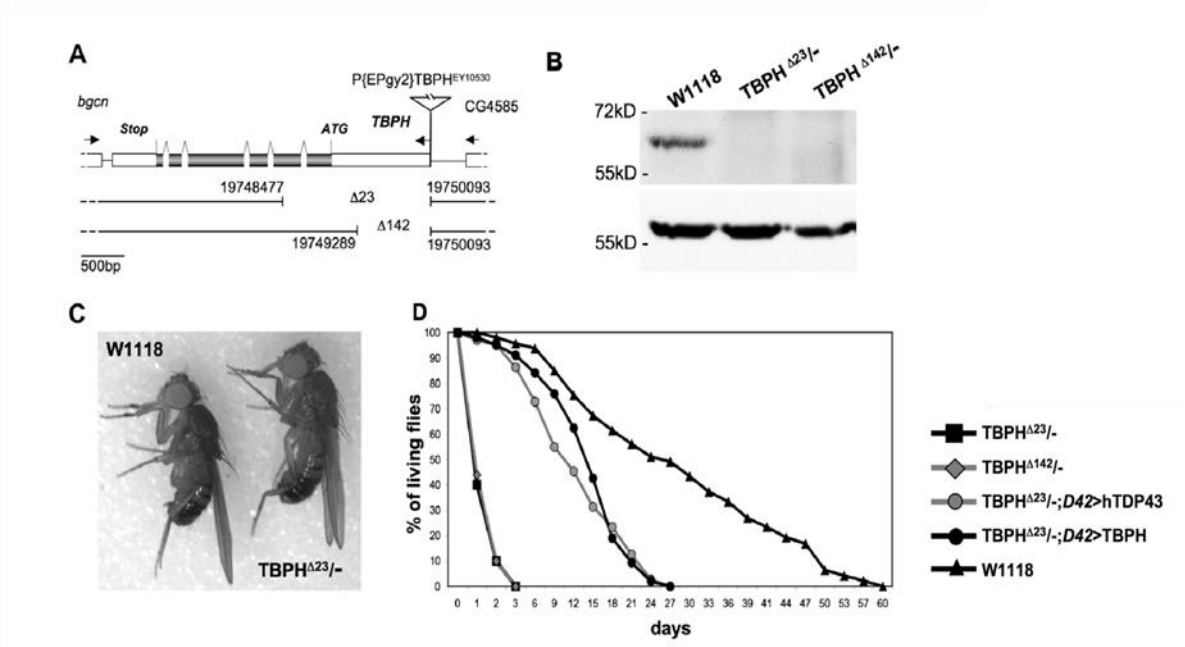

Figure 20 Loss of TBPH in *Drosophila* impacts negatively on life span and Locomotion. (A) Schematics of TBPH mutant alleles. (B) Western blot detects no endogenous protein in mutant fly heads (upper panel) tubulin was a loading control (bottom panel). (C) physical appearances of wild type controls and TBPH mutant flies are similar with no observable differences. (D) Expressing *Drosophila* or human TDP-43 transgene in the neurons recovers the reduction in life span recorded in TBPH mutant flies. Adapted from (Feiguin *et al.* 2009).

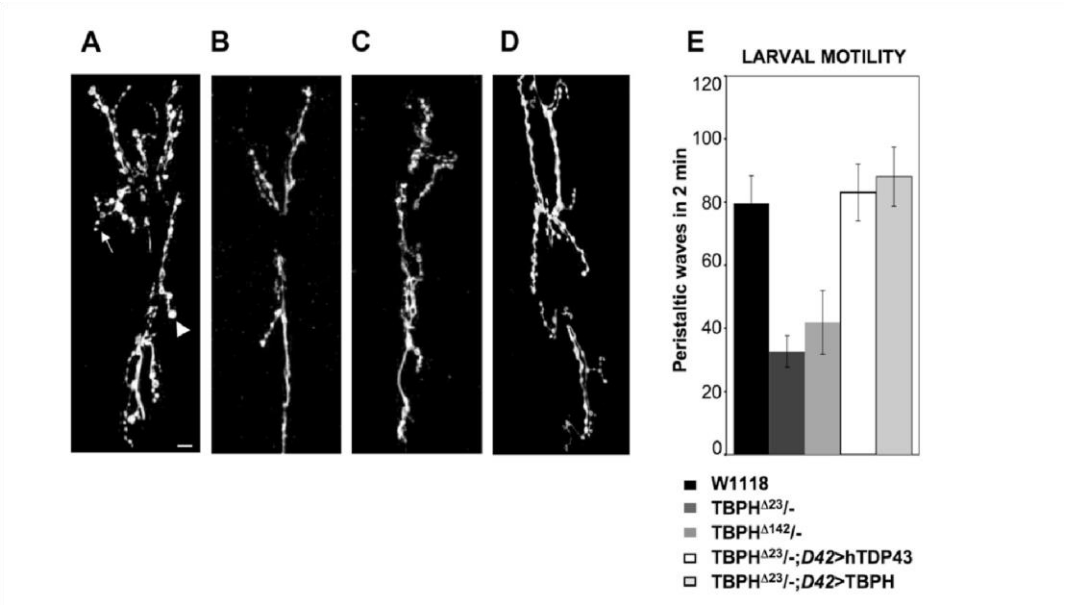

Figure 21 Anatomical defects at Neuromuscular Junction of TBPH mutant Flies. (A) Confocal images of motoneurons presynaptic terminals at muscles 6 and 7 in wild type third instar larvae stained with anti-HRP antibodies, reveals the branching pattern and the presence of big (arrowhead) and small (arrow) synaptic boutons. (B) and (C) Similar staining and anatomical position for TBPHD23 and TBPHD142 homozygous larvae respectively, show reduced axonal branching pattern and number of synaptic boutons. (D) TBPHD23 minus third instar larvae rescued by expressing UAShTDP-43 in motoneurons with D42-GAL4 shows recovery of presynaptic complexity with increased formation of synaptic boutons and axonal terminal branching. Magnification 63. (E) Number of peristaltic waves observed during 2 minutes in 120 h third instar larvae. n = 20 for each genotype, error bars indicate S.D.; $P < 0.0001$ calculated by ANOVA. Adapted from (Feiguin *et al.,* 2009).

Moreover, the levels of some pre-synaptic vesicular proteins such as Syntaxin, Synapsin, and cysteine string protein (CSP) were reduced when TBPH was silenced in neurons. Also the levels of Futsch, was found to be down-regulated in TBPH mutant flies presupposing a possible alteration in the function of microtubules (Figure 22). TDP-43 has a critical role in the formation and maintenance of the *Drosophila* NMJ, a specialised synapse from where features of motor neuron degeneration can be seen and deduced.

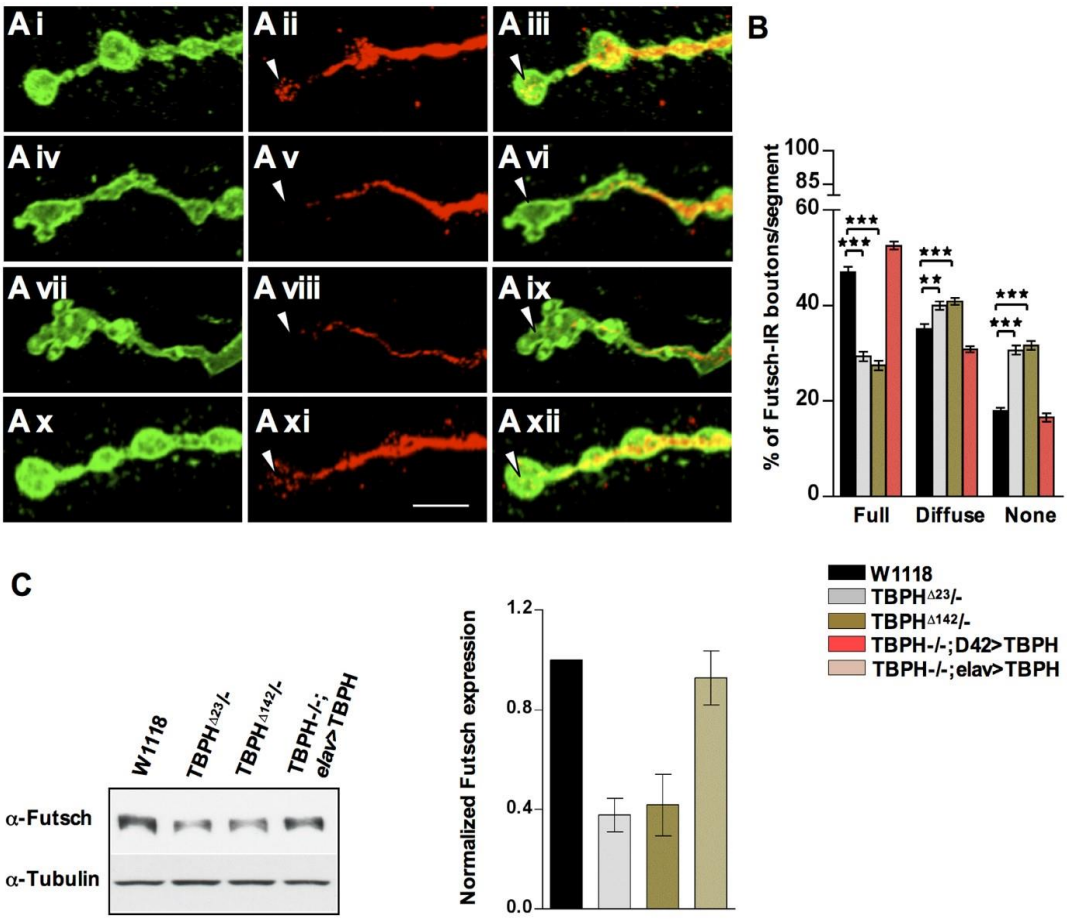

Figure 22 Depletion of TBPH interferes with microtubule organization through mediation of Futsch action. (A) Confocal images showing futsch staining at the terminal synaptic boutons of wild type (Ai–Aiii), TBPHD23 (Avii–Aix), TBPHD142 (Aiv–Avi). Note the complete absence of *futsch* at the most distal, newly formed, boutons in TBPH null Arrow heads point to the apparent absence of futsch at the newly formed boutons which are distalmost. (Ax–Axii) Expression of TBPH protein in the neurons recovers *futsch* staining in TBPH null larvae. (B) Quantifications of *futsch* staining pattern in muscle 6–7 abdominal segment II showing increased number of diffused *futsch* and *futsch* negative boutons in TBPH null alleles compared to wild type. $n=15$ larvae. **p<0.01 and ***p<0.001 calculated by one-way ANOVA. (C) Western blot analysis and the respective histogram confirmed the reduced *futsch* expression levels in TBPH null fly heads compared to wild type. $n=4$. Adapted from (Godena *et al.,* 2011).

2.0 AIM AND OBJECTIVES OF THE RESEARCH

2.1 Aim

The aim of the study was to characterize the Futsch/MAP1B rescue of locomotion defects in a *Drosophila* model of Amyotrophic Lateral Sclerosis.

2.2 The Objectives were:

- To investigate if silencing *tbph* was sufficient to exert an effect on Futsch levels and its role in the anatomy of the NMJ.
- To determine the best driver for the expression of Futsch in the neurons of TBPH mutant flies.
- To check if expressing Futsch in the neurons of TBPH mutant flies was sufficient to recover their ALS-like phenotypes with respect to motility, anatomy of the NMJ and levels of some synaptic proteins.
- To investigate the effects of Futsch on Rab4 rescue of motility in TBPH mutant flies and vice versa.
- To investigate the role of Futsch in synaptic vesicle recycling in TBPH mutant flies.
- To investigate the effect of Futsch on synaptic growth signalling (BMP pathway) in TBPH mutant flies.

3.0 MATERIALS AND METHODS

3.1 Fly stocks

w[1118]

Oregon R

w[1118]; TBPHΔ23/Cyo-GFP (Feiguin *et al.,* 2009)

w[1118]; TBPHΔ142/Cyo-GFP (Feiguin *et al.,* 2009)

uas-EP10756; TBPHΔ23/Cyo-GFP (Godena *et al.,* 2011)

w[1118]; UAS-mCD8::GFP/Cyo (#5137, BDSC)

w[1118]; UAS-MitoGFP/TM3SB

w[1118]; TBPHΔ23/Cyo-GFP; UAS-MitoGFP/TM3SB

w[1118]; ELAV-GAL4/Cyo-GFP

w[1118]; nSYB-GAL4/Cyo-GFP

w[1118]; D42-GAL4/Cyo-GFP

w[1118]; OK6-GAL4/Cyo-GFP

w[1118]; UAS-RAB4 GFP/TM3SB

w[1118]; TBPHΔ23/Cyo-GFP; UAS-RAB4 GFP/TM6B

w[1118]; TBPHΔ23/Cyo-GFP; UAS-RAB5 GFP/TM6B

w[1118]; UAS-TBPH/Cyo-GFP

w[1118]; UAS-TBPH RNAi (#ID38377, VDRC)

w[1118]; UAS-GFP RNAi (#9330, BDSC)

w[1118]; UAS-GFP RNAi (#9331, BDSC)

w[1118], P{UAS-dicer2, w[+]} (#60007, VDRC)

3.2 *Drosophila* techniques

3.2.1 Fly stocks and crosses

Some of the fly stocks were prepared in other laboratories and were gifts from friends and colleagues, some of them were prepared during the course of this study while others were purchased from the Bloomington *Drosophila* stock centre (Indiana; https//bdsc.indiana.edu/), the *Drosophila* genetic resource centre (Kyoto; https://kyotofly.kit.jp/cgibin/stocks/index.cgi), and *Drosophila* stock centre (Vienna; https://stockcenter.vdrc.at/control/main). Stocks were stored at room temperature for short term use or at 18°C for long term use. They were flipped into new tubes weekly or bi-monthly depending on the temperature in which they were kept. Flies were grown in small vials containing fly food in small aliquots (Figure 23). Experimental crosses of ten females and three males per vial were maintained in an incubator with set conditions of 60% humidity, 25°C, 12 hours light and 12 hours dark

cycles. The recipe for the fly food is written in Table 1 and the procedure described.

Figure 23 An empty fly vial with fresh food.

Table 1 Constituents of the Fly food and the required quantity

Ingredients	Quantity
yeast	1000g
agar	100g
cornflour	466g
sugar	666g
propionic acid	66ml
water	17l

In summary, about 15l of the water was boiled and the yeast was dissolved in a small portion of the boiled water. Agar was added to the boiling water and stirred intermittently to prevent overflow. The cornmeal was dissolved in the remaining 2l of water and added to the boiling agar. The mixture was stirred well. The dissolved yeast was added into the boiling mixture and stirred periodically. The food was cooled to about 65°C and the propionic acid was added. Food was stirred well and aliquoted into small vials shown in Figure 23 while it was just warm to touch. Not hot! The food was allowed to cool completely (overnight was used) before closing each vial with cotton wool. Food was stored at 4°C until required for maximum of 4weeks.

3.2.2 Larva Movement (Crawling)

The third instar larvae known as the wandering larvae were carefully picked from the food, washed in a drop of clean demineralised water and taken to the UV lamp microscope for selection using markers like the GFP or tubby. The larva were carefully selected and placed in a 6cm dish containing 0.7% agarose to prevent them from drying out. Each larva was placed in the middle of a 10cm dish containing 0.7% agarose and allowed 30s for acclimatization. Then, the number of peristaltic movements of the larva in 120s was counted. A larva moves by contractile waves originating from the posterior segments that move anteriorly from segment to

segment (Figure 24). About 20-30 larvae were counted per genotype. The counted larvae were transferred into a fresh vial of food and allowed to complete their cycles. This is to ensure the right genotypes were selected as the eclosed flies can confirm this.

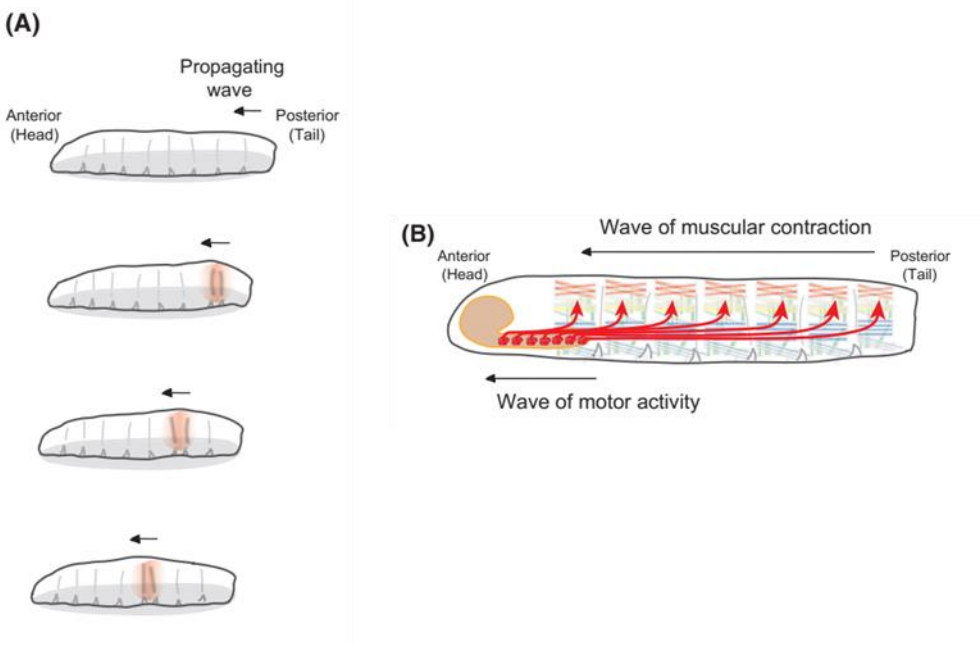

Figure 24 Larval locomotion system (A) Schematics showing larval peristaltic locomotion by propagating waves that moves from the posterior to the anterior part of the larva segmentally. (B) Basic architecture of the Drosophila larval neuromuscular system. Image adapted from (Kohsaka *et al.,* 2012)

3.3 Larva NMJ immunohistochemistry

Third instar larvae were selected as described above into 6cm plate containing 0.7% agarose. Each larva was washed and placed on a sylgard plate for dissection in a drop of HL3 solution (128mM NaCl, 2mM KCl, 4mM $MgCl_2$, 0.1mM $CaCl_2$, 35.5mM Sucrose and 5mM Hepes (pH 7.2) . The larva was pinned at both ends and a midline incision was made with a spring scissors between both pins (Austerlic Insect Pins 0.1mm

diameter, Fine Science Tools, Germany). The internal organs were removed and the remaining larva wall was carefully washed with the HL3 (Figure 25). It was then fixed using 4% PFA in PBS for about 20minutes except for glutamate receptors that fixation was done with methanol for 5mins at -20°C.

Table 2 Primary antibodies used with their dilution rate

Primary Antibodies		
Name (supplier)	Host	Dilution (NMJ)
αGFP (#A11122, Invitrogen)	Rabbit	1 : 300
αHRP (#323-005-021 Jackson)	Rabbit	1 : 150
αHRP conjugated with alexa fluor 555 (#123-165-021 Jackson)	Goat	1 : 150
αDlg (#4F3c, DSHB)	Mouse	1 : 250
αGluRIIA (#8B4D2c, DSHB)	Mouse	1 : 15
αFutsch (#22C10s, DSHB)	Mouse	1 : 50
αsynapsin (#3C11-c, DSHB)	Mouse	1 : 15
αsyntaxin (#8C3-s, DSHB)	Mouse	1 : 15
αcsp (#6D6-c, DSHB)	Mouse	1 : 15
αacetylated tubulin	Mouse	1 : 2000
αGFP (#A10262, Invitrogen)	Chicken	1 : 1000
αPmad-1 (#sc12353 Santa cruz)	Rabbit	1 : 1000
FM1-43 dye (# T35356 Life Technologies)	-	4mM final concentration

Table 3 Secondary antibodies used with their dilution rate

Secondary Antibodies		
Name (supplier)	Host	Dilution (NMJ)
Alexa Fluor® 488 αmouse (#A11001) or αrabbit (#A11008), (Life Technologies)	Goat	1 : 500
Alexa Fluor® 555 αmouse (#A21422) or αrabbit (#A21428), (Life Technologies)	Goat	1 : 500
Alexa Fluor® 647 αchicken (#A21449, Life Technologies)	Goat	1:500
αmouse-HRP (#32430, Pierce)	Goat	1 : 150
αrabbit-HRP (#32460, Pierce)	Goat	1 : 500

Larvae were kept in HL3 on ice till dissection was completed (<3hours) and they were washed in PBST (PBS 1x supplemented with 0.1% (v/v) Tween20) thrice for 5minutes each. Blocking was done for 30minutes in a solution of 5% NGS (Normal Goat Serum, Chemicon) in PBST. The blocking solution was used to dilute the primary antibodies (

Table **2**) and the larvae were incubated in it overnight at 4°C. The next day, primary antibodies were removed and the larvae were washed thrice for 10minutes each in PBST. They were then blocked as previously described and incubated for 2hrs in secondary antibodies (Alexa Fluor® Secondary antibodies, Life Technologies) (Table 3) diluted in the blocking solution. This incubation was in the dark and at room temperature. Larvae were washed in PBST thrice for 20minutes each to remove excess antibodies and they were then incubated in slowfade®Gold antifade (Life Technologies) reagent overnight at 4°C. The Larvae were then mounted in slowfade on glass slides, cover-slipped and scanned by a Carl Zeiss LSM 990 airyscan confocal microscope.

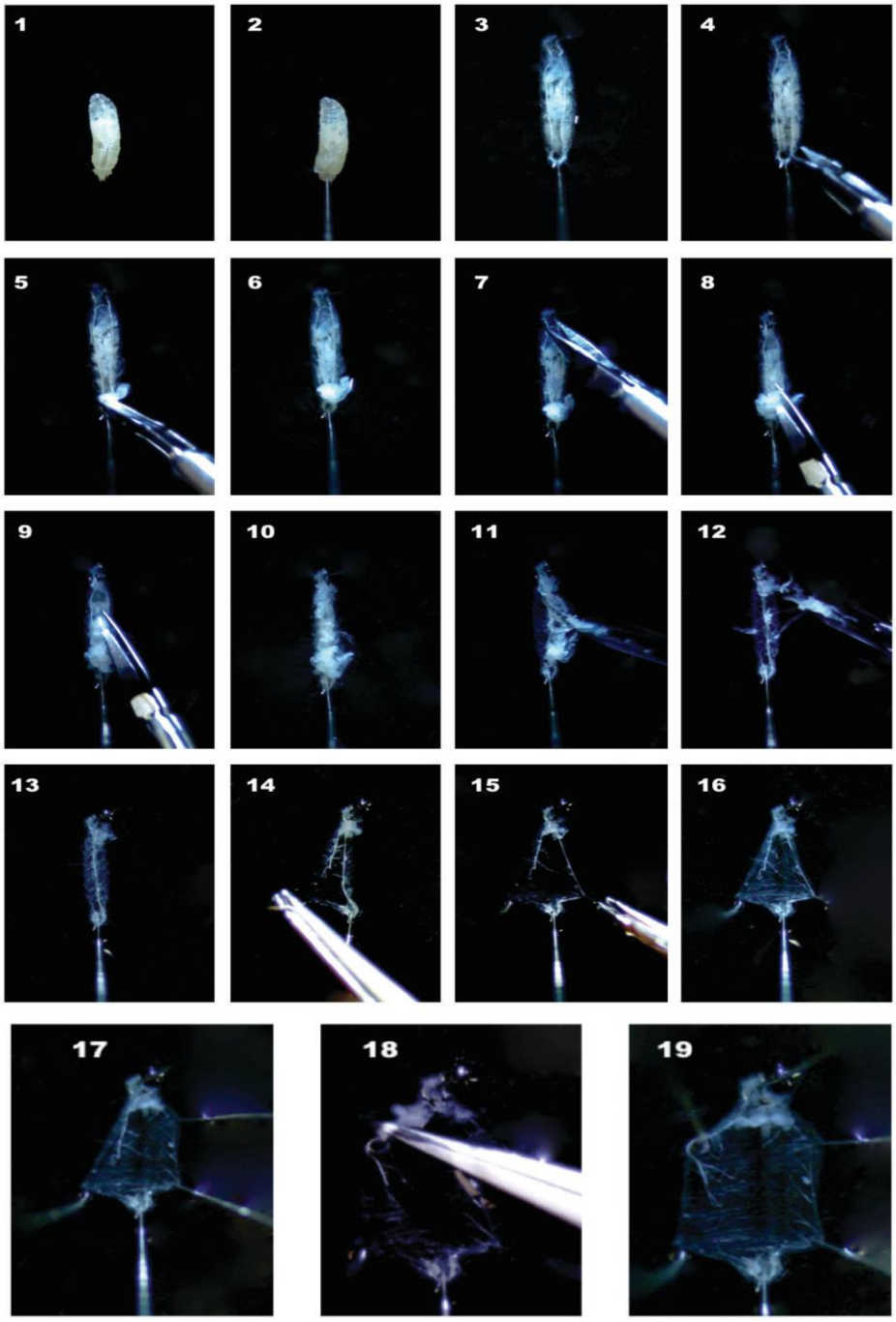

Figure 25 Steps involved in the dissection of a single larva. Adapted from (klima *et al.,* 2021)

3.3.1 Shape of Boutons

Boutons of the NMJs stained with HRP were used for this analysis. The NMJs were acquired with the airyscan confocal microscope using exactly the same settings for all genotypes involved. The bouton was categorized as regular when the circumference was round and smooth with an equal or almost equal axes. It was irregular when the circumference was not smooth and in a shape other than round with obviously unequal axes (Figure 26).

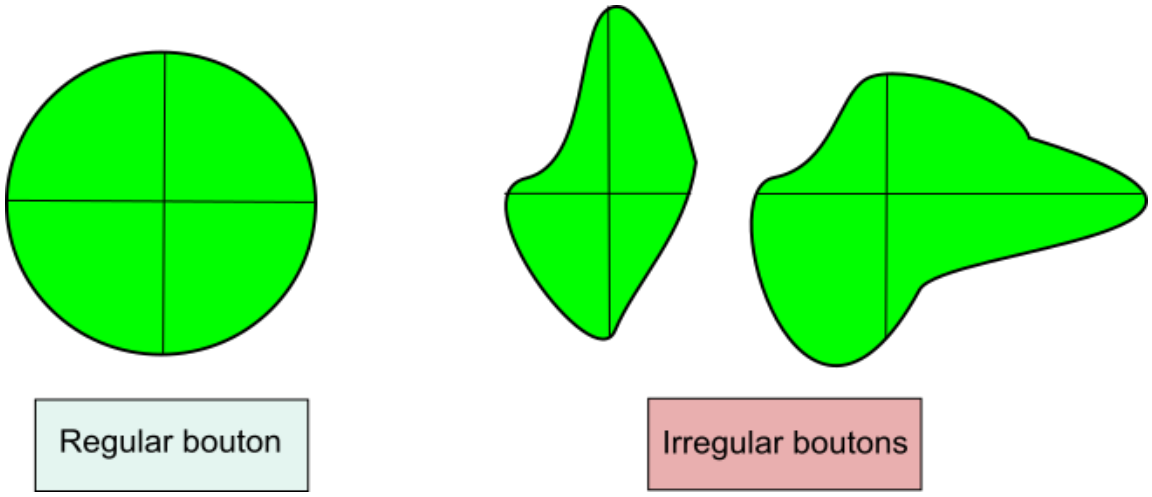

Figure 26 Regular and Irregular boutons. Regular boutons are circular and irregular boutons appear in different shapes and sizes. (Adapted from Strah, 2019).

3.3.2 Number of Branches

Primary, secondary and tertiary branches of a HRP-stained NMJ were all counted together and recorded (Figure 27) using images taken with the airyscan confocal microscope as described above.

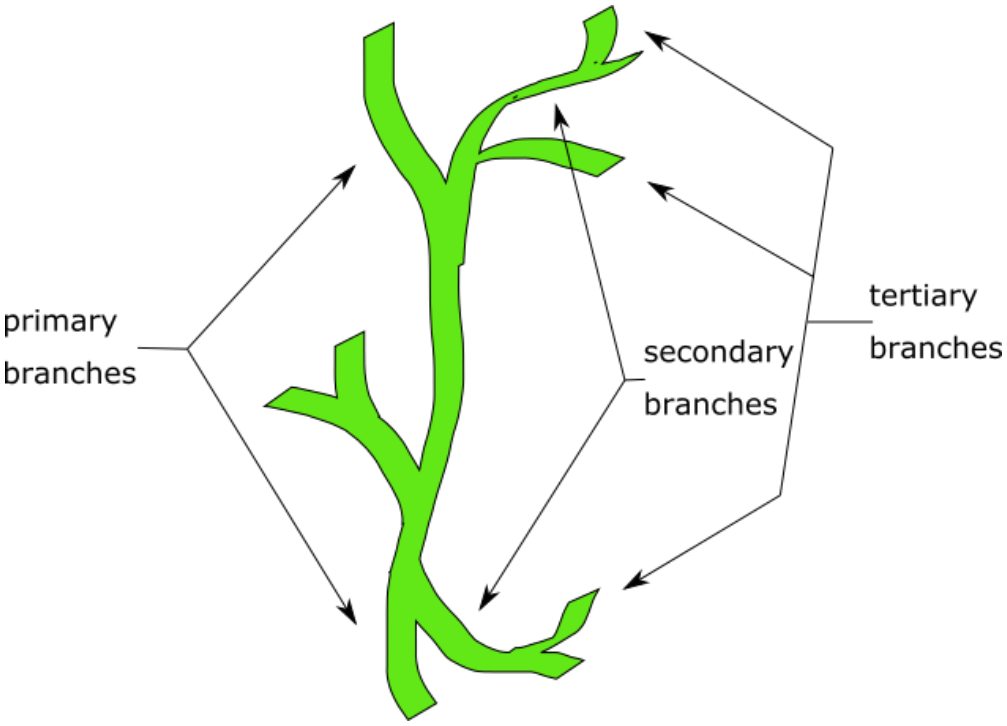

Figure 27 Schematic representation of the different types of branches in a Larva NMJ adapted from Strah, 2019.

3.4 Pre and post synaptic markers quantification

The larvae double or triple labelled with HRP and antibodies against pre and or post synaptic markers using the previously described immunohistochemical methods were used. Confocal images of the involved genotypes were taken at fixed settings using the 63X oil objective lens and processed using imagej software. Only the boutons of NMJs between muscles 6 and 7 in the second and third abdominal segments of each larva were considered (Figure 28). Using imagej, each bouton was marked as a region of interest (ROI) on the HRP-stained image of the

NMJ and the intensities were measured. These ROIs are then used to measure the intensities of the same areas (boutons) on the marker-of-interest's image. The maximum intensities of the makers were taken and normalised against the HRP values. The obtained ratios were statistically analysed using Microsoft excel and Graphpad prism.

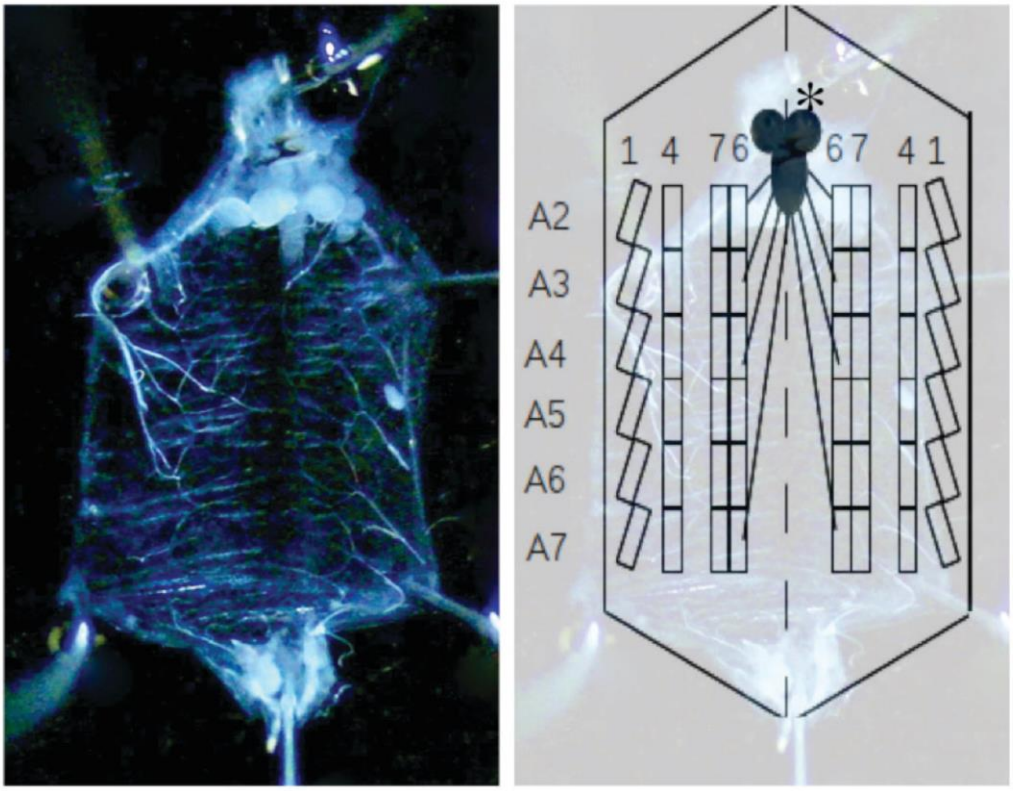

Figure 28 Location of the muscles 6 and 7 in the abdominal segments of a dissected larva. Adapted from ICGEB Drosophila course 2018 manual.

3.5 FM1-43 labelling of synaptic vesicle trafficking

(N-(3triethylammoniumpropyl)4(4(dibutylamino)styryl)pyridinium dibromide) FM1-43 is a styryl dye that is used to visualize the localization and recycling of the vesicles at synapses (Verstreken *et al.,* 2008). This protocol was for live imaging and all solutions were prepared and used fresh (Table 4).

Table 4 Recipe for the preparation of HL3 solutions

HL3 for Dissection	HL3 for FM1-43
110Mm NaCl	25Mm NaCl
5mM KCl	90mM KCl
10mM $NaHCo_3$	10mM $NaHCo_3$
5mM Hepes	5mM Hepes
35mM Sucrose or 30mM sucrose+ 5mM Threalose	35mM Sucrose or 30mM sucrose+ 5mM Threalose
10mM $MgCl_2$	10mM $MgCl_2$
	0.5M $CaCl_2$
Bring PH to 7.2	Bring PH to 7.2

Each larva was quickly dissected in HL3 as previously described ensuring that the motor neurons emerging from the ventral cord were cut. Incubation for primary stimulation was done at room temperature in the

dark using the stimulation solution (1ml HL3 for FM1-43, 1µl FM1-43 from a 4mM stock, and 3µl $CaCl_2$ from a 0.5M stock) for 1minute. Larva was then washed 5times in HL3 for dissection for 1 minute each to remove the excess dye that was not incorporated. At the 3rd wash, HRP conjugated (1: 150) was diluted in the HL3 to highlight the synaptic boutons. Incubation time was 3minutes. At the end of the fifth wash, a generous amount of HL3 was added to the larva in the sylgard plate and we proceeded to the Nikon microscope for live imaging of the synaptic boutons at X40 and X63. Again, only the NMJs between muscle 6 and 7 in the second and third abdominal segments were considered. This whole process was termed “Loading” and it corresponds to endocytosis. After the acquisitions of the “loading” images, the larva was drained and again stimulated in the dark at room temperature using the stimulation solution (without FM1-43) for 10minutes. It was then washed 5 times for 1 minute each. This process corresponds to exocytosis and was termed “Unloading”. Live images of the unloaded boutons were taken immediately after the fifth wash in excess HL3. Care was taken to image the same NMJs that were “loaded” using exactly the same settings of the microscope. All the images were processed using imagej software and the maximum intensity of the FM1-43 dye in both loading and unloading were recorded for each bouton. Graphpad prism and Microsoft excel were

used for statistical analysis of the generated values. 10-15 larvae per genotype involved were tested and imaged.

3.6 Isogenization of TBPH stocks to generate clean TBPH null flies

Since creating the TBPH mutant flies by Feiguin *et al.,* 2009, the flies have been in constant use in the laboratory and may have acquired some mutations or other modifications in their genome to aid survival. Thus, the need to isogenize the stocks arose as we intend to have the flies on the same genetic background. Also, to ensure that the *tbph* deletion is the only mutation present in the TBPH mutant flies. The process which involved back-crossing of the male heterozygous flies with virgins of the genotype of their mothers (in this case, was a balancer, Lpin/CyoGFP) is depicted in Figure 29. The back-crosses were done 8times and at the end, genomic DNA extraction confirmed the deletion of *tbph* in both mutants. So, only one of the resultant new stocks was expanded as four identical experiments for each genotype were set. The stocks were expanded (one each for Δ23, Δ142 and w1118) and the protocol below to collect clean mutant flies (Δ23/Δ23 and Δ142/Δ142) for sequencing was performed.

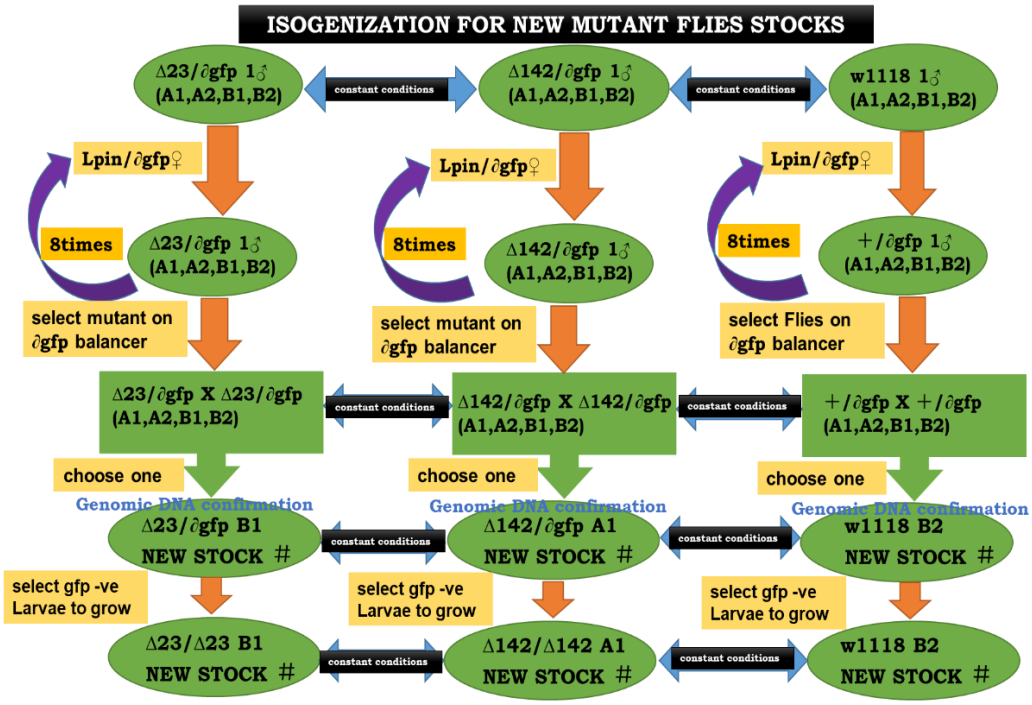

Figure 29 Schematics showing steps involved in the preparation of clean TBPH mutant flies.

The collection plates garnished with a drop of yeast paste were prepared fresh using the egg media (Table 5) and each genotype (Δ23/CyoGFP, Δ142/CyoGFP and w1118) had a plate correctly labelled fixed to a collection cage containing the corresponding flies for mating (70 females and 30 males). The plates filled with embryos were collected after every 12hours and kept in the incubator at 25°C. After 72hours, the GFP-negative larvae for each genotype were selected and placed into vials of fly food correctly labelled. The vials containing maximum of 25larvae each were incubated at 25°C and allowed to complete metamorphosis into adult flies. The heads of these flies were collected and stored in RNAlater solution.

Table 5 Constituents of the Fly egg food-media and the required quantity

***Drosophila* egg media**
400ml distilled water
57.6ml apple juice
14.08g agarose Stirred well
Autoclaved for 1hour in the kitchen Left to cool and stirred
3.2ml propionic acid and 80 nipargin were added
Aliquoted into 6cm collection plates.

3.7 Statistical analysis

This was done using Microsoft excel and Graphpad prism v5.1. One-way ANOVA with Bonferroni's post-hoc, Krushka Wallis with Dunn's post-hoc, T-test with Mann-Whitney and Wilcoxon corrections were applied as statistical tests as required. Values are expressed as mean and standard error of mean (SEM) in all figures. $P<0.05$ was taken to be statistically significant.

4.0 RESULTS

4.1 The level of Futsch was reduced at the NMJ in TBPH mutant flies

As published in the reports of Godena *et al.,* 2011, the level of Futsch is reduced in TBPH mutant flies as we observe at the beginning of this thesis work. Our observations reported in Figure 30 shows a significant reduction of Futsch staining in TBPH mutants when compared with all other genotypes. In addition, it was evident that Futsch reached the terminal boutons in all the genotypes depicted except in the case of TBPH null mutant. There was also a significant difference in the levels of Futsch in the Futsch rescue group compared with the control that was wildtype for TBPH, where Futsch level was significantly lower than in the rescue group. This confirms the efficiency of the Elav-gal4 driver used.

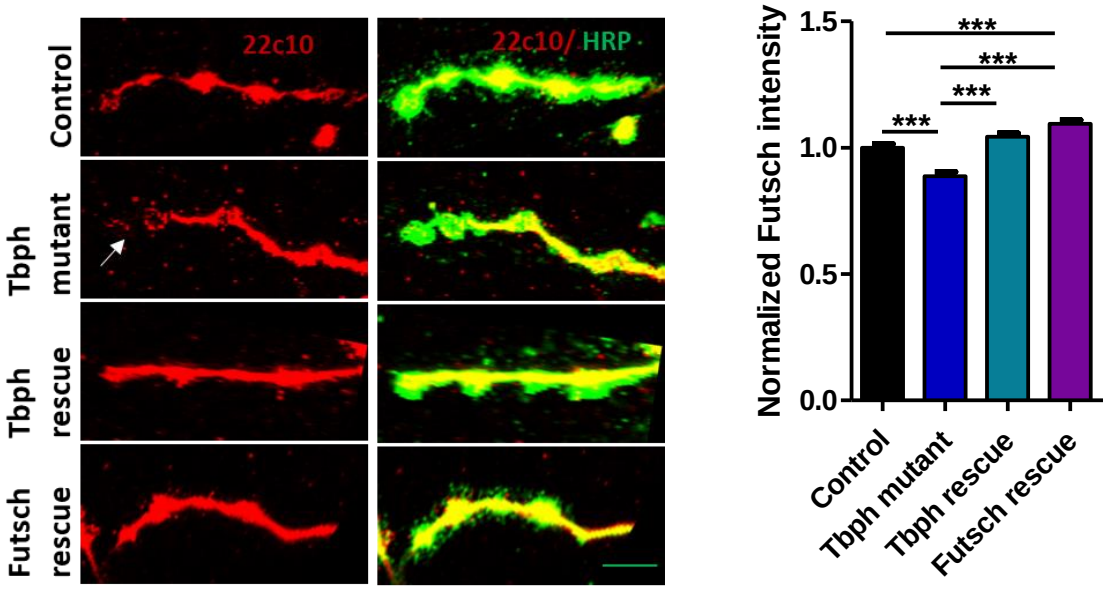

Figure 30 Futsch was reduced at the NMJ of TBPH mutant flies. Confocal images showing the NMJs between muscles 6 and 7 double-labelled with anti- HRP (in green) and anti Futsch (in red). Note the Futsch staining at the terminal boutons in all the groups except the *tbph* mutant where it is absent (white arrow). Graph shows the quantification of Futsch intensity in the boutons normalized on HRP. Genotypes: Elav-gal4/+ (Control), tbphΔ23elav-gal4/tbphΔ23; UAS-gfp-mcd8/+ (tbph mutant), tbphΔ23elav-gal4/UAS-tbphΔ23 (tbph rescue) and UAS-Ep10751; tbphΔ23elav-gal4/tbphΔ23 (Futsch rescue) N=25 per genotype. Scale bar is 20µm. Error bars are SEM. ***p<0.0001 as calculated using ANOVA with Bonferroni's correction.

4.2 Silencing TBPH in neurons produced similar phenotypes to *TBPH* mutant flies with respect to Futsch.

Having observed a reduced level of Futsch at the NMJ of TBPH mutant flies, we decided to check if silencing of TBPH in neurons rather than complete absence is sufficient to exert the same effect on the Futsch protein level at the NMJ. Therefore, we silenced TBPH in neurons using RNAi against TBPH while RNAi against GFP was used as a control. Both larva motility and the structure of their NMJs were analysed.

4.2.1 Larva motility was impaired when TBPH was silenced in neurons

As shown in Figure 31, a motility defect was observed upon TBPH silencing in neurons similar to null TBPH mutants. The larval movement was significantly slower than the control where TBPH was at a wildtype level. The movement reduction observed was approximately 50% of the control.

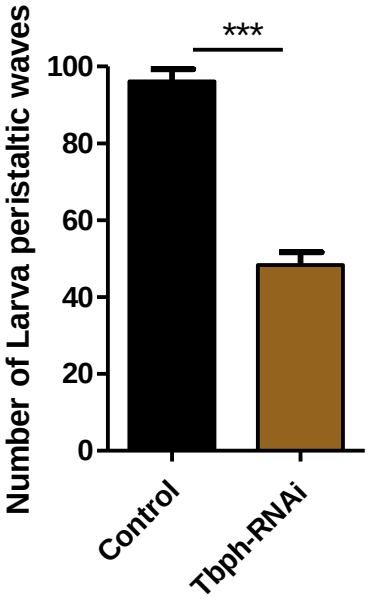

Figure 31 Motility of larva was impaired when TBPH was silenced in neurons. Larva peristaltic movements were observed and recorded in 120s for each larva. Genotypes: Dicer(X); Elav-gal4/+; UAS-SiRNA-gfp/+ (Control) and Dicer(X); Elav-gal4/+; UAS-Tbph-RNAi/+ (Tpbh-RNAi). N=30 per genotype. Error bars are SEM. ***p<0.0001 as calculated using t-test.

4.2.2 The number of branches and boutons of the NMJ were reduced following TBPH silencing in neurons

The NMJ was further characterised by evaluating possible alterations in the number of branches and boutons. Figure 32 shows a reduction in the

number of branches of the NMJ from 100% to 70% and the number of boutons to 68%. The shape of the boutons was also negatively affected (Figure 33). There was almost a double increase in the percentage of irregular boutons (about 56%) when TBPH was silenced in neurons as compared to the control that had 32% irregular boutons.

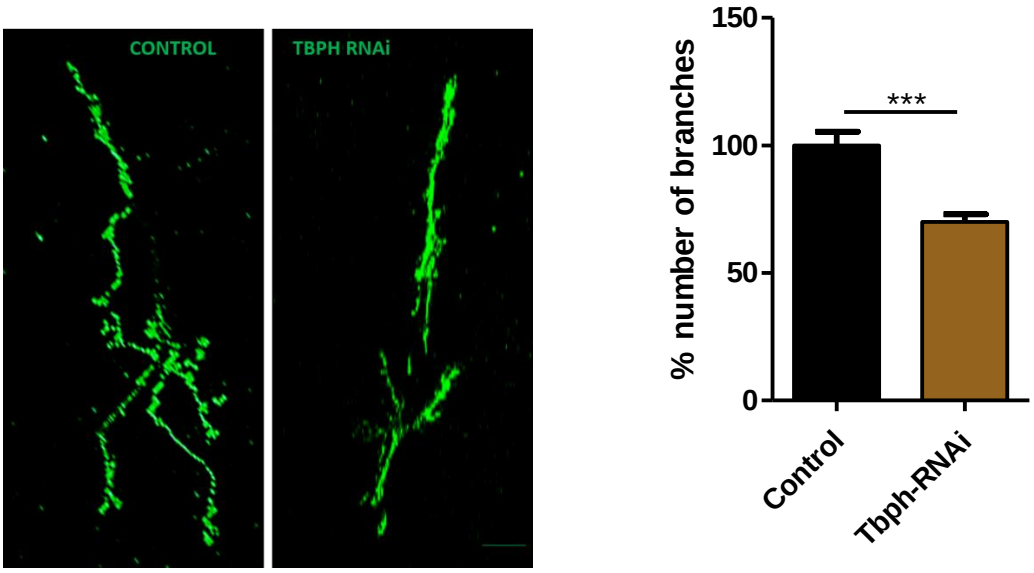

Figure 32 The number of branches was reduced at the NMJ when TBPH was silenced in neurons. Panel shows representative confocal images of the NMJs between muscles 6 and 7 stained with anti-HRP. Graph shows the quantification of the branches. Genotypes: Dicer(X); Elav-gal4/+; UAS-SiRNA-gfp/+ (Control) and Dicer(X); Elav-gal4/+; UAS-Tbph-RNAi/+ (Tpbh-RNAi). Scale bar is 10µm. N= 25 per genotype. Error bars are SEM. **p<0.001 as calculated using t-test.

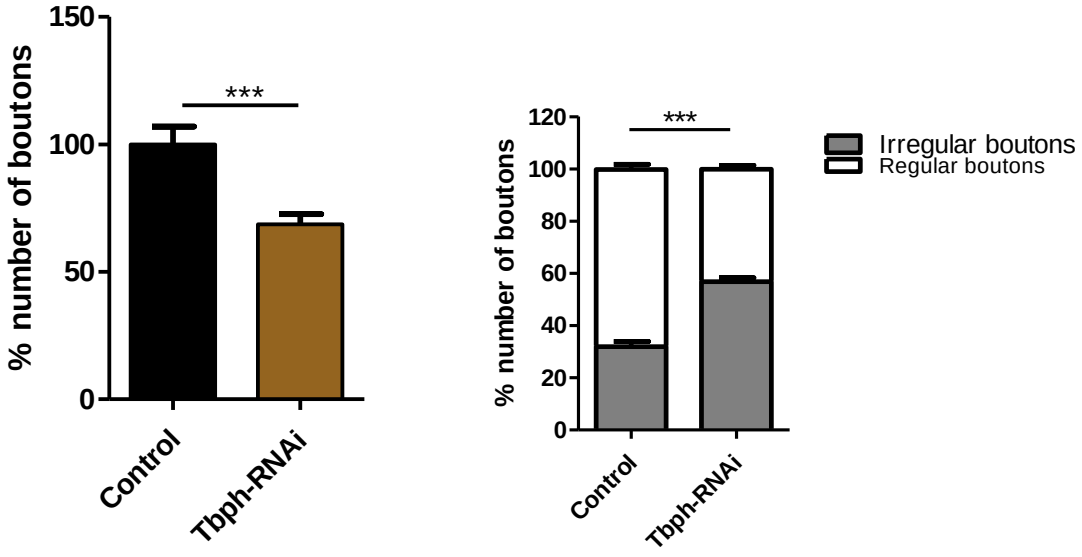

Figure 33 The number and shape of boutons were affected when TBPH was silenced in neurons. Left graph shows the number of boutons per NMJ and the right graph shows the quantification of the shape of the boutons into regular and irregular all of which were negatively impacted and statistically significant. Genotypes: Dicer(X); Elav-gal4/+; UAS-SiRNA-gfp/+ (Control) and Dicer(X); Elav-gal4/+; UAS-Tbph-RNAi/+ (Tpbh-RNAi). N= 25 per genotype. Error bars are SEM. ***p<0.001 as calculated using t-test.

4.2.3 The level of Futsch at the NMJ was reduced when TBPH was silenced in neurons

Having observed a motility defect upon TBPH silencing similar to TBPH deficiency, we proceeded to larva dissection and NMJ staining for Futsch. As depicted in Figure 34, a significant reduction in the level of Futsch was detected for TBPH silencing. Futsch level dropped from 1.0 to about 0.84. Noteworthy is the distribution of Futsch that was absent at the terminal boutons when TBPH was silenced also similar to what is observed in the TBPH mutant flies.

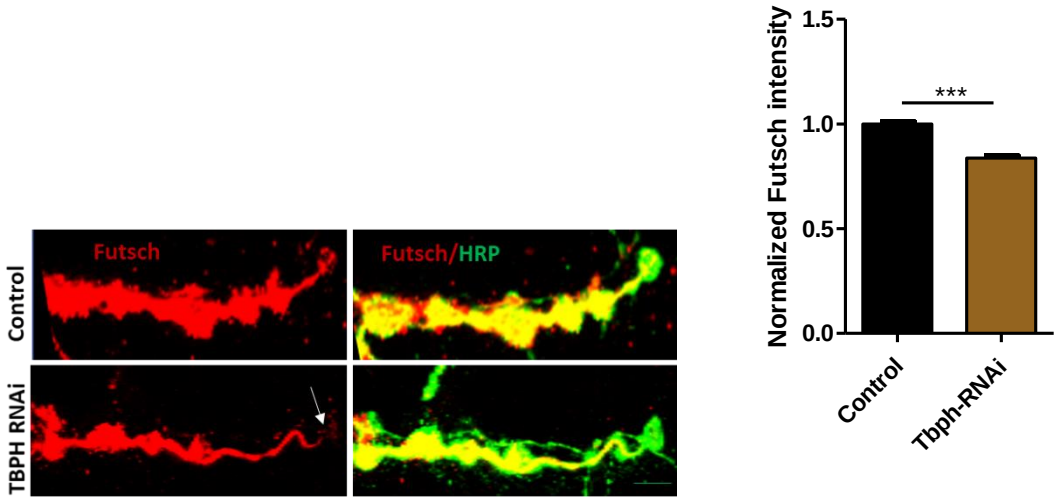

Figure 34 The level of Futsch was reduced at the NMJ when TBPH was silenced in neurons. Panel shows representative confocal images of the NMJs between muscles 6 and 7 double-labelled with anti- HRP (in green) and anti Futsch (in red). Note the futsch staining at the terminal bouton present in the control and absent when tbph was silenced (white arrow). Genotypes: Dicer(X); Elav-gal4/+; UAS-SiRNA-gfp/+ (Control) and Dicer(X); Elav-gal4/+; UAS-Tbph-RNAi/+ (Tpbh-RNAi). Graph shows quantification of Futsch intensity in the boutons normalized on HRP. N= 30 per genotype. Scale bar is 20µm. Error bars are SEM. ***p<0.0001 as calculated using t-test.

4.3 Larva motility was significantly improved with expression of Futsch in TBPH mutant flies.

Having observed that the silencing of TBPH exclusively in the neurons is sufficient to exert a detrimental effect on Futsch at the NMJ, we decided to increase Futsch level by expressing it in the neurons of TBPH mutant flies by means of several drivers (Figure 35 and Figure 36) and performing crawling assay of third instar larvae to verify if Futsch expression might recover the TBPH null motility phenotype. Several drivers were tested in order to find the one with the optimal recovery potency.

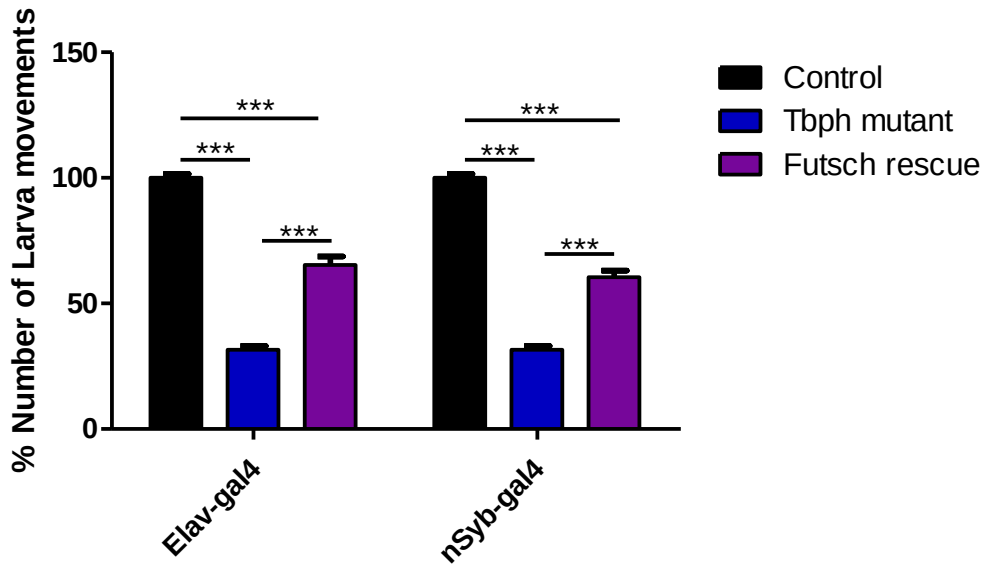

Figure 35 Overexpression of Futsch with pan-neuronal drivers in TBPH mutant flies recovers larva motility defect. This was done using the pan-neuronal drivers Elav-gal4 and nSyb-gal4. A partial recovery of the motility defect was observed when compared with the control in 120seconds. Genotypes: Elav-gal4/+ (Control), tbphΔ23elav-gal4/tbphΔ23; UAS GFP-mCD8/+ (Tpbh mutant) and is EP10751; tbphΔ23elav-gal4/tbphΔ23 (Futsch rescue) nSyb-gal4/+ (Control) tbphΔ23nSyb-gal4/tbphΔ23; UAS GFP-mCD8/+ (Tpbh mutant) and EP10751; tbphΔ23nSyb-gal4/tbphΔ23 (Futsch rescue) Error bars are SEM. N= 30 per genotype. ***p<0.0001 as calculated using ANOVA with Bonferroni's correction.

Both of the pan neuronal drivers Elav-gal4 and nSyb-gal4 used for Futsch expression produced a significant rescue of the motility defects seen in TBPH mutant flies (65% and 60% respectively, Figure 35). The motor-neuron specific drivers Ok6-gal4 and D42-gal4 were also used and they resulted in a lesser rescue of motility defect that was also significant (48% and 45% respectively, Figure 36). In conclusion, the pan neuronal drivers performed better than the motor-neuron specific drivers. Since Elav-gal4 was the driver with the best rescue, we selected it as the driver of choice for subsequent experiments (Figure 35 left graph).

Nevertheless, it is imperative to note that all the drivers produced a significant recovery of the motility defect of TBPH mutant flies when expressing Futsch rather than GFP. So, we can postulate that Futsch has a positive impact on larva motility when expressed even in a subset of motor neurons.

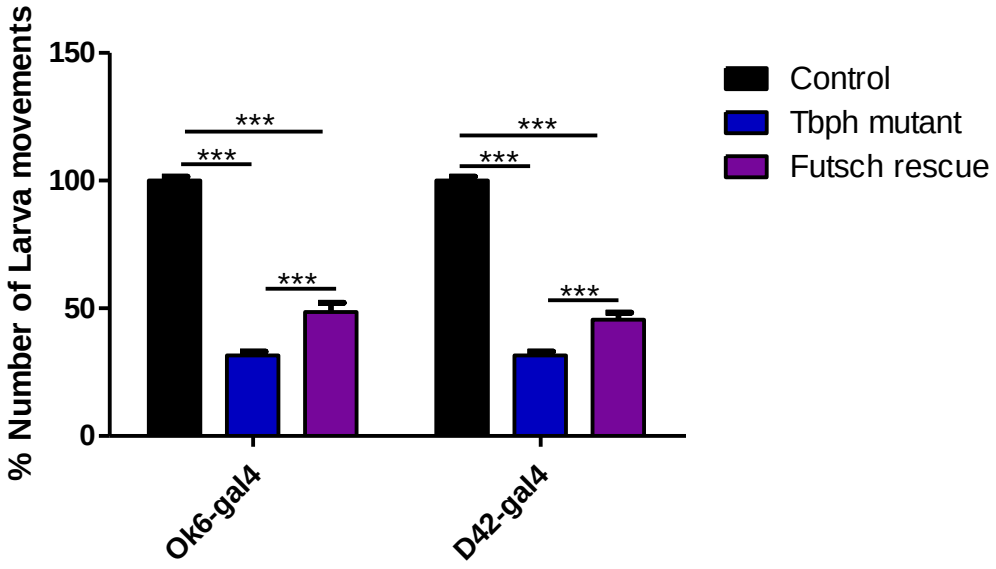

Figure 36 Overexpression of Futsch with motor-neuron specific drivers in TBPH mutant flies recovers larva motility defect. This was done using the motor neuron specific drivers ok6-gal4 and D42-gal4. A partial recovery of the motility defect was observed when compared with the control in 120seconds. Genotypes: OK6-gal4/+ (Control), tbphΔ23OK6-gal4/tbphΔ23; UAS GFP-mCD8/+ (Tpbh mutant) and EP10751; tbphΔ23OK6-gal4/tbphΔ23 (Futsch rescue). D42-gal4/+ (Control), tbphΔ23D42-gal4/tbphΔ23; UAS GFP-mCD8/+ (Tpbh mutant) and EP10751; tbphΔ23D42-gal4/tbphΔ23 (futsch rescue). Error bars are SEM. N= 30 per genotype. ***$p<0.0001$ as calculated using ANOVA with Bonferroni's corrections.

The control flies that were wildtype for TBPH, performed significantly better at 100% (across all the drivers) than the Futsch recovery group which was not surprising as only the expression of TBPH is expected to produce a full recovery. However, the statistical significant difference

between the performances of the mutants and the Futsch rescue group was sufficient to report a rescue.

4.5 The structural integrity of the NMJ was recovered in TBPH mutant flies expressing Futsch in their neurons

Following the promising results obtained with the third instar larva peristaltic movements of TBPH mutant flies expressing Futsch, we proceeded to dissection in order to check their NMJs. As expected, there was significant rescue of the anatomy of the NMJ in the mutants when they expressed Futsch as compared to controls (Figure 37). Both the shape and number of boutons were rescued as observed from the quantification of the NMJs (Figure 38).

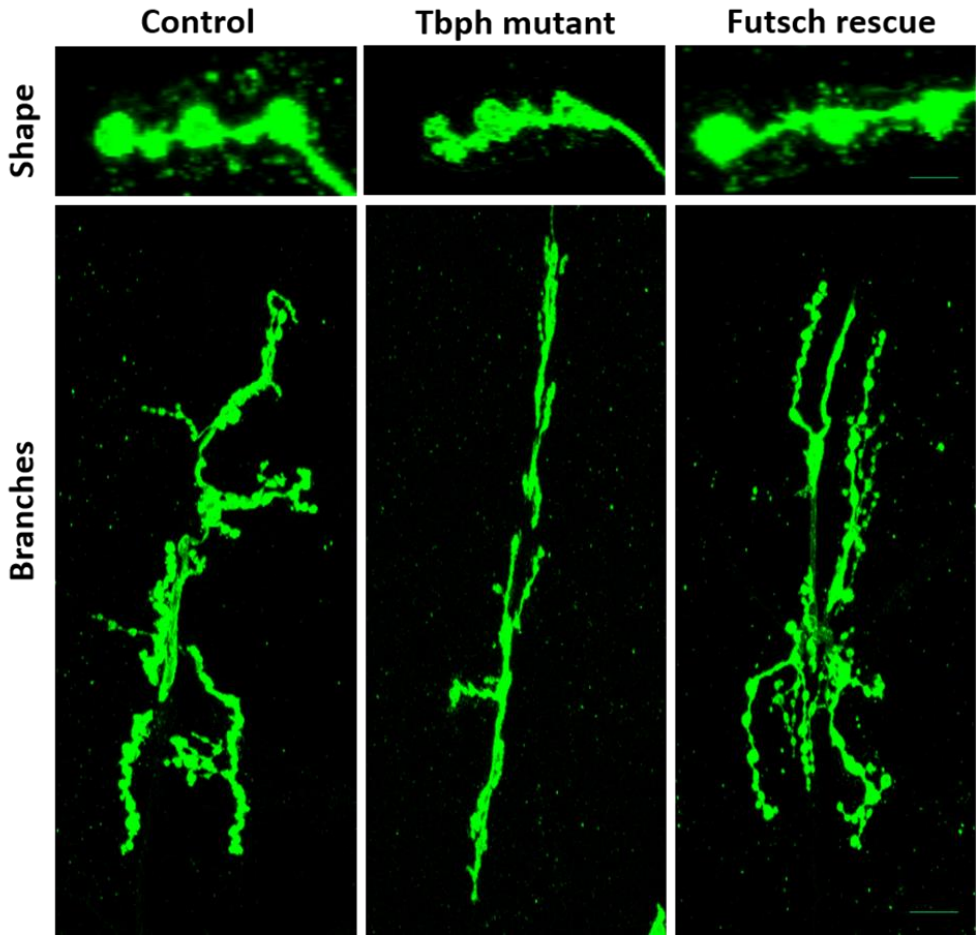

Figure 37 The Anatomy of the NMJ was recovered in TBPH mutant flies expressing Futsch. The representative confocal images showing the NMJs between muscles 6 and 7 labelled with HRP. Top panel shows the recovery of shape. Note the round shape of the terminal boutons in the control and Futsch rescue groups which is absent in the mutant. Bottom panel shows the full NMJs. The recovery of the branching and whole junction integrity is apparent. Genotypes: Elav-gal4/+ (Control), tbphΔ23elav-gal4/tbphΔ23; UAS GFP-mCD8/+ (Tpbh mutant) and EP10751; tbphΔ23elav-gal4/tbphΔ23 (Futsch rescue). Scale bar is 20µm. N= 30 per genotype.

Feiguin *et al.,* 2009 reported mis-shaped boutons as a characteristic of TBPH mutant flies. We observed this feature (Figure 37 top panel) and in fact, TBPH mutant flies expressing GFP had the highest number of irregular (mis-shaped) boutons (about 85% on average) when compared with Futsch expressing larvae (about 62%) and the control flies that were wildtype for TBPH (about 29%). Reduced number of branches and

boutons were also reported as features of TBPH mutant flies. Both features were significantly rescued by Futsch expression in TBPH mutant flies. From 68% to 96% for branches and 63% to 95% for the bouton number (Figure 38). It is worthy to note that there was no statistical significance between the control flies that were wildtype for TBPH at 100% and the TBPH mutant flies expressing Futsch at 96% and 95% respectively for the branches and bouton number. This implies a more than partial recovery of the branches and boutons, an indication of growth of the NMJ.

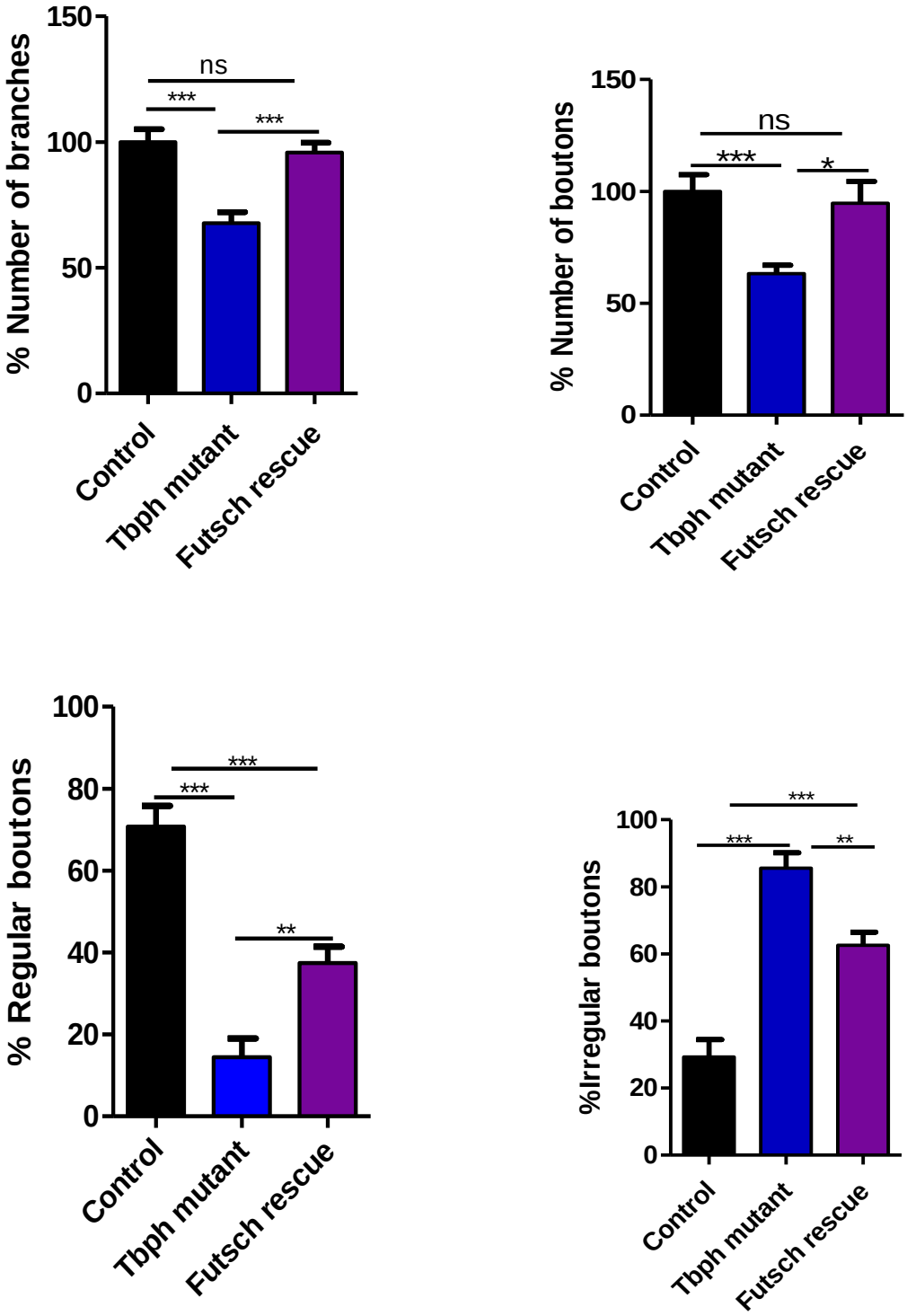

Figure 38 The number of branches and boutons of the NMJ were recovered in TBPH mutant flies expressing Futsch. Top panel graphs show the normalized quantification of the Bouton numbers and Branches both of which were recovered by Futsch. Bottom panel graphs show the quantification of the boutons with respect to shape as regular and irregular. The mutants had the lowest number of regular bouton which were partly recovered by the expression of Futsch. Genotypes: Elav-gal4/+ (Control), tbphΔ23elav-gal4/tbphΔ23; UAS GFP-mCD8/+ (Tpbh mutant) and EP10751; tbphΔ23elav-gal4/tbphΔ23 (Futsch rescue). Error bars are SEM. N= 30 per genotype. *p<0.01 **p<0.001 ***p<0.0001, ns not significant as calculated using ANOVA with Bonferroni's corrections.

4.6 Larva motility was not improved in TBPH mutant flies expressing Tau

We decided to check if the results obtained with Futsch with respect to rescue of motility will be similar to that of Tau by virtue of both proteins being microtubule associated proteins in the same “Classical” group. So, we expressed Tau in the neurons of TBPH mutant flies and performed a crawling assay of the third instar larvae. The graph in Figure 39 reports the observation made from this experiment. There was no difference between the TBPH mutant flies and those that expressed Tau. So, there was no recovery of the motility. Interestingly, when the larvae were dissected and the NMJs checked, there was a good recovery of the anatomy of the NMJ in TBPH mutant flies expressing Tau (Figure 39 micrograph). We can then say that we have an anatomical rescue similar to that observed when the flies expressed Futsch but the rescue was not functional because the larvae still retained their motility defects in contrast to the rescue observed with Futsch. This reiterate the fact that the rescue obtained with the expression of Futsch is not only associated to its function as a microtubule associated protein but also probably because it is involved in a unique mechanism devoid of Tau’s action.

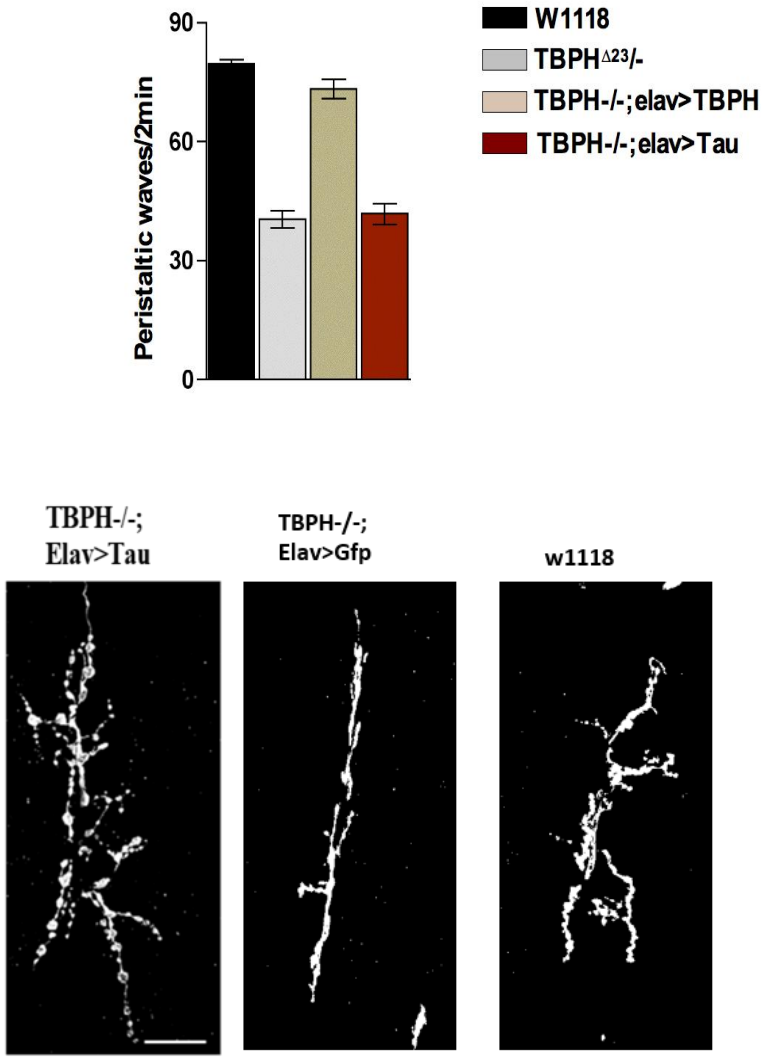

Figure 39 Overexpression of Tau in the neurons of TBPH mutant flies did not recover motility defect in Larvae. This was done using 3rd instar larvae motility assay and no recovery of motility was observed when compared with the control (w1118) in 120seconds as seen in the graph. Micrographs show representative images from the NMJ between muscles 6 and 7 labelled with with anti-HRP. Recovery of the anatomy of the junction with respect to branches and boutons is apparent. Error bars are SEM. N= 30 per genotype. (Courtesy in conjunction with Giulia Romano).

4.7 Futsch recovers the levels of some pre-synaptic vesicular proteins at the NMJ in TBPH mutant flies

Having observed both anatomical and functional recoveries of the NMJs with Futsch expression in TBPH mutant flies, we proceeded to check some pre-synaptic proteins using immunohistochemistry. These proteins

were reported by Romano *et al.,* 2014 to be downregulated in TBPH mutant flies and they include synapsin, syntaxin, CSP and acetylated tubulin (Godena *et al.,* 2011). All of which were recovered in TBPH mutant flies expressing Futsch in varying degrees.

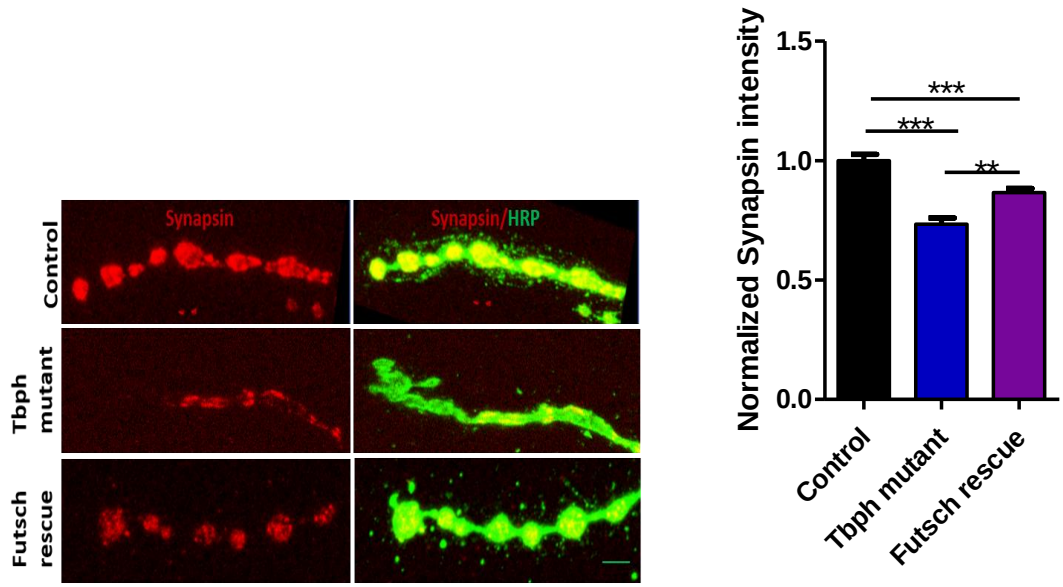

Figure 40 The level of synapsin was rescued in TBPH mutant flies expressing Futsch. Panels are representative confocal images showing the NMJs between muscles 6 and 7 double-labelled with anti-HRP (in green) and anti-synapsin (in red). Note the intensity of the synapsin staining. Graph shows quantification of synapsin intensity in the boutons normalized on HRP. Genotypes: Elav-gal4/+ (Control), tbphΔ23elav-gal4/tbphΔ23; UAS GFP-mCD8/+ (Tpbh mutant) and EP10751; tbphΔ23elav-gal4/tbphΔ23 (Futsch rescue). Scale bar is 20µm. N=30 per genotype. Error bars are SEM. ***p<0.0001 **p<0.001 as calculated using ANOVA with Bonferroni's correction.

Figure 40 shows the observation made when the NMJs were stained for synapsin. There was a significant rescue of synapsin levels when the flies expressed Futsch (about 0.87) compared to when they expressed GFP (about 0.73). The control flies that were wildtype for TBPH were 1.00 and were significantly greater than both previous groups.

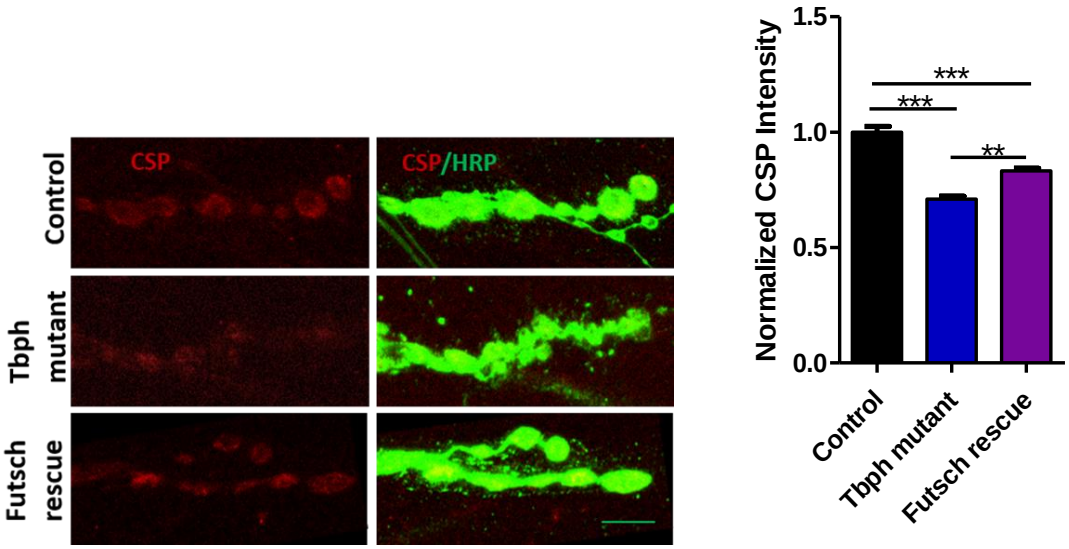

Figure 41 The level of Csp was rescued in TBPH mutant flies expressing Futsch. Panels are representative confocal images showing the NMJs between muscles 6 and 7 double-labelled with anti-HRP (in green) and anti-Csp (in red). Note the intensity of the Csp staining. Graph shows quantification of Csp intensity in the boutons normalized on HRP. Genotypes: Elav-gal4/+ (Control), tbphΔ23elav-gal4/tbphΔ23; UAS GFP-mCD8/+ (Tpbh mutant) and EP10751; tbphΔ23elav-gal4/tbphΔ23 (Futsch rescue). Scale bar is 20µm. N=25 per genotype. Error bars are SEM. ***p<0.0001 **p<0.001. as calculated using ANOVA with Bonferroni's correction.

The level of Csp was also rescued when Futsch was expressed in TBPH mutant flies (about 0.83) compared to when they expressed GFP (about 0.71). The control flies that were wildtype for TBPH at 1.00 were significantly greater than both previous groups (Figure 41).

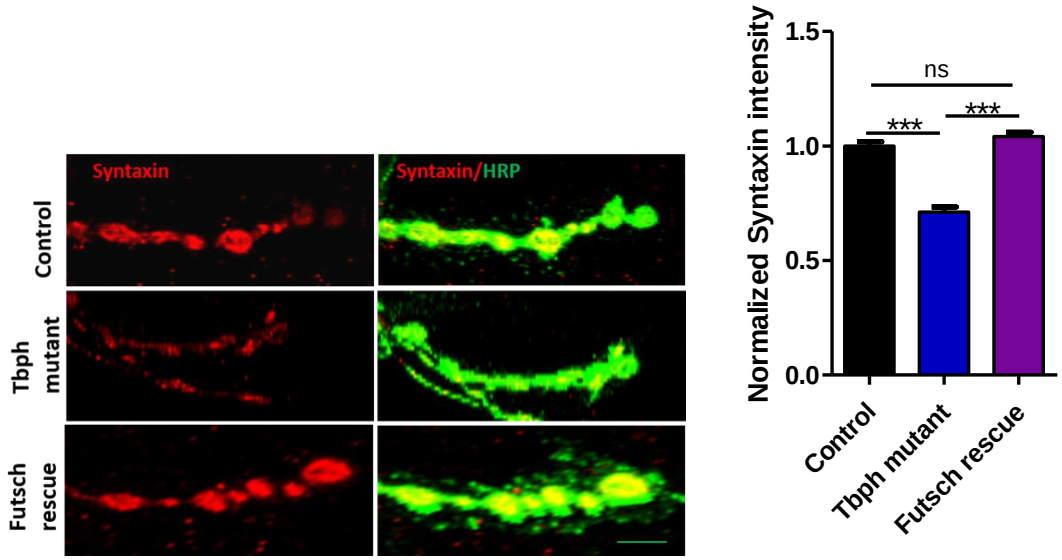

Figure 42 The level of syntaxin was rescued in TBPH mutant flies expressing Futsch. Panels are representative confocal images showing the NMJs between muscles 6 and 7 double-labelled with anti-HRP (in green) and anti-syntaxin (in red). Note the intensity of the syntaxin staining. Graph shows quantification of syntaxin intensity in the boutons normalized on HRP. Genotypes: Elav-gal4/+ (Control), tbphΔ23elav-gal4/tbphΔ23; UAS GFP-mCD8/+ (Tpbh mutant) and EP10751; tbphΔ23elav-gal4/tbphΔ23 (Futsch rescue). Scale bar is 20µm. N= 25 per genotype. Error bars are SEM. ***p<0.0001 ns= not significant as calculated using ANOVA with Bonferroni's correction.

There was a complete recovery of syntaxin when TBPH mutant flies expressed Futsch because there was no significant difference between the Futsch rescue group (about 1.04) and the control flies that were wildtype for TBPH (about 1.00). Both groups were expressing significantly greater than TBPH mutant flies expressing GFP at about 0.71 (Figure 42).

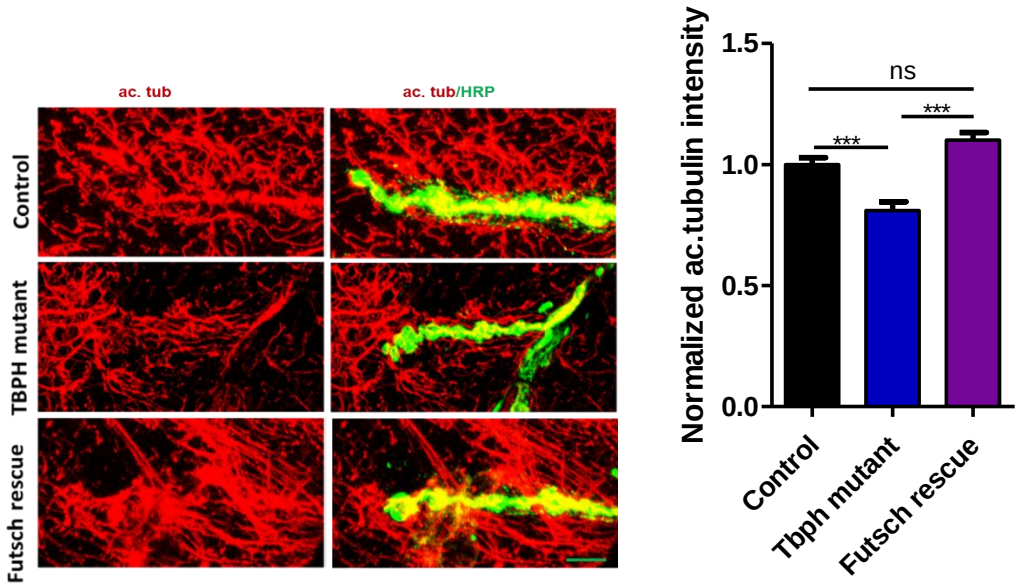

Figure 43 The level of acetylated tubulin was rescued in TBPH mutant flies expressing Futsch. Panels are representative confocal images showing the NMJs between muscles 6 and 7 double-labelled with anti-HRP (in green) and anti-acetylated tubulin (in red). Note the intensity of the acetylated tubulin staining. Graph shows quantification of acetylated tubulin intensity in the boutons normalized on HRP. Genotypes: Elav-gal4/+ (Control), tbphΔ23elav-gal4/tbphΔ23; UAS GFP-mCD8/+ (Tpbh mutant) and EP10751; tbphΔ23elav-gal4/tbphΔ23 (Futsch rescue). Scale bar is 20µm. N= 30 per genotype. Error bars are SEM. ***p<0.0001 ns= not significant as calculated using ANOVA with Bonferroni's correction.

In Figure 43, we report the observations made when NMJs were stained for acetylated tubulin. There was a complete recovery of acetylated tubulin when TBPH mutant flies expressed Futsch (about 1.10) because there was no statistical significance when compared with the control flies that were wildtype for TBPH (at 1.00). TBPH mutant flies expressing GFP was about 0.81 and was significantly lesser than the other two groups.

4.8 Futsch recovers the levels of some post-synaptic proteins at the NMJ of TBPH mutant flies

The levels of Dlg and glutamate receptors IIA (GluRIIA) were checked given the positive observations made with the pre-synaptic proteins. Both protein levels were recovered with Futsch expression in TBPH mutant flies.

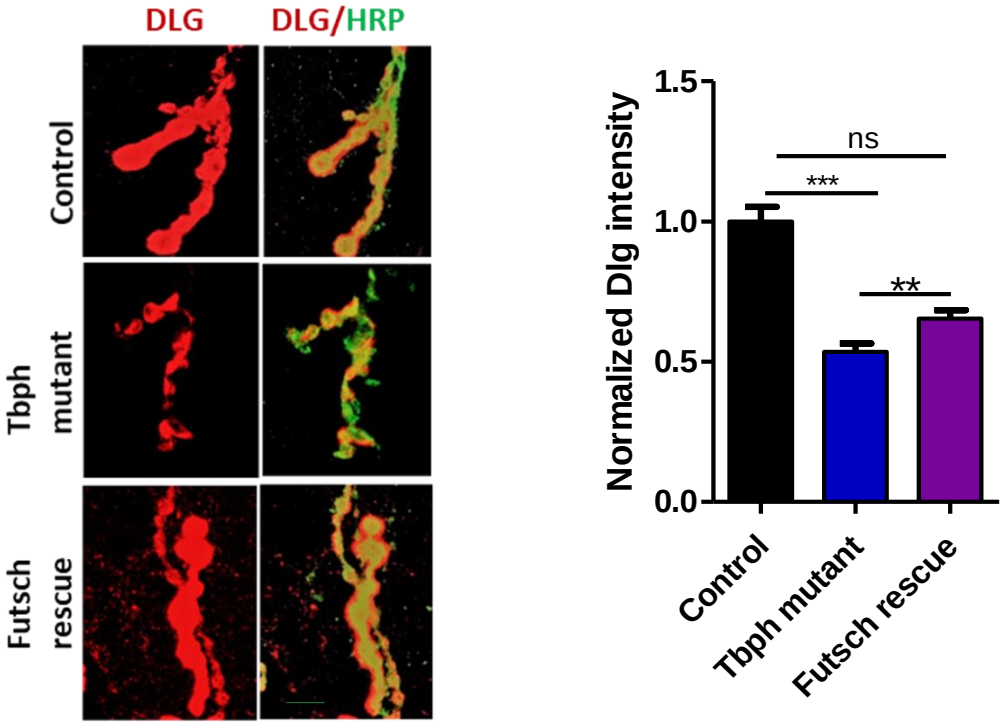

Figure 44 The level of Dlg was rescued in TBPH mutant flies expressing Futsch. Panels are representative confocal images showing the NMJs between muscles 6 and 7 double-labelled with anti-HRP (in green) and anti-dlg (in red). Note the intensity of dlg staining. Graph shows quantification of dlg intensity in the boutons normalized on HRP. Genotypes: Elav-gal4/+ (Control), tbphΔ23elav-gal4/tbphΔ23; UAS GFP-mCD8/+ (Tpbh mutant) and EP10751; tbphΔ23elav-gal4/tbphΔ23 (Futsch rescue). Scale bar is 20µm. N= 30 per genotype. Error bars are SEM. ***p<0.0001 **p<0.001 ns= not significant as calculated using ANOVA with Bonferroni's correction.

Dlg level was significantly recovered in TBPH mutant flies expressing Futsch (about 0.65) compared to when they expressed GFP (about 0.54).

The control flies that were wildtype for TBPH was 1.00 and was greater than both previous groups (Figure 44).

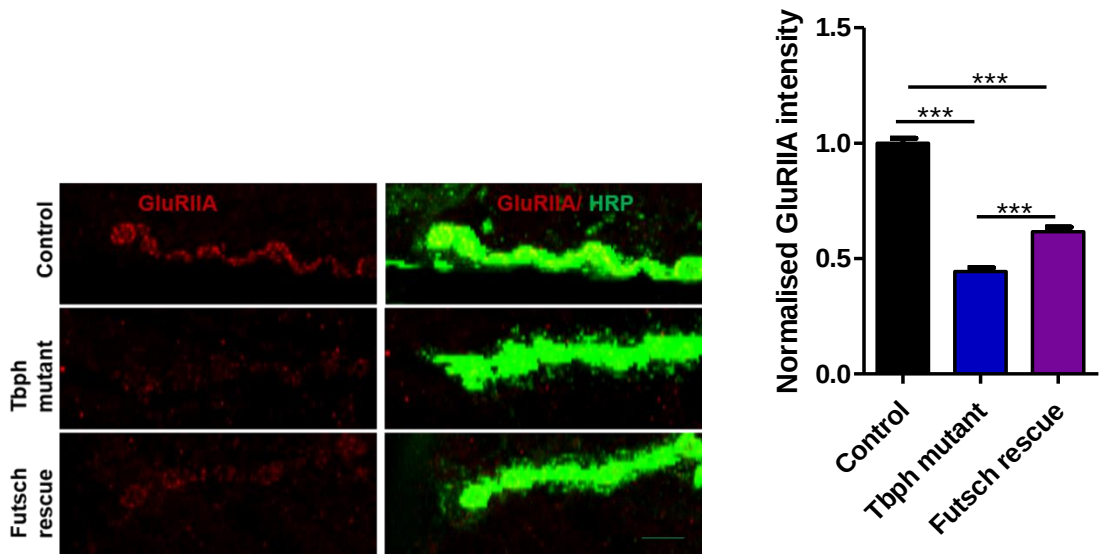

Figure 45 The level of glutamate receptors IIA was rescued in TBPH mutant flies expressing futsch. Panels are representative confocal images showing the NMJs between muscles 6 and 7 double-labelled with anti-HRP (in green) and anti-GluRIIA (in red). Note the intensity of GluRIIA staining. Graph shows quantification of GluRIIA intensity in the boutons normalized on HRP. Genotypes: Elav-gal4/+ (Control), tbphΔ23elav-gal4/tbphΔ23; UAS-GFP-mCD8/+ (Tpbh mutant) and EP10751; tbphΔ23elav-gal4/tbphΔ23 (Futsch rescue). Scale bar is 20µm. N=25 per genotype. Error bars are SEM. ***p<0.0001 as calculated using ANOVA with Bonferroni's correction.

Figure 45 shows a significant rescue of GluRIIA when TBPH mutant flies expressed Futsch (0.62) compared to when they expressed GFP (about 0.44). The control in wildtype condition for TBPH was significantly better than both groups at 1.00.

4.9 More mitochondria were localized at the NMJ in TBPH mutants.

In order to attempt to document axonal transport indirectly, we checked the localization of mitochondria at the NMJ by IHC using the mean

intensity of mito-GFP (a mitochondria import signal fused with GFP) staining. Mitochondria are perfect cargoes that must be transported from the soma to the NMJs where they are required to power synaptic processes that are highly energy intensive. In addition, defective mitochondria must find their way back to the soma for proper degradation. So, mitochondria are thought to be a good read-out of axonal transport. TBPH mutants have a significantly higher intensity of mito-GFP than the control that is wildtype for TBPH (Figure 46) averaging 1.14 and 1.00 respectively.

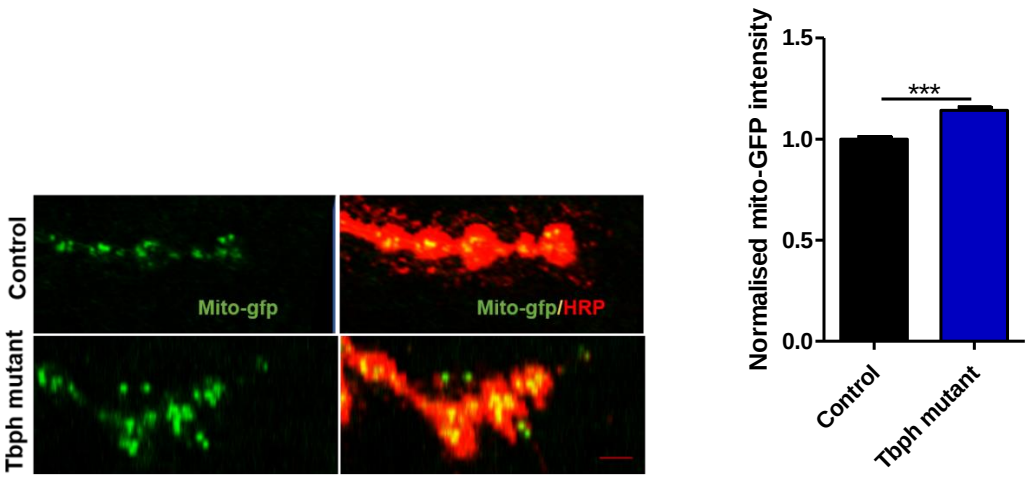

Figure 46 More mitochondria were present at the NMJ in TBPH mutant flies. Panel shows representative confocal images of the NMJ between muscles 6 and 7 double-labelled with HRP (in red) and mito-gfp (in green). The graph shows quantification of the mito-GFP intensity in the boutons and the mutants have a significant higher mean intensity than the control. Genotypes: Elav-gal4/+; UAS mito-GFP/+ (Control) and tbphΔ23elav-gal4/tbphΔ23; UAS mito-GFP/+ (Tbph mutant). Scale bar is 20µm. N= 25 per genotype. Error bars are SEM. ***p<0.0001 as calculated using t-test.

Also, the expression of mito-GFP did not alter the typical TBPH mutant locomotion defects as reported in the crawling assay (Figure 47). The control with wildtype condition for TBPH moved twice as fast as the mutant

with about 100 movements in 120s as compared to the mutants that had 43 movements in the same time frame.

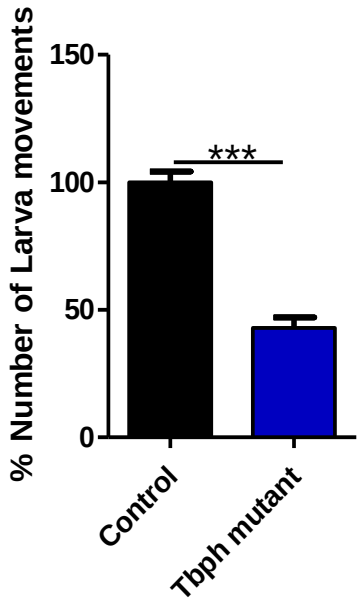

Figure 47 Motility of Larva was impaired in TBPH mutant flies expressing mito-GFP. Larva peristaltic movements were observed and recorded in 120s for each larva. Genotypes: Elav-gal4/+; UAS-mito-GFP/+ (Control) and tbphΔ23elav-gal4/tbphΔ23; UAS-mito-GFP/+ (Tbph mutant). N= 30 per genotype. Error bars are SEM. ***p<0.0001 as calculated using t-test.

4.10 Analysis of the synaptic vesicle recycling at the *Drosophila* NMJ using FM1-43 dye.

FM1-43 is a fluorescent dye used as a synaptic vesicle marker to visualise and analyse endocytosis from the presynaptic membrane and also to study the exocytosis kinetics of pre-labelled vesicles. The process of synaptic vesicle recycling involves simultaneously both endocytosis which corresponds to loading of the dye and exocytosis which corresponds to unloading of the dye. For the test experiment, a Chemical (KCl) stimulation was achieved by immersing dissected larvae (w1118) in a "stimulation fluid" that is required to "load" FM1-43 into vesicles in a

process simulating endocytosis. As control experiment, more dissected larvae (w1118) were immersed in a “dissection fluid” that was designed to be non-stimulatory and the process of loading was initiated. Comparing the intensities of FM1-43 in these two experiments, Loading was more successful in the experiment using the stimulation fluid than in the one using the dissection fluid (Figure 48).

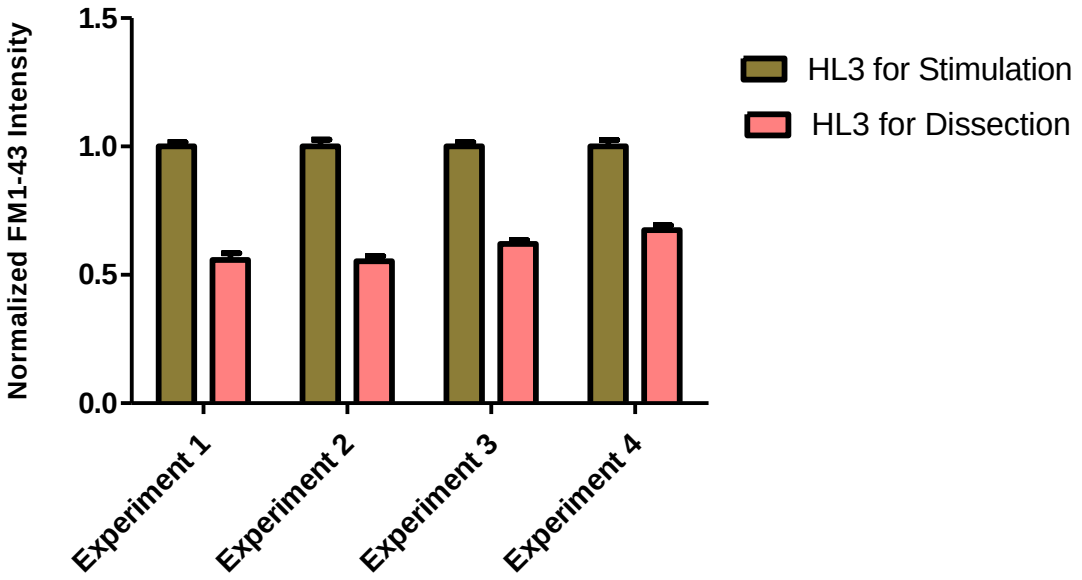

Figure 48 Quantification of FM1-43 intensity in synaptic boutons during “loading” in w1118 flies. Using the dissection solution in place of the stimulation fluid loaded a significantly lesser amount of FM1-43. N= 20. Error bars are SEM

Approximately half the quantity of FM1-43 loaded using the stimulation fluid was loaded when the dissection solution was used. The four experiments ran with these two fluids in w1118 were very consistent as they all produced similar results (Figure 48). Thus, we proceeded to the

experiments of checking the synaptic vesicle recycling in w1118 and TBPH mutant flies using the stimulation fluid.

4.11 The synaptic vesicle recycling is impaired in TBPH mutant flies.

In order to test the role of TBPH in the exo-endocytic cycling of synaptic vesicles, we decided to check the process of vesicle recycling through the use of FM1-43. This cycle was stimulated and monitored. Recordings were reported in Figure 49. Both genotypes, the control (w1118) and TBPH mutant "loaded" and "unloaded" at significantly different rates. The control had a turnover of about 42% while TBPH mutant larvae had about 24%, almost half that of the control.

In more details, while the control loaded 100% of vesicles at the synapse and unloaded about 58% of that leaving approximately 42% in the boutons (Figure 49), the TBPH mutant flies on the other hand, loaded about 84% of boutons and unloaded approximately 60% of that leaving approximately 24% in the boutons. So, the turnover of the synaptic vesicle recycling was significantly higher in the control than in TBPH mutant flies.

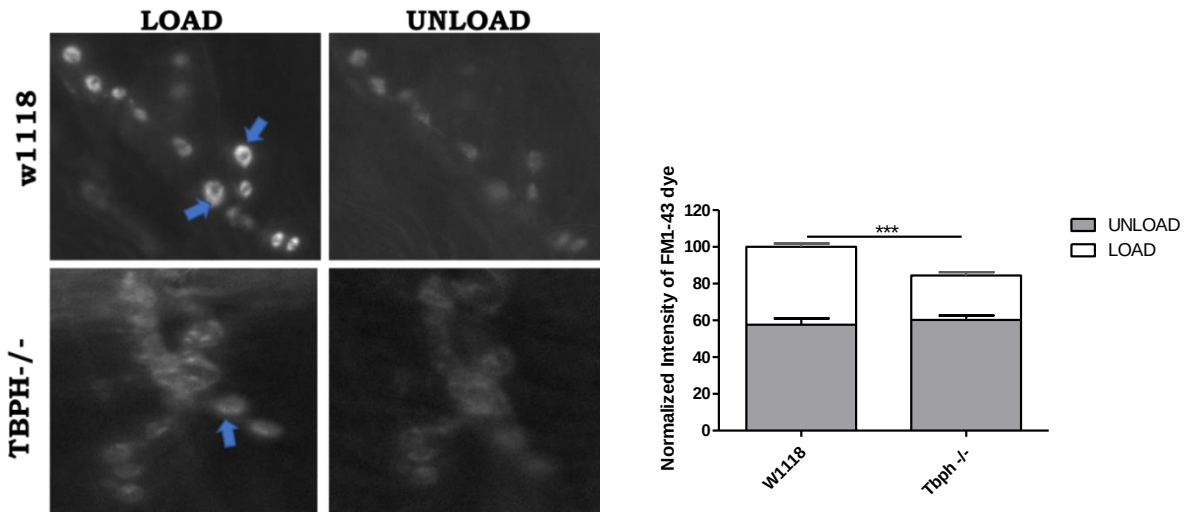

Figure 49 TBPH mutant flies have impaired synaptic vesicle recycling. Panel shows images from live microscopy of the NMJ between muscles 6 and 7 visualized by FM1-43 dye. Graph shows the quantification of FM1-43 intensity in the boutons as they undergo endocytosis (Load) and exocytosis (Unload). Note the blue arrows showing the sub-boutonic structures. N= 20 per genotype. Error bars are SEM. ***p<0.0001 as calculated using t-test.

Noteworthy, we observed the presence of some structures in the boutons shaped like “doughnuts” (blue arrows in Figure 49) that were deeply perfused with FM1-43 dye resulting with high intensities as reported in Figure 50. The control had significantly greater number of these structures than the TBPH mutant flies. Consequently, TBPH mutant flies had significantly more boutons without these structures (Figure 50).

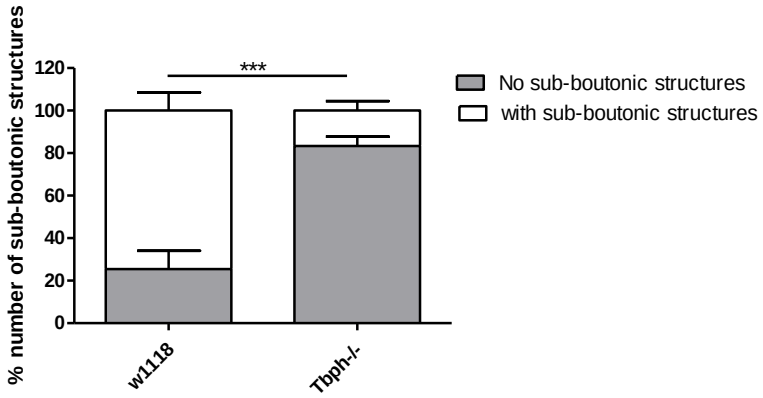

Figure 50 Quantification of localization of FM1-43 in synaptic boutons. TBPH mutant flies had lesser number of sub-boutonic structures. N= 20 per genotype. Error bars are SEM. ***p<0.0001 as calculated using t-test.

4.12 The synaptic vesicle recycling was improved in TBPH mutant flies expressing Futsch

Having recovered in the Futsch rescue flies, synaptic proteins such as synapsin, syntaxin and Csp that are associated with the vesicles at the synapse, we proceeded to check if there would be a recovery of the impairment observed in the synaptic vesicle recycling of TBPH mutant flies by Futsch. There was a rescue of the vesicle recycling in the mutants as there was a significant improvement in the turnover rates of the vesicles (Figure 51). The control that was wildtype for TBPH had a turnover of about 45%, the TBPH mutant had about 20%, the rescue by TBPH and Futsch had 43% and 35% respectively. So, we report a recovery by Futsch rescue.

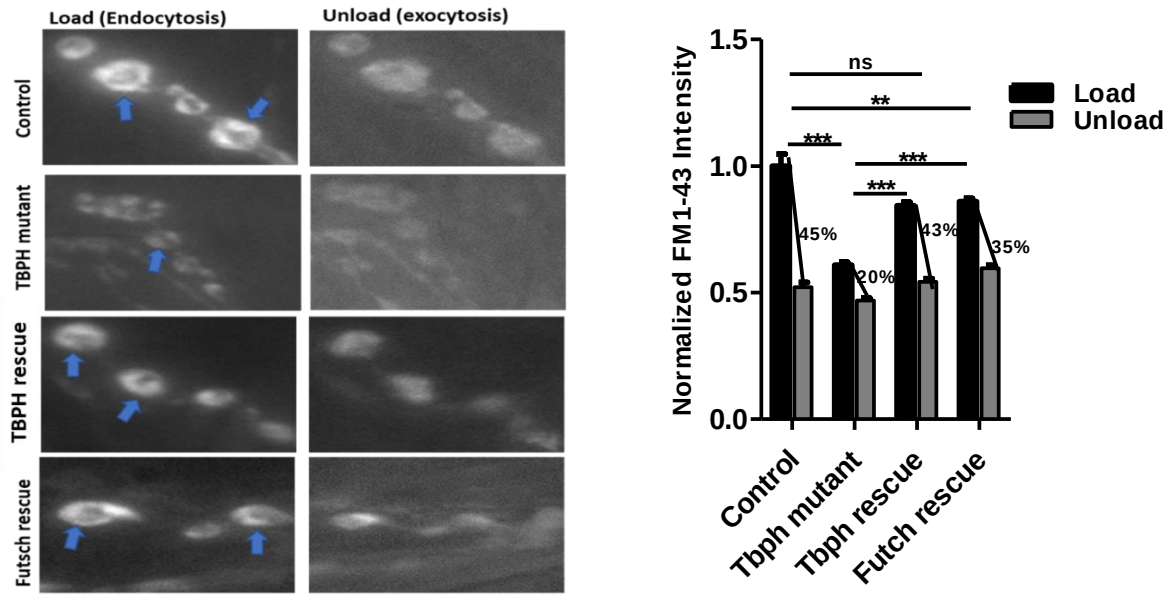

Figure 51 Synaptic vesicle recycling was improved in TBPH mutant flies expressing Futsch. Panel shows images from live microscopy of the NMJ between muscles 6 and 7 visualized by FM1-43 dye. Graph shows the quantification of FM1-43 intensity in the boutons as they undergo endocytosis (Load) and exocytosis (Unload). Note the blue arrows showing the sub-boutonic structures. Genotypes: Elav-gal4/+ (Control), tbphΔ23elav-gal4/tbphΔ23; UAS-GFPmCD8/+ (tbph mutant), tbphΔ23elav-gal4/UAS-tbphΔ23 (tbph rescue) and EP10751; tbphΔ23elav-gal4/tbphΔ23 (Futsch rescue). Scale bar is 20µm. N= 20 per genotype. Error bars are SEM. ***p<0.0001 **p<0.001 ns= not significant as calculated using ANOVA with Bonferroni's correction

Also, there was a recovery of the sub-boutonic structures with sequestrated FM1-43 in TBPH mutant flies expressing Futsch. About 72% of boutons had no sub-boutonic structures in TBPH mutant flies compared to about 34% in the mutants expressing Futsch. The percentages of boutons having no sub-boutonic structures of FM1-43 in the control that were wildtype for TBPH and in the mutants expressing TBPH (TBPH rescue) were 25% and 30% respectively (Figure 52). So, Futsch exerted an improvement in this regard too.

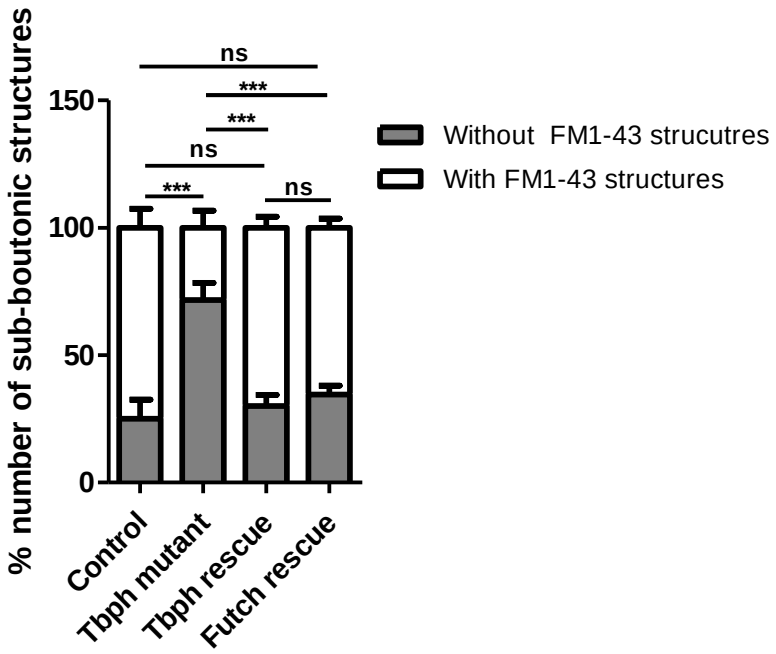

Figure 52 Quantification of localization of FM1-43 in synaptic boutons. TBPH mutant flies had a significant lesser number of boutons with sub-boutonic structures. Genotypes: Elav-gal4/+ (Control), tbphΔ23elav-gal4/tbphΔ23; UAS-GFP-mCD8/+ (tbph mutant), tbphΔ23elav-gal4/UAS-tbph (tbph rescue) and EP10751; tbphΔ23elav-gal4/tbphΔ23 (Futsch rescue) N=25 per genotype. N= 20 per genotype. Error bars are SEM. ***p<0.0001, ns= not significant as calculated using ANOVA with Bonferroni's correction.

4.13 The Rab4 and Rab5 rescue of TBPH mutant flies defects

4.13.1 Rab4-GFP rescues motility defect in TBPH mutant flies

Taking into consideration the results obtained with the synaptic vesicle recycling and the recovery of acetylated tubulin levels, a key player of the cytoskeleton, we proceeded to some proteins of vesicular trafficking, Rab4 and Rab5, both of which were GFP-tagged. TBPH mutant flies expressing Rab4-GFP in their neurons significantly improved their larvae motility while those expressing Rab5-GFP did not (Figure 53) as there was no significant difference between the performances of the Rab5-GFP rescue flies and TBPH mutants. Both groups averaged about 42

movements in 2minutes while those expressing Rab4-GFP and the control that was wildtype for TBPH averaged about 68 and 100 movements in the same time frame respectively Figure 53).

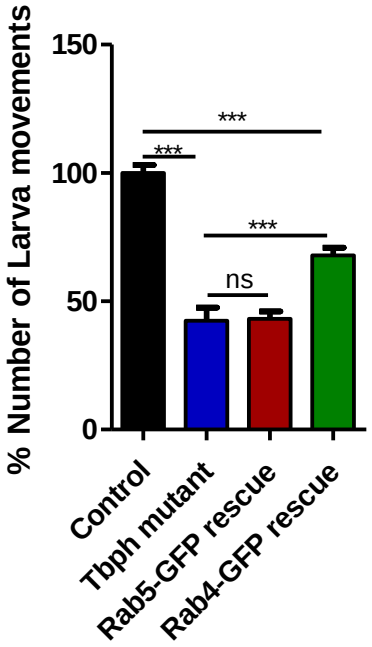

Figure 53 Motility of larva was improved in TBPH mutant flies expressing Rab4-GFP. Larva peristaltic movements were observed and recorded in 120s for each larva. Rab4-GFP showed a significant rescue of motility compared with Rab5-GFP and TBPH mutant flies. Genotypes: Elav-gal4/+; UAS-Rab4-GFP/+ (Control), tbphΔ23elav-gal4/tbphΔ23; UAS-lacZ/+ (Tpbh mutant), tbphΔ23elav-gal4/tbphΔ23; UAS-Rab5-GFP/+ (Rab5-GFP rescue) and tbphΔ23elav-gal4/tbphΔ23; UAS-Rab4-GFP/+ (Rab4-GFP rescue). N=25 per genotype. Error bars are SEM. ***p<0.0001, ns = not significant as calculated using ANOVA with Bonferroni's correction.

4.13.2 Rab5 expressed more than Rab4 at the NMJ in TBPH mutant flies

Analysing the NMJ of both Rab4 and Rab5 GFP conjugated rescue larvae, we observed that the intensity of Rab5-GFP was significantly

higher than that of Rab4-GFP's. However the higher expression level did not correlate with an increased phenotypic read out in motility (Figure 53 Figure 54). The level of Rab5-GFP at 1.25 is almost double that of Rab4-GFP at 0.73 (Figure 56) while the control with the expression of Rab4-GFP in a TBPH wildtype background was 1.00.

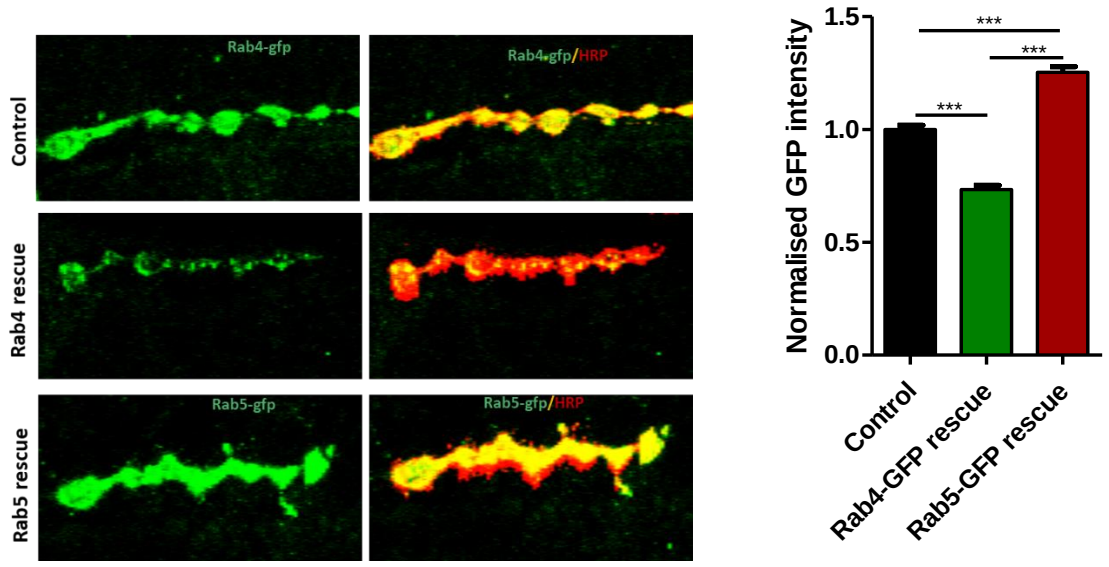

Figure 54 The level of Rab5-GFP was higher in TBPH mutant flies. Panels are representative confocal images showing the NMJs between muscles 6 and 7 stained with anti- HRP (in red) and anti-gfp (in green). Note the intensity of the Rab-gfp staining. Graph shows quantification of the Rab-GFP intensity in the boutons normalized on HRP. Genotypes: Elav-gal4/+; UAS-Rab4-GFP/+ (Control), tbphΔ23elav-gal4/tbphΔ23; UAS-Rab5-GFP/+ (Rab5-GFP rescue) and tbphΔ23elav-gal4/tbphΔ23; UAS-Rab4-GFP/+ (Rab4-GFP rescue). N=25 per genotype. Scale bar is 20μm. Error bars are SEM. ***p<0.0001 as calculated using ANOVA with Bonferroni's correction.

4.13.3 Rab4 and Rab5 recovered Futsch levels at the NMJ in TBPH mutant flies

Using IHC, we checked the level of Futsch at the NMJ in TBPH mutant flies expressing Rab4-GFP and Rab5-GFP given the recovery of motility

recorded with Rab4-GFP rescue flies. Both Rab proteins produced a recovery of Futsch levels at the NMJ (Figure 55). There was a significant difference in the intensities of Futsch measured in the control expressing Rab4-GFP in a TBPH wildtype background (1.00) compared with TBPH mutants expressing both Rab4-GFP and Rab5-GFP (about 0.90 and 0.87 respectively). Both Rab rescue groups were significantly higher than TBPH mutant expressing LacZ that averaged about 0.64.

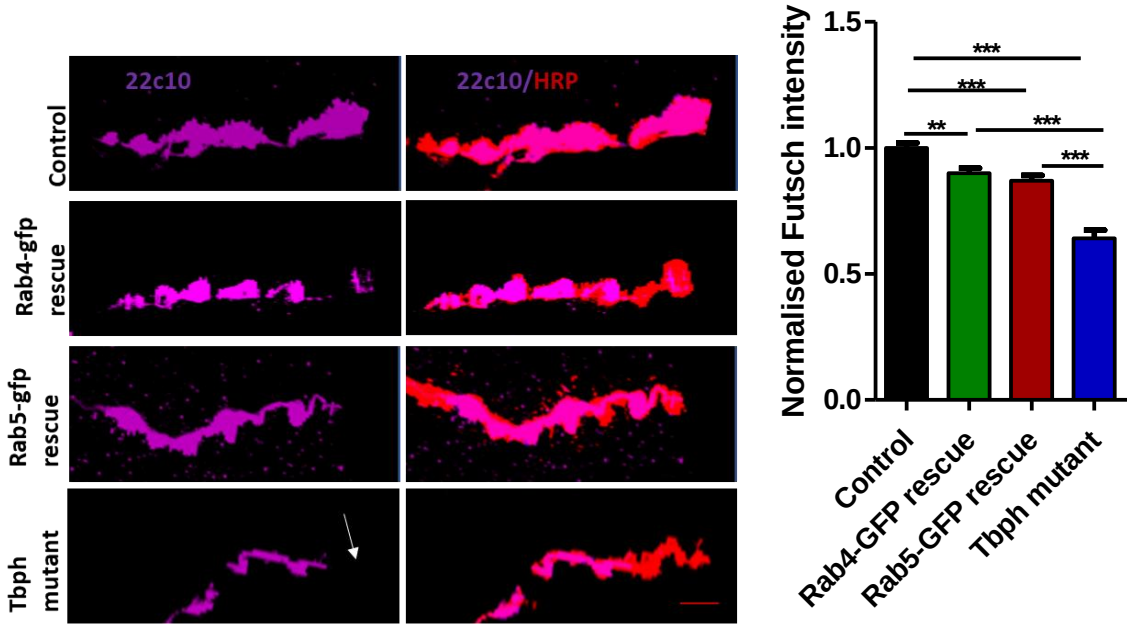

Figure 55 The Rab proteins 4&5 recover Futsch level at the NMJ in TBPH mutant flies. Panel shows representative confocal images of the NMJs between muscles 6 and 7 double-labelled with anti-HRP (in red) and anti Futsch (in purple). Note the Futsch staining at the terminal bouton present in all the groups except in tbph mutant (white arrow). Graph shows quantification of Futsch intensity in the boutons normalized on HRP. Genotypes: Elav-gal4/+; UAS-Rab4-GFP/+ (Control), tbphΔ23elav-gal4/tbphΔ23; UAS-Rab4-GFP/+ (Rab4-GFP rescue), tbphΔ23elav-gal4/tbphΔ23; UAS-Rab5-GFP/+ (Rab5-GFP rescue), and tbphΔ23elav-gal4/tbphΔ23; UAS-lacZ/+ (Tpbh mutant). N= 25 per genotype. Scale bar is 20µm. Error bars are SEM. **p<0.001, ***p<0.0001 as calculated using ANOVA with Bonferroni's corrections.

4.13.4 Rab4 and Rab5 improve the number of NMJ branches in TBPH mutant flies

Also of note is the recovery of branches of the NMJ observed in both rescue groups of the Rab proteins. TBPH mutants expressing Rab4-GFP percentage number of branches averaged about 87% while those expressing Rab5-GFP had an average of 76%. Both groups have significantly higher percentage of branches than TBPH mutants with an average of 51%. The control expressing Rab4-GFP in a TBPH wildtype background was significantly higher than all other genotypes with a 100% number of branches (Figure 56).

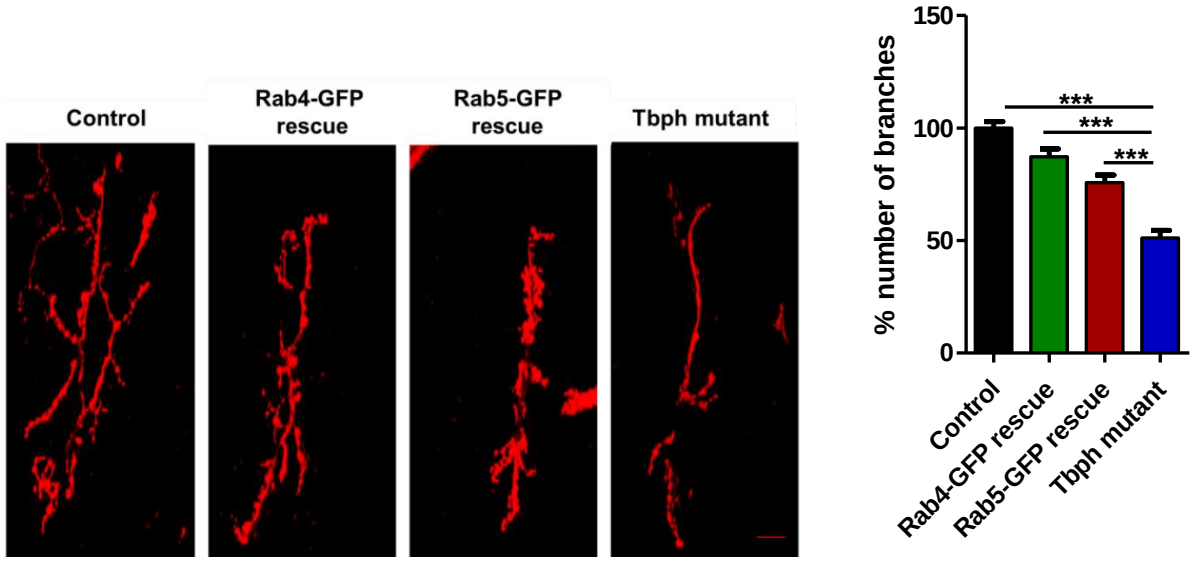

Figure 56 The number of branches of the NMJ was improved in TBPH mutant flies expressing Rab proteins 4&5. Both rescue groups performed significantly better than TBPH mutant flies and a bit lesser than the control. NMJ was labelled with HRP. Genotypes: Elav-gal4/+; UAS-Rab4-GFP/+ (Control), tbphΔ23elav-gal4/tbphΔ23; UAS-Rab4-GFP/+ (Rab4-GFP rescue), tbphΔ23elav-gal4/tbphΔ23; UAS-Rab5-GFP/+ (Rab5-GFP rescue), and tbphΔ23elav-gal4/tbphΔ23; UAS-lacZ/+ (Tpbh mutant). N= 25 per genotype. Scale bar is 20µm. N=25 per genotype. Error bars are SEM. ***p<0.0001. * p<0.01 as calculated using ANOVA with Bonferroni's corrections.

4.13.5 The level of acetylated tubulin at the NMJ was recovered in TBPH mutant flies expressing Rab4 or Rab5

Having observed both the recovery of larva motility and that of Futsch at the NMJ of the Rab4-GFP rescue flies similar to that obtained with Futsch, we decided to check the level of acetylated tubulin at the NMJ in an attempt to make a connection between Futsch and Rab4. Figure 57 shows the results of the observations made. Indeed, there was a recovery of acetylated tubulin in TBPH mutant flies expressing Rab4-GFP and in those expressing Rab5-GFP with values averaging 0.91 and 0.93 respectively. All genotypes averaged significantly higher intensities of acetylated tubulin than TBPH mutant flies expressing LacZ with a value of 0.69. There was no statistical difference between the control expressing Rab4-GFP in a TBPH wildtype background with a value of 1.00 and both Rab rescue groups.

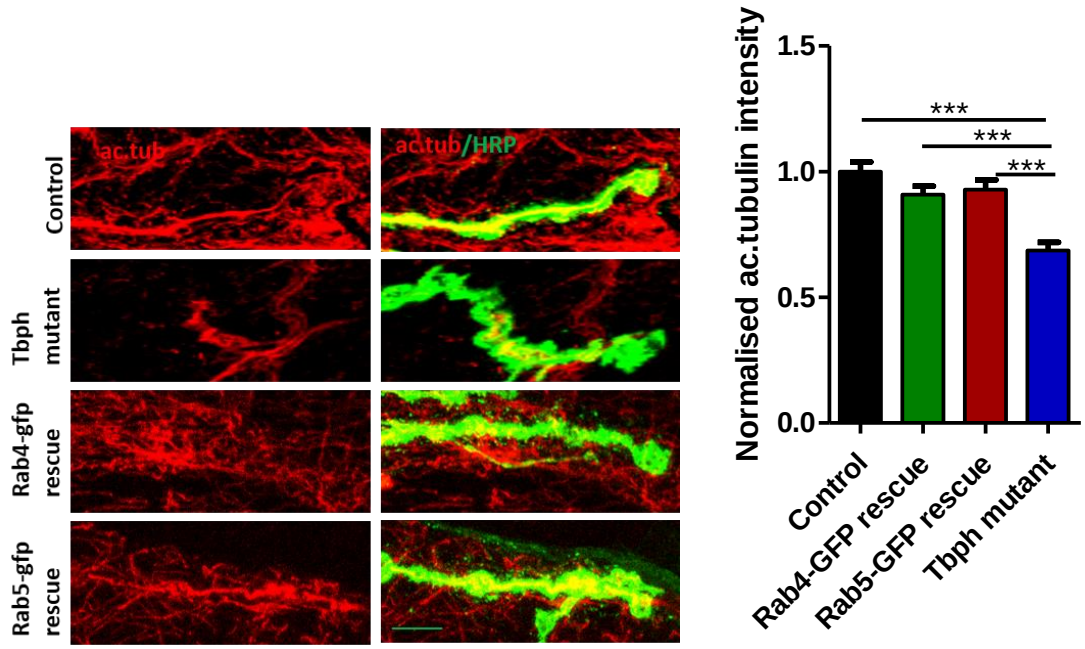

Figure 57 The level of acetylated tubulin was recovered in TBPH mutant flies expressing Rabs 4&5. Panels are representative confocal images showing the NMJs between muscles 6 and 7 double-labelled with anti-HRP (in green) and anti-acetylated tubulin (in red). Note the intensity of acetylated tubulin staining. Graph shows quantification of acetylated tubulin intensity in the boutons normalized on HRP. Genotypes: Elav-gal4/+; UAS-Rab4-GFP/+ (Control), tbphΔ23elav-gal4/tbphΔ23; UAS-Rab4-GFP/+ (Rab4-GFP rescue), tbphΔ23elav-gal4/tbphΔ23; UAS-Rab5-GFP/+ (Rab5-GFP rescue), and tbphΔ23elav-gal4/tbphΔ23; UAS-lacZ/+ (Tpbh mutant). N= 25 per genotype. Scale bar is 20μm. N=25 per genotype. Error bars are SEM. ***p<0.0001 as calculated using ANOVA with Bonferroni's correction.

4.13.6 The level of Syntaxin at the NMJ was not recovered in TBPH mutant flies expressing Rab4 or Rab5

Syntaxin level at the NMJ was checked by IHC in TBPH mutant flies expressing Rab4-GFP and Rab5-GFP. No recovery of syntaxin was observed for both of the Rab proteins. TBPH mutant flies expressing LacZ had an average intensity of syntaxin of 0.82, while those expressing Rab4-GFP and Rab5-GFP resulted in intensities of 0.83 and 0.81 respectively. The control expressing Rab4-GFP in a TBPH wildtype background was significantly higher than all other groups at an average of 1.00 (Figure 58).

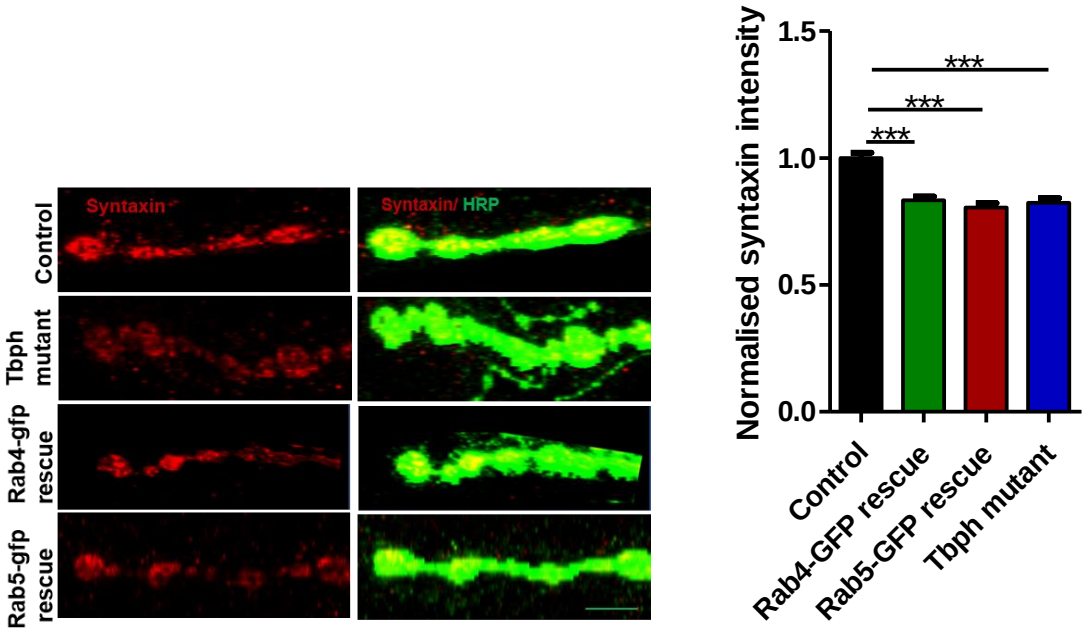

Figure 58 The level of Syntaxin was not recovered in TBPH mutant flies expressing Rabs 4&5. Panels are representative confocal images showing the NMJs between muscles 6 and 7 double-labelled with anti-HRP (in green) and anti-syntaxin (in red). Note the intensity of syntaxin staining. Graph shows quantification of syntaxin intensity in the boutons normalized on HRP. Genotypes: Elav-gal4/+; UAS-Rab4-GFP/+ (Control), tbphΔ23elav-gal4/tbphΔ23; UAS-Rab4-GFP/+ (Rab4-GFP rescue), tbphΔ23elav-gal4/tbphΔ23; UAS-Rab5-GFP/+ (Rab5-GFP rescue), and tbphΔ23elav-gal4/tbphΔ23; UAS-lacZ/+ (Tpbh mutant). N=20 per genotype. Scale bar is 20µm. N=20 per genotype. Error bars are SEM. ***p<0.0001 as calculated using ANOVA with Bonferroni's correction.

4.14 The level of pMad at the NMJ was reduced in TBPH mutant flies

From the observations of recovery of the functional anatomy of the NMJ by Futsch, it was evident that Futsch promotes the growth of this specialised synapse. So, we decided to check its involvement in a growth signalling pathway and we chose the bone morphogenetic protein (BMP) growth signalling. Phosphorylated BMP pathway effector Mad (pMad) localizes to both the soma in the ventral cord (nuclear pMad) and the NMJ (synaptic pMad). While the role of the nuclear pMad is said to be

modulation of BMP target genes, that of synaptic pMad is yet to be fully understood and suggestions are made about a possible local synaptic activity rather than an involvement in retrograde translocation to the nuclei only.

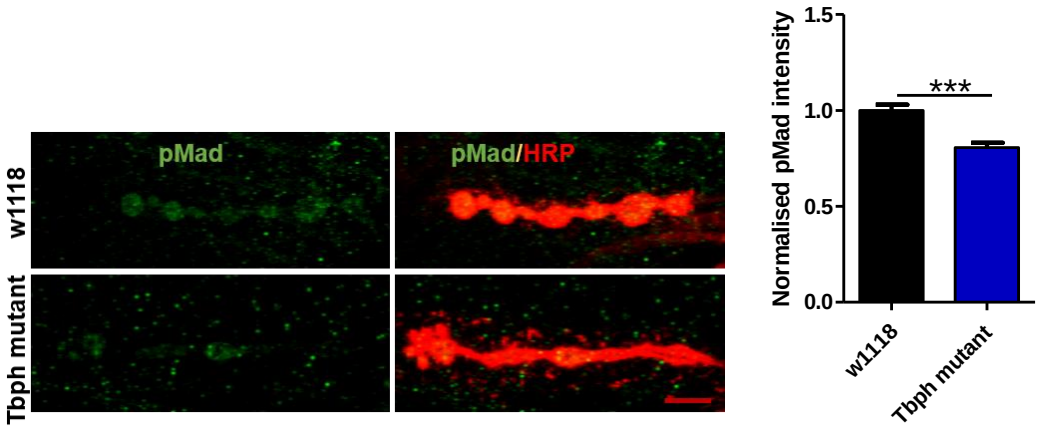

Figure 59 The level of pMad was reduced in TBPH mutant flies. Panels are representative confocal images showing the NMJs between muscles 6 and 7 double-labelled with anti-HRP (in red) and anti-pMad (in green). Note the intensity of pMad staining. Graph shows shows quantification of pMad intensity in the boutons normalized on HRP. Genotypes: w1118 (Control) and tbph mutant is tbphΔ23/ tbphΔ23. Scale bar is 20μm. N=25 per genotype. Error bars are SEM. ***p<0.0001 as calculated using student t-test.

Given this incitement, the levels of pMad was quantified at the NMJ of w1118 and TBPH mutant flies. There was a significant difference in the intensities of the pMad between the control and TBPH mutant flies with averages of about 1.00 and 0.80 respectively (Figure 59).

4.14 The level of pMad at the NMJ was improved in TBPH mutant flies expressing Futsch

Having observed a significant difference in the intensities of the synaptic pMad between w1118 and TBPH mutant flies, we proceeded to check its

level in the Futsch rescue flies using TBPH rescue as a positive control (Figure 60). TBPH mutant flies expressing Futsch had an increased synaptic pMad level with a value of 0.85 when compared with those expressing GFP with a value of 0.78. The TBPH mutant flies rescued with TBPH and the control flies in a TBPH wildtype condition averaged 0.96 and 1.00 respectively (Figure 60).

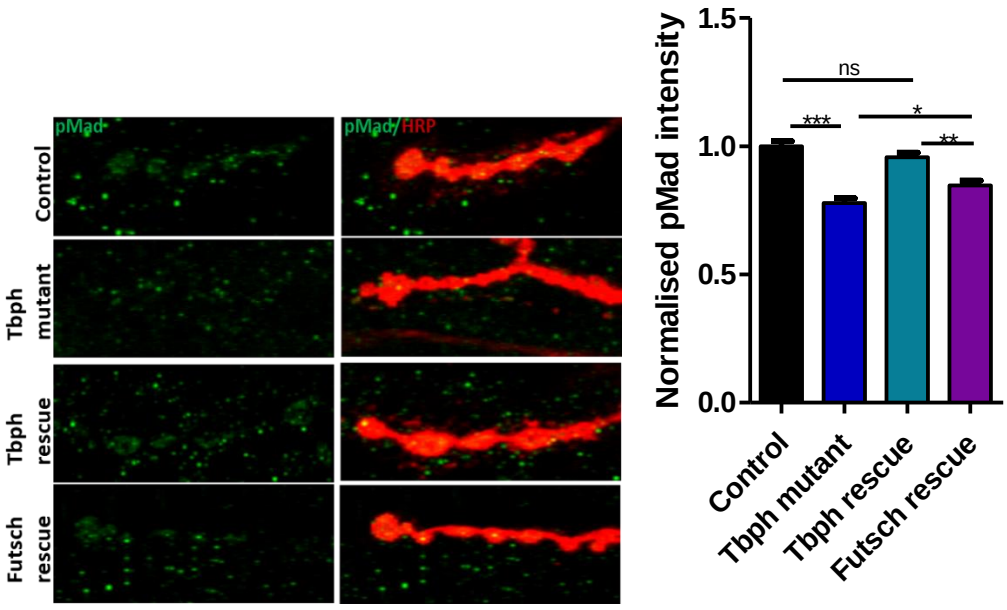

Figure 60 The level of pMad was improved in TBPH mutant flies expressing futsch. Panels are representative confocal images showing the NMJs between muscles 6 and 7 double-labelled with anti-HRP (in red) and anti-pMad (in green). Note the intensity of pMad staining. Graph shows quantification of pMad intensity in the boutons normalized on HRP. Genotypes: Elav-gal4/+ (Control), tbphΔ23elav-gal4/tbphΔ23; UAS-GFP-mCD8/+ (Tpbh mutant), tbphΔ23elav-gal4/UAS-tbphΔ23 (Tbph rescue) and EP10751; tbphΔ23elav-gal4/tbphΔ23 (futsch rescue). Scale bar is 20µm. N=20 per genotype. Error bars are SEM. *p<0.01, **p<0.001, ***p<0.0001, ns = not significant as calculated using One-way ANOVA.

4.15 The level of pMad at the NMJ was improved in TBPH mutant flies expressing Rab4 or Rab5

We proceeded to check the level of pMad in the Rab-GFP rescue flies having observed a difference in the Futsch rescue flies. TBPH mutant flies

expressing Rab4-GFP gave a significant rescue of pMad at the NMJ with a value of 0.78 compared with the mutant flies expressing LacZ that had a value of about 0.70. Interestingly, the mutant flies expressing Rab5-GFP gave a higher rescue of pMad with a value of about 0.87 while the Control flies expressing Rab4-GFP in a TBPH wildtype background had a value of 1.00 (Figure 61).

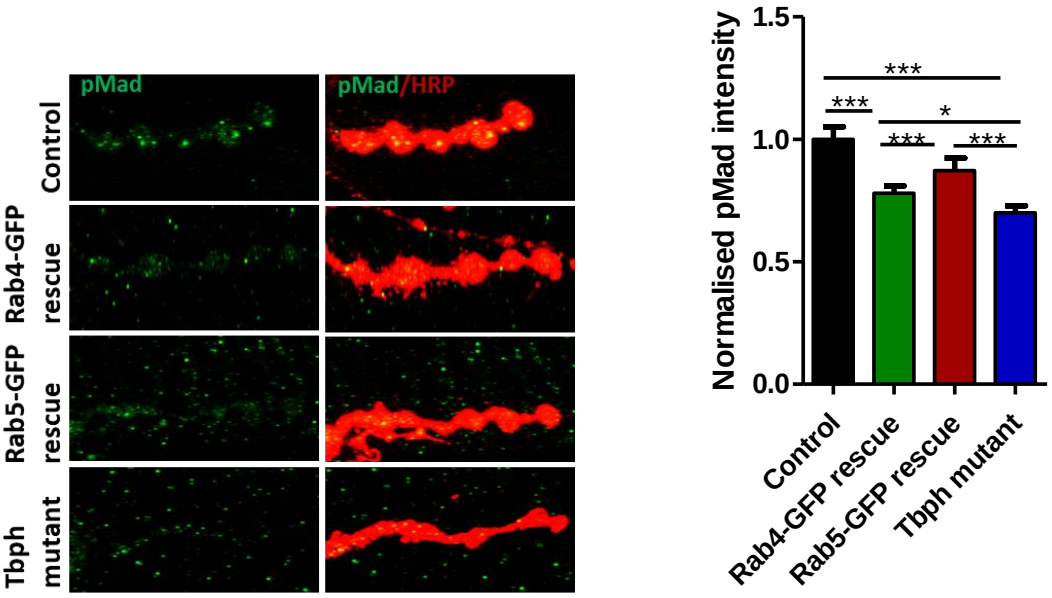

Figure 61 The level of pMad was improved in TBPH mutant flies expressing Rab proteins 4&5. Panels are representative confocal images showing the NMJs between muscles 6 and 7 double-labelled with anti-pMad (in green) and anti-HRP (in red). Note the intensity of pMad staining. Graph shows quantification of pMad intensity in the boutons normalized on HRP. Genotypes: is Elav-gal4/+; UAS-Rab4-GFP/+ (Control), tbphΔ23elav-gal4/tbphΔ23; UAS-Rab4-GFP/+ (Rab4-GFP rescue), tbphΔ23elav-gal4/tbphΔ23; UAS-Rab5-GFP/+ (Rab5-GFP rescue) and tbphΔ23elav-gal4/tbphΔ23; UAS-LacZ/+ (Tpbh mutant). Scale bar is 20µm. N=15 per genotype. Error bars are SEM. *p<0.01, ***p<0.0001, ns = not significant as calculated using One-way ANOVA.

5.0 DISCUSSION

5.1 Silencing TBPH in neurons produced similar effects to its complete knockout with respect to Futsch functions

Motility defect is a known classic feature of TBPH mutant flies reported by Feiguin *et al.,* 2011 and Romano *et al.,* 2014. On average, these larvae crawled less than half the number of times the wildtype flies did. So, we can say they have less than 50% motility function (Figure 31). Silencing TBPH in the neurons similar to a complete knockout, also produced an almost identical phenotype whereby the larvae crawled about half the number of times the control did. This implies that the larvae having TBPH silenced in their neurons lost approximately 50% of their motility function which was sufficient to produce a significant defect. The observation of this ALS-like phenotype prompted further investigations into what the NMJs look like and whether the protein level and the localization of Futsch was affected or not, considering that Futsch is a known translational target of TBPH (Coyne *et al.,* 2014). Futsch was found to be about 22% reduced at the NMJ and this difference was sufficient to elicit “Futsch” dysfunction because the number of branches and boutons were also reduced and importantly the shape of the boutons were also affected (Figure 34,Figure 32 and Figure 33). These features are all those associated with reduced Futsch levels as seen in TBPH mutant flies. Also, of note is the distribution

of Futsch which was ominuously absent in the terminal boutons when TBPH was silenced (Figure 34). This is an important observation because growth occurs at the terminal boutons and Futsch is required to stabilize the microtubule cytoskeleton responsible for the maintenance of the shape of both old and newly formed boutons in order to maximise their functions (Roos *et al.,* 2000) and efficacy.

5.2 Futsch recovered motility in TBPH mutant flies best with Elav-gal4

Pan neuronal driver Elav-gal4 was found to be the best driver for the expression of Futsch in the neurons of TBPH mutant flies. This conclusion was drawn from observations made from the results of the larva movements carried out using different drivers (Figure 35Figure 36) from which Elav-gal4 gave the highest numerical value of recovery. nSyb-gal4, another pan neuronal driver also performed significantly better than the motor neuron specific drivers but Elav-gal4 scored higher (Figure 35). One may be tempted to think that D42-gal4 and OK6-gal4 should perform better since they are motor neuron drivers and are directly involved in the disease (having a localised effect on ALS) but this was not the case as reported from the observations made. Indeed, the reverse was the case with the pan neuronal drivers performing better than the motor neuron specific drivers. We attributed this to the probable multiple roles of Futsch. It could be responsible for the availability of other important proteins and

factors involved in different pathways in the neuronal system in addition to its relationship with TDP-43. So, using a driver with a broader spectrum of functions not limited to only the motor neurons may make available these “factors” hence, a better functional read-out was obtained. Importantly, Elav-gal4 is tested and trusted because it is known as one of the most commonly used and reliable driver for gene expression in the nervous system. Thus, its performance here was not surprising and unexpected (Shiraishi *et al.,* 2014).

Irrespective of the driver used for the gene expression, it was clear that Futsch produced a rescue of an important phenotypic defect of TBPH mutant flies, locomotion (here observed as larva motility). This was an impressive feat because even the motor neuron drivers when used were able to exert a positive effect on motility implying a very cogent action of Futsch in the neurons. How and what exactly Futsch did in TBPH mutant larvae to elicit a recovery of motility dysfunction remained an important subject of the project.

5.3 Futsch recovered NMJ abnormalities associated with microtubules and synaptic growth in TBPH mutant flies

Hummel *et al.,* 2000 demonstrated Futsch to be important for axonal and dendritic growth. NMJ abnormalities seen in TBPH mutant flies such as mis-shaped boutons, reduced number of branches and bouton’s number

(Feiguin *et al.,* 2009) were recovered by expressing Futsch in their neurons. Some criteria by which growth is quantified at the NMJ include shape of boutons, and number of branches and boutons among others. Roos *et al.,* 2000 reported Futsch to be necessary for synaptic growth in *Drosophila*. Godena *et al.,* 2011 and Coyne *et al.,* 2014 demonstrated a connection between TDP-43 and Futsch at the NMJ by reporting a decrease in Futsch level in TBPH mutant flies and in the spinal cords of ALS patients respectively. An observation that is corroborated by this study too (Figure 30).

It is generally accepted that development and growth at the NMJ occur by addition and stabilization of new boutons through division of old boutons. A function regulated by the microtubule cytoskeleton as they are important for synaptic organization and plasticity. Futsch has been found to be necessary for the maintenance of this process thereby controlling growth at the NMJ (Roos *et al.,* 2000) More so, the shape of the boutons is important not only for growth but also for synaptic functions related to their surface area such as neurotransmission, thus it is important for optimal functioning of the specialized synapse. All of which are regulated by the microtubule cytoskeleton that are responsible for the maintenance of the architecture necessary to stabilize the boutons during division. Normal Futsch function is important for smooth running of this process. So, our

observations of a recovery of synaptic growth in TBPH mutant flies expressing Futsch with respect to boutons and branches (Figure 37Figure 38), expands and substantiate the claims of Godena *et al.,* 2011 and is in direct accordance with available literature. The overall integrity and stabilization of the NMJ appear to be regulated by Futsch but not only by virtue of its association with the microtubule cytoskeleton. If this were to be singularly so, we should observe similar effects when another microtubule associated protein is substituted for Futsch in the quest of locomotion rescue. Tau is a MAP that belongs to the same classical group as Futsch and expressing Tau in the neurons of TBPH mutant flies failed to produce a recovery of motility in the larvae. A sharp contrast to what was observed with Futsch. Interestingly, Tau also gave a recovery of the anatomy of the NMJ but it was not enough to translate into a functional phenotype (Figure 39). We therefore believe that Futsch is probably involved in another pathway that may not be directly related with its status as a microtubule associated protein as there is a level of functional redundancy in the MAPs which Tau was not able to replicate here.

5.4 Microtubules were more stabilized at the NMJ of TBPH mutant flies when Futsch was expressed in their neurons

Recovery of functions involving stable microtubules such as branches and bouton shapes made it imperative to check the level of stabilized microtubules. Acetylation is a key post translational modification of tubulin

and is widely accepted as a measure of stability. A good recovery of acetylated tubulin, consequently, stable microtubules was observed with neuronal Futsch overexpression in TBPH mutant flies which confirms the functional MAP action of Futsch (Figure 43). In line with the reported lower levels of Futsch in these flies, Godena *et al.,* 2011 also observed a concurrent reduction in the quantity of their synaptic “stable” (acetylated) microtubules. Worthy of note was the distribution of the “stable” microtubules that were recovered with TBPH expression. They were present in the terminal boutons where Futsch was also found but they were ominously absent in the TBPH mutant flies (Figure 43). This reiterate the importance of Futsch function in the maintenance of bouton stability and overall NMJ growth. This result obtained with acetylated tubulin by Futsch was indeed quite important as it gave more than probable credence to the previously obtained results because now we have a direct link of Futsch to the microtubules in its recovery quest.

5.5 The levels of pre-synaptic vesicular proteins were recovered by Futsch in TBPH mutant flies

Having observed the recovery of motility and overall integrity of the NMJ in TBPH mutant flies by Futsch, we were curious to understand how futsch was able to do this especially when another MAP, Tau, was not able to exert such a functional recovery. So, we decided to check the levels of some presynaptic proteins involved with synaptic vesicles to gain

an insight into the direction through which Futsch follows to elicit this recovery. Given the fact that it also recovered stable microtubules that are known as the ‘highway’ for cellular transportation. Could the overall functional readout of improved motility be a result of better synaptic output by way of more efficient synaptic vesicles and trafficking?

Synapsin, Syntaxin and CSP are all proteins involved with synaptic vesicles. All of these proteins were downregulated at the NMJ of TBPH mutant flies (Romano *et al.,* 2014) and we found that Futsch was able to recover them to significantly appreciable levels. Synapsins are neuron-specific phosphoproteins that have been implicated in the clustering of synaptic vesicles especially those in the ‘reserve pool’ (Hilfiker *et al.,* 1999). They are known to interact with the vesicles and the cytoskeletal architecture thereby keeping the vesicles together in readiness for exocytosis to sustain neurotransmission. (Winther *et al.,* 2015) confirmed the clustering action of synapsin at the *Drosophila* NMJ in a synergistic association with dap160, a protein also involved in synaptic vesicle tethering. Genetic studies involving the NMJs of *C. elegans* and *D. melanogaster* revealed syntaxin to be involved in a trimeric SNARE (soluble *N*-ethylmaleimide sensitive factor attachment receptor) complex that is necessary for priming of synaptic vesicles. The complex is formed by synaptobrevin, syntaxin and SNAP-25 (soluble *N*-ethylmaleimide

sensitive factor attachment protein 25) (Richmond & Broadie, 2002) and is thought to drive the process of exocytosis. Romano *et al.,* 2014 reported a possible translational connection between syntaxin and TBPH implying that the reduction we see in the levels of syntaxin at the NMJ could also play a role in the synaptic defects seen in TBPH mutant flies. It is pertinent to note that Futsch has also been reported as a translational target of TBPH (Coyne *et al.,* 2014). Cysteine string protein (CSP) is also involved with the synaptic vesicles and it functions to maintain the spatial arrangement of SNAP 25 to enhance its recruitment into the SNARE complex at the membrane ready for fusion (Burgoyne & Morgan, 2015). Futsch recovery of these downregulated synaptic vesicle proteins in TBPH mutant flies (Figure 40Figure 41 Figure 42) prompted us to proceed in the direction of the synaptic vesicle recycling as a probable means or part of the mechanism involved by which Futsch exert its rescue of ALS-like motility defects. Before we check the synaptic vesicle recycling, it made good sense to check the level of some post-synaptic proteins too since all these vesicular proteins are pre-synaptic.

5.5 Post synaptic proteins Dlg and GluRIIA were recovered by Futsch in TBPH mutant flies

TBPH was found to be necessary for the organization and maintenance of post synaptic structures at the neuromuscular junction. Strah *et al.,* 2020 reported an interaction between TBPH and the mRNA of Dlg

implying a regulatory function on its expression level both in neurons and skeletal muscles. In accordance with this report, we have also observed a reduction in the level of Dlg at the NMJ of TBPH mutant flies (Figure 44) which gives credence to the report of a concomitant reduction of its mRNA levels in this same flies. Why Futsch, a microtubule associated protein recovers this Dlg reduction in TBPH mutant flies is probably due to the fact that Futsch is necessary for the growth and maintenance of axons and dendrites which are important for neurotransmission from the pre to the post synaptic compartments for effective functioning. Also of note, both proteins were found to be downregulated in ALS patients (Coyne *et al.,* 2014; Strah *et al.,* 2020) and TBPH exerts a regulatory action on them so, this can also have a contributory role in the mechanism. Post synaptic clustering of glutamate receptors is important to maintain transmission at the synapse (Romano *et al.,* 2018). They reported glutamic acid decarboxylase (Gad1) to be required for the clustering of GluRIIA at the NMJ as GluRIIA was found to be reduced in TBPH mutant flies. Furthermore, they observed a higher level of extracellular glutamate levels. We also observed a reduction in the clusters of post synaptic GluRIIA at the NMJ in TBPH mutant flies (Figure 45) which is in agreement with the glutamate excitotoxicity theory (as a result of reduced glutamate receptors) as a contributory mechanism of ALS disease and progress. Futsch probably improves the clustering of these receptors via

similar mechanism by which it is involved in the clustering of synaptic vesicles for efficient neurotransmission.

5.6 More mitochondria were localized at the NMJ of TBPH mutant flies

The role of mitochondria dysfunction in the pathogenesis of ALS and other TDP-43 proteinopathies has been discussed. Recently, Wang *et al.,* 2019 reported ultrastructural damages to the mitochondria along with functional impairments in TDP-43 proteinopathies using a combination of cell and animal model systems while comparing with samples from patients. Damage to this organelle has been reported to precede motor neuron degeneration (also in SOD1 mouse model) making its intervention a potential therapeutic target. Interestingly, we observed that the intensity of mito-GFP (a mitochondrial import signal fused to GFP) was higher in TBPH mutants (Figure 46) when compared with the wildtype. This could be because more mitochondria are transported to the NMJ to compensate for the inefficiency of the synapse as they are mainly responsible for providing the energy required to maintain the synaptic processes that are majorly active. So, we can tentatively say that the transport of mitochondria to the NMJ in TBPH mutant flies appear to be unaffected by the loss of TBPH and Futsch while the reverse is the case for synaptic vesicles. Unfortunately, nothing can be postulated regarding the efficient functioning of the mitochondria at NMJs since the use of mito-GFP only

allows the quantification and presence of mitochondria. The higher mito-GFP intensity detected at the NMJ of TBPH mutants could be due to their inability to move quickly or freely back to the soma with a consequent backlog of inefficient and/ old mitochondria that should be degraded that translate into a higher intensity of mito-GFP reported in TBPH mutants.

5.7 Futsch has a role in synaptic vesicle recycling in TBPH mutant flies

The use of FM1-43 dye to demonstrate synaptic vesicle recycling at the NMJ in *Drosophila* larvae provides a good method to gain an insight into the workings of vesicular trafficking at the synapse and its role in effective neurotransmission. In order to sustain neurotransmission, an efficient recycling of vesicles has to take place (Verstreken *et al.,* 2008). Having recovered through Futsch the expression level of some proteins associated with synaptic vesicles, it was a further positive confirmation to observe that also the impaired synaptic vesicle recycling in TBPH mutant flies (Figure 51) was rescued by Futsch. A complete vesicle cycle includes both exocytosis and endocytosis. Regarding exocytosis, Futsch was found to be necessary for normal neurotransmitter (glutamate) release and maintenance of active zones in *Drosophila* (Lepicard *et al.,* 2014). These authors observed a reduction in the amplitude of evoked excitatory junctional currents (eEJC) in Futsch mutants and proposed a reduction in the mean number of synaptic vesicles released upon

stimulation as a causative factor. This is because they did not observe any changes in the spontaneous synaptic vesicle release as measured by the miniature excitatory junctional currents' (mEJC) amplitude and frequency. So, they concluded that loss of Futsch causes a presynaptic dysfunction in glutamate release at the NMJ in *Drosophila* as a consequence of a decreased number of vesicles in the readily releasable pool (RRP). Expressing Futsch in the neurons of TBPH mutant flies was probably able to rescue this pre-synaptic defect of reduced vesicular release thereby improving the turnover of the recycling process (Figure 51). This can also make available "synapsin" that is responsible for clustering these vesicles in the pool keeping them together and making them available upon stimulation. All of these, consequently make the synapse (NMJ) more efficient in its function and could translate phenotypically as improved motility. Worthy of mention is also the recovery of these "sub-boutonic structures" which contained sequestered FM1-43 clearly detectable by its high intensity there (Figure 52). Even if it is not yet clear what these structure are, and further studies are necessary to elucidate their functions, what came to light is the fact that, since FM1-43 labels vesicles, they contain more vesicles than elsewhere in the boutons. Could this sub-boutonic structures contain vesicles in the readily releasable pool (RRP)? Given that reduction of vesicles in the RRP

has been observed to be a consequence of Futsch absence (Lepicard *et al.,* 2014).

5.8 Neuronal expression of the Rab4 and Rab5 recovers some TBPH mutant flies defects

The Rab family of GTPases is a family of endosomal proteins important as regulators of endosomal trafficking. Rab4 and Rab5 are localized to the early endosomes and they have roles in recycling of internalised vesicles and endosomal fusion respectively. While Rab4 has been implicated in the control of vesicle recycling from the early endosomal compartment to the recycling compartment and back to the plasma membrane, Rab5 is thought to regulate the initial transport of Clathrin-coated vesicles from the plasma membrane to the early endosomes, their tethering and eventual fusion (Zerial & McBride, 2001).

Microtubule-dependent motor proteins transport vesicles including the Rabs from the Golgi apparatus to various parts of the cell where they are required. There is a conserved machinery of Kinesin-Rab interaction from mammalian cells to *Drosophila*. Early endosomes with Rab5 associate with Khc-73 (mammalian KIF13) and Dynein while vesicles associated with Rab4 interact with Kinesin-2 and 3 (Dey *et al.,* 2017) These interactions imply that the Rab proteins travel along the microtubule-dependent pathway bidirectionally (both retrograde and anterograde) so,

it was not very surprising to find that the expression of Rab4 in the neurons of TBPH mutant flies recovered motility (Figure 53) and acetylated tubulin levels (Figure 57) similar to those obtained when Futsch, a microtubule associated protein was expressed in the same flies. This is because Rab4 transport on the Futsch-dependent stable microtubules provides a plausible point of contact for signalling between the two proteins which could explain their similar rescue patterns. Also of note is the fact that the NMJ branching was also improved by both proteins (Figure 56). It was interesting to see that expressing either Rab4 or Rab5 in the neurons of TBPH mutant flies was sufficient to recover the levels of Futsch at the NMJ (Figure 55). This observation of Futsch recovery made the motility rescue in the larvae and branching of the NMJ observed in the Rab-GFP rescue flies understandable. On the contrary, Dey *et al.*, 2017 found that reduced flow of Rab4-positive vesicles to the ventral ganglion of the larva enhanced motility although not in a TBPH mutant background. The relationship between Futsch and the Rab proteins appears to be microtubule related for the main purpose of transport as the Rab proteins were also able to recover the levels of acetylated tubulin which is a marker of stable microtubules, the generic function of Futsch. It is however interesting to observe that Rab4 was also able to recover the level of pMad, an effector in the BMP signalling pathway in a manner similar to that of Futsch (Figure 60Figure 61) which was mildly significant but

apparently enough to exert a direly needed physiological response and rescue. We therefore speculate, that these two proteins (Futsch and Rab4) seems to be required in a similar tightly controlled levels and are involved in a biological process(es) devoid of Rab5. Why Rab4 and not Rab5 was able to recover motility in TBPH mutant flies is still obscure. Could it be that Rab4 is more effective in its action of balancing the vesicular traffic between the recycling and degradation pathways? This action is quite important for the maintenance of general metabolism and special cellular features such as secretion and transmission. Indeed, both Rab proteins recovered the level of Futsch and pMad and even though, Rab5-GFP's level was almost double the level of Rab4-GFP when expressed in the TBPH mutant flies (Figure 54), its phenotypic readout of motility was not recovered and its larvae retained their motility defects similarly to the TBPH mutant flies (Figure 53).

5.9 Futsch improved the level of synaptic pMad in TBPH mutant flies

Phosphorylated mad is an important component of the BMP signalling pathway without which the growth signal coming from the muscle does not reach the nucleus of the connecting motor neuron. Mothers against *dpp*, (*Mad*) is phosphorylated by the BMP receptors wishful thinking (*wit*), saxophone (*sax*) and thickvein (*tkv*) upon receiving the glass boat bottom (*gbb*) signal from the underlying muscle. This in turn forms a complex with

medea (*Medea*) that facilitates translocation to the nucleus where it modulates the expression of target genes in the motor neuron (Aberle *et al.,* 2002; Marqués *et al.,* 2002; McCabe *et al.,* 2003; Rawson *et al.,* 2003). Loss of BMP signalling has been shown to alter Futsch distribution in motor neurons (Ellis *et al.,* 2010). Consistent with this claim is the observed mild but significant recovery of this BMP transducer that is significantly lost in TBPH mutant mutants by Futsch (Figure 60). Deshpande *et al.,* 2016 also reported a dramatic loss of pMad in TBPH mutants which is in accordance with reduced synaptic BMP signalling. Of note are previous works documenting Futsch as a key player in synaptic growth through its effect on microtubule network and stability (Roos *et al.,* 2000, Hummel *et al.,* 2000, Godena *et al.,* 2011). Also reported is a direct link between loss of microtubule stability and synaptic growth which presupposes a direct action for Futsch, a known microtubule stabilizer. A Futsch-dependent regulation of microtubule stability as a main target for BMP signalling in the regulation of synaptic growth has been proposed (Nahm *et al.,* 2013). Nahm and colleagues observed that dysregulated BMP signalling manifesting as synaptic growth defects were totally suppressed by Futsch mutations. They showed *Drosophila* fragile x mental retardation protein (dFMRP), a translational repressor of Futsch (Zhang *et al.,* 2001) acts downstream of BMP signalling to modulate the levels of Futsch which is tightly regulated to maintain microtubule stability

and in effect, neuronal viability. Although, the modulation of synaptic growth by Futsch was shown to be regulated by the BMP signalling pathway, the strength of the synaptic transmission was observed to be devoid of Futsch action (Ball *et al.,* 2010).

5.10 The interplay of vesicle recycling, Futsch and the BMP signalling in dTDP-43's ALS

TDP-43-induced synaptic growth defects are similar to those observed in reduced BMP signalling at the NMJ such as reduced bouton number and size (Rawson *et al.,* 2003). Its mis-regulation heavily affected the synaptic BMP signalling but not the nuclear BMP signalling. This indicates that the signalling defect occur upstream of Mad as a negative regulator of Mad (*Dad*) was able to suppress the NMJ's growth reductions induced by dTDP-43 (Deshpande *et al.,* 2016). Could TDP-43 also be a target of the BMP signalling? It is possible that the actions of dFMRP and TDP-43 on Futsch could be opposingly synergistic depending on the modulatory signaling of the BMP (Figure 62).

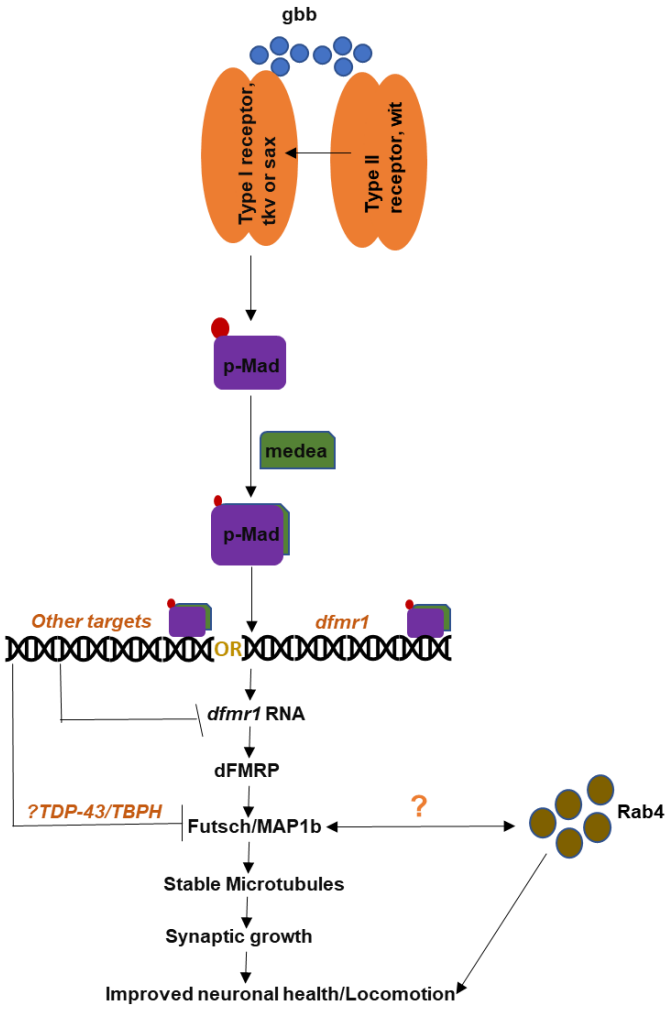

Figure 62 Schematic of a proposed BMP signalling model at the Drosophila NMJ. This supports a model where TBPH and dFMRP exerts an opposing synergistic effect on futsch to modulate microtubule stability and synaptic growth at the NMJ resulting in improved locomotion. Rab4 may act as a sensor for Futsch to modulate this action or Futsch may be a sensor for Rab4 to regulate endosomal trafficking rate to improve function. Future studies will be aimed at making this clarification.

A non-canonical role for synaptic pMad was proposed by (Sulkowski *et al.,* 2014). They suggested that the BMP signalling pathway monitors synaptic activity to adjust growth through the monitoring of presynaptic "BMP receptors-pMad dependent complexes" and the activities of post synaptic glutamate receptors IIA without requiring any *gbb* signal. So, synaptic pMad acts like a 'sensor' for the BMP signalling to adjust the

synaptic growth accordingly (Sulkowski *et al.,* 2014). GluRIIA was significantly reduced in TPBH mutant flies which apparently corelates with reduced synaptic pMad, a measure of reduced BMP signalling. Futsch was able to improve the level of GluRIIA when expressed in the neurons of TBPH mutant flies. This gives us another possible pathway Futsch may be involved in.

Traffic through the recycling endosomes was shown to be required to decrease BMP signalling and TDP-43 caused a loss of this signal by sequestrating BMP receptors from early to recycling endosomes (Deshpande *et al.,* 2016). This could explain why Rab4 involved in the regulation of the early-recycling-degradation pathway was able to recover motility of TBPH mutant larva and Rab5 involved in endocytic budding did not, given their respective actions. Futsch could be interacting with Rab4 to increase the recycling rate of the BMP receptors or even its ligand. More studies are in order to uncover this important link.

Data from the mammalian systems also suggest BMP signalling as a regulator of MAPs, a group into which Futsch (MAP1B) belongs. Using mammalian neuron cultures, BMP7 (mammalian homologue of *Drosophila gbb*) has been described as a regulator of microtubule stabilization through the phosphorylation of MAP2 (Podkowa *et al.,* 2010; Withers *et al.,* 2000). Similar report was given by (Björkblom *et al.,* 2005)

where MAP2 was implicated as an effector of the JUN kinase 1 enzyme in the maintenance of dendritic architecture. Spichthyin (NIPA1), Spastin and Spartin are proteins involved in the neurodegenerative disease, HSP (hereditary spastic paraplegia) and are localized to endosomes. They have been found to be inhibitors of the BMP signalling pathway both in *Drosophila* and mammalian systems (Nahm *et al.,* 2013; Tsang *et al.*, 2009; Tsang *et al.,* 2007). This is through their regulatory roles in the internalization and endosomal trafficking of BMP receptors. Thus, a common role of pathological importance for BMP signalling in various neurodegenerative diseases is presumable.

In a *Drosophila* model of ALS, (Ratnaparkhi *et al.,* 2008) observed a corresponding loss of pMad when VAPB (vesicle associated protein B) level was reduced and vice versa. Also, the level and distribution of Futsch was also impaired in VAP mutants suggesting a direct effect on microtubules. VAP levels were found to be reduced in ALS patients and mutant SOD transgenic mice (Teuling *et al.,* 2007). Smad (Mad) has been reported to bind directly to microtubules and only dissociate to return to the nucleus upon the microtubules undergoing phosphorylation (Dong et al., 2000). (Wang *et al.,* 2007) found that BMP signalling is required for microtubule stability in motor neurons and loss of *tkv* (Thickvein) resulted in defective microtubules and reduced tubulin. So, all of these taken

together gives credence to the observation of Futsch recovering not only synaptic proteins but also vesicle recycling and a BMP effector protein all of which are deficient in our TDP-43 model of ALS.

Evidence that the BMP signalling may be impaired in human ALS patients is gradually coming to light. A report by (Nakamura *et al.,* 2008) showed a significant reduction in the levels of nuclear pSmad and also found cytoplasmic round hyaline inclusions containing sequestrated pSmad. These are reported in specimens of motor neurons from human sporadic ALS spinal cords. So, upregulating the BMP signalling in the neurons through Futsch and Rab4 actions seems to be a viable therapeutic scheme of action worthy of future pursuit.

Research into identifying biomarkers of ALS progression in humans yielded smad 1, 3, and 8 (Mad in *Drosophila*) as biomarkers of disease progression in the skeletal muscles harvested from a cohort of ALS patients. This was confirmed using the SOD1 mouse model (Yi *et al.,* 2014). Also, identified is the TGF-beta (*gbb* in *Drosophila*) family of ligand in the muscles as a marker of disease progression. This, the authors confirmed using the C2C12 muscle cell lines (Yi *et al.,* 2015). Their results corelated with an increase in the expression and levels of the ligand, the described smads, and muscle weakness in ALS patients as the disease progresses. So, the smads and the TGF-beta ligand are viable as

biomarkers that could predict ALS disease progression in humans. This is an important feat because it provides a good diagnostic approach into discovering the disease early before clinical symptomatic manifestations and could help to improve the prognosis while research into its cure is on-going.

6.0 Conclusions and Recommendations

6.1 Conclusions

The discovery of mutations in proteins associated with microtubule organization and stability in human diseases such as ALS, Hereditary spastic paraplegias, fragile X mental retardation, among others (Ellis *et al.*, 2010) gave credence to the stature of microtubule wholeness in neuronal function. BMP signalling has been implicated in the maintenance of microtubule architecture (Wang *et al.,* 2007). In characterizing the role of Futsch/MAP1B in the rescue of locomotion defects in a TDP-43 model of ALS, we were able to observe and understand that Futsch is important in a variety of processes at the neuromuscular junction. TBPH mutants, our model of ALS have major dysfunctions in Futsch levels and distribution, microtubule stability and in processes involving stable microtubules such as axonal transport. Futsch expression was able to resolve this microtubule defect and other synaptic proteins loss thus, enhancing the viability of the motor neurons probably through a more active and effective BMP signalling response resulting from improved vesicle recycling of its receptors. This is presumably one of the reasons why expressing Futsch in the neurons of TBPH mutant flies was sufficient to significantly recover one of the major symptoms of the disease that is a direct read-out of motor neuron degeneration, defective locomotion.

Targeting endosomal trafficking of the BMP receptors/effectors remain a future therapeutic target to return the growth signalling function as there is observed recycling defects in TDP-43 induced ALS which was improved by Futsch expression. So, Futsch is also another probable candidate for therapeutic tests.

6.2 Some recommendations

Listed below are some of the experiments that we would be interested to perform to deeply investigate the relationship of Futsch, vesicle recycling and the BMP signalling.

- It would be interesting to see if Futsch recovers the levels of Rab4 as Rab4 was able to significantly improve its levels.
- Further experiments are required to test the localization of Rab4 in the boutons at the NMJ preferably using the FM1-43 dye protocol. It would be interesting to see their co-localization on live imaging.
- The unravelling of the exact nature of the sub-boutonic structures observed is also worthy of future pursuits.
- In addition, more experiments are required to test Futsch and Rab4 recovery of BMP receptors and transducers preferably using their respective mutants or even double mutants.

REFERENCES

Aberle, H., Haghighi, A. P., Fetter, R. D., McCabe, B. D., Magalhães, T. R., & Goodman, C. S. (2002). Wishful thinking encodes a BMP type II receptor that regulates synaptic growth in Drosophila. *Neuron*, *33*(4), 545–558. https://doi.org/10.1016/S0896-6273(02)00589-5

Al-Chalabi, A., Jones, A., Troakes, C., King, A., Al-Sarraj, S., & Van Den Berg, L. H. (2012). The genetics and neuropathology of amyotrophic lateral sclerosis. *Acta Neuropathologica*. https://doi.org/10.1007/s00401-012-1022-4

Al-Chalabi, A., Van Den Berg, L. H., & Veldink, J. (2017). Gene discovery in amyotrophic lateral sclerosis: Implications for clinical management. *Nature Reviews Neurology*. https://doi.org/10.1038/nrneurol.2016.182

Alami, N. H., Smith, R. B., Carrasco, M. A., Williams, L. A., Winborn, C. S., Han, S. S. W., … Taylor, J. P. (2014). Axonal Transport of TDP-43 mRNA Granules Is Impaired by ALS-Causing Mutations. *Neuron*, *81*(3), 536–543. https://doi.org/10.1016/j.neuron.2013.12.018

Anderson, P., & Kedersha, N. (2008). Stress granules: the Tao of RNA triage. *Trends in Biochemical Sciences*. https://doi.org/10.1016/j.tibs.2007.12.003

Andrieux, A., Salin, P., Schweitzer, A., Bégou, M., Pachoud, B., Brun, P., … Job, D. (2006). Microtubule Stabilizer Ameliorates Synaptic Function and Behavior in a Mouse Model for Schizophrenia. *Biological Psychiatry*. https://doi.org/10.1016/j.biopsych.2006.03.048

Atwood, H. L., Govind, C. K., & Wu, C. F. (1993). Differential ultrastructure of synaptic terminals on ventral longitudinal abdominal muscles in Drosophila larvae. *Journal of Neurobiology*, *24*(8), 1008–1024. https://doi.org/10.1002/neu.480240803

Aulas, A., & Vande Velde, C. (2015). Alterations in stress granule dynamics driven by TDP-43 and FUS: a link to pathological inclusions in ALS? *Frontiers in Cellular Neuroscience*. https://doi.org/10.3389/fncel.2015.00423

Ayala, Y. M., De Conti, L., Avendaño-Vázquez, S. E., Dhir, A., Romano, M., D'Ambrogio, A., … Baralle, F. E. (2011). TDP-43 regulates its mRNA levels through a negative feedback loop. *EMBO Journal*. https://doi.org/10.1038/emboj.2010.310

Baetz, N. W., & Goldenring, J. R. (2013). Rab11-family interacting proteins define spatially and temporally distinct regions within the dynamic Rab11a-dependent recycling system. *Molecular Biology of the Cell*. https://doi.org/10.1091/mbc.e12-09-0659

Ball, R. W., Warren-Paquin, M., Tsurudome, K., Liao, E. H., Elazzouzi, F., Cavanagh, C., … Haghighi, A. P. (2010). Retrograde BMP signaling controls synaptic growth at the nmj by regulating trio expression in motor neurons. *Neuron*, *66*(4), 536–549. https://doi.org/10.1016/j.neuron.2010.04.011

Barber, S. C., Mead, R. J., & Shaw, P. J. (2006). Oxidative stress in ALS: A mechanism of neurodegeneration and a therapeutic target. *Biochimica et Biophysica Acta - Molecular Basis of Disease*. https://doi.org/10.1016/j.bbadis.2006.03.008

Benard, G., Bellance, N., James, D., Parrone, P., Fernandez, H., Letellier, T., & Rossignol, R. (2007). Mitochondrial bioenergetics and structural network organization. *Journal of Cell Science*. https://doi.org/10.1242/jcs.03381

Bilican, B., Serio, A., Barmada, S. J., Nishimura, A. L., Sullivan, G. J., Carrasco, M., … Chandran, S. (2012). Mutant induced pluripotent stem cell lines recapitulate aspects of TDP-43 proteinopathies and reveal cell-specific vulnerability. *Proceedings of the National Academy of Sciences*. https://doi.org/10.1073/pnas.1202922109

Björkblom, B., Östman, N., Hongisto, V., Komarovski, V., Filén, J. J., Nyman, T. A., … Coffey, E. T. (2005). Constitutively active cytoplasmic c-Jun N-terminal kinase 1 is a dominant regulator of dendritic architecture: Role of microtubule-associated protein 2 as an effector. *Journal of Neuroscience*, *25*(27), 6350–6361. https://doi.org/10.1523/JNEUROSCI.1517-05.2005

Blizzard, C. A., Southam, K. A., Dawkins, E., Lewis, K. E., King, A. E., Clark, J. A., & Dickson, T. C. (2015). Identifying the primary site of

pathogenesis in amyotrophic lateral sclerosis - vulnerability of lower motor neurons to proximal excitotoxicity. *Disease Models & Mechanisms*. https://doi.org/10.1242/dmm.018606

Bodakuntla, S., Jijumon, A., Villablanca, C., Gonzalez-Billault, C., & Janke, C. (n.d.). *Microtubule-associated proteins: structuring the cytoskeleton*. https://doi.org/10.1016/j.tcb.2019.07.004ï

Bordet, T., Buisson, B., Michaud, M., Drouot, C., Galea, P., Delaage, P., … Pruss, R. M. (2007). Identification and Characterization of Cholest-4-en-3-one, Oxime (TRO19622), a Novel Drug Candidate for Amyotrophic Lateral Sclerosis. *Journal of Pharmacology and Experimental Therapeutics*. https://doi.org/10.1124/jpet.107.123000

Bowling, A. C., Schulz, J. B., Brown, R. H., & Beal, M. F. (1993). Superoxide Dismutase Activity, Oxidative Damage, and Mitochondrial Energy Metabolism in Familial and Sporadic Amyotrophic Lateral Sclerosis. *Journal of Neurochemistry*. https://doi.org/10.1111/j.1471-4159.1993.tb07478.x

Brand, H., & Perrimon, N. (n.d.). *402 A*.

Brandt, R. (2001). Cytoskeletal mechanisms of neuronal morphogenesis. *Zoology*. https://doi.org/10.1078/0944-2006-00027

Brenner, D., Mü, K., Wieland, T., Weydt, P., Bö Hm, S., Lulé, D. E., … Weishaupt, J. (n.d.). *LETTER TO THE EDITOR NEK1 mutations in familial amyotrophic lateral sclerosis*. https://doi.org/10.1093/brain/aww033

Brunden, K. R., Lee, V. M. Y., Smith, A. B., Trojanowski, J. Q., & Ballatore, C. (2017). Altered microtubule dynamics in neurodegenerative disease: Therapeutic potential of microtubule-stabilizing drugs. *Neurobiology of Disease*, *105*, 328–335. https://doi.org/10.1016/j.nbd.2016.12.021

Buratti, E., & Baralle, F. E. (2009). Chapter 1 The Molecular Links Between TDP-43 Dysfunction and Neurodegeneration. *Advances in Genetics*. https://doi.org/10.1016/S0065-2660(09)66001-6

Buratti, E., & Baralle, F. E. (2010). The multiple roles of TDP-43 in pre-mRNA processing and gene expression regulation. *RNA Biology*, *7*(4), 420–429. https://doi.org/10.4161/rna.7.4.12205

Burgoyne, R. D., & Morgan, A. (2015). Cysteine string protein (CSP) and its role in preventing neurodegeneration. *Seminars in Cell and Developmental Biology*, *40*, 153–159. https://doi.org/10.1016/j.semcdb.2015.03.008

Bush, M. S. (1996). An analysis of an axonal gradient of phosphorylated MAP 1B in cultured rat sensory neurons. *European Journal of Neuroscience*. https://doi.org/10.1111/j.1460-9568.1996.tb01208.x

Carletti, B., Passarelli, C., Sparaco, M., Tozzi, G., Pastore, A., Bertini, E., & Piemonte, F. (2011). Effect of protein glutathionylation on neuronal cytoskeleton: A potential link to neurodegeneration. *Neuroscience*. https://doi.org/10.1016/j.neuroscience.2011.05.060

Cartelli, D., Ronchi, C., Maggioni, M. G., Rodighiero, S., Giavini, E., & Cappelletti, G. (2010). Microtubule dysfunction precedes transport impairment and mitochondria damage in MPP+-induced neurodegeneration. *Journal of Neurochemistry*. https://doi.org/10.1111/j.1471-4159.2010.06924.x

Cassimeris, L. (2010). Microtubule Associated Proteins in Neurons. *Encyclopedia of Neuroscience*, 865–870. https://doi.org/10.1016/B978-008045046-9.00725-7

Chen, H., Qian, K., Du, Z., Cao, J., Petersen, A., Liu, H., … Zhang, S. C. (2014). Modeling ALS with iPSCs reveals that mutant SOD1 misregulates neurofilament balance in motor neurons. *Cell Stem Cell*. https://doi.org/10.1016/j.stem.2014.02.004

Chiang, P.-M., Ling, J., Jeong, Y. H., Price, D. L., Aja, S. M., & Wong, P. C. (2010). Deletion of TDP-43 down-regulates Tbc1d1, a gene linked to obesity, and alters body fat metabolism. *Proceedings of the National Academy of Sciences*. https://doi.org/10.1073/pnas.1002176107

Chiò, A., Logroscino, G., Hardiman, O., Swingler, R., Mitchell, D., Beghi, E., & Traynor, B. G. (2009). Prognostic factors in ALS: A critical review. *Amyotrophic Lateral Sclerosis*. https://doi.org/10.3109/17482960802566824

Clark, J. A., Yeaman, E. J., Blizzard, C. A., Chuckowree, J. A., & Dickson, T. C. (2016). A Case for Microtubule Vulnerability in Amyotrophic Lateral Sclerosis: Altered Dynamics During Disease. *Frontiers in Cellular*

Neuroscience, *10*(September), 1–16. https://doi.org/10.3389/fncel.2016.00204

Cogliati, S., Frezza, C., Soriano, M. E., Varanita, T., Quintana-Cabrera, R., Corrado, M., … Scorrano, L. (2013). Mitochondrial cristae shape determines respiratory chain supercomplexes assembly and respiratory efficiency. *Cell*. https://doi.org/10.1016/j.cell.2013.08.032

Coyne, A. N., Siddegowda, B. B., Estes, P. S., Johannesmeyer, J., Kovalik, T., Daniel, S. G., … Zarnescu, D. C. (2014). Futsch/MAP1B mRNA Is a Translational Target of TDP-43 and Is Neuroprotective in a Drosophila Model of Amyotrophic Lateral Sclerosis. *Journal of Neuroscience*. https://doi.org/10.1523/jneurosci.2526-14.2014

Cueille, N., Blanc, C. T., Popa-Nita, S., Kasas, S., Catsicas, S., Dietler, G., & Riederer, B. M. (2007). Characterization of MAP1B heavy chain interaction with actin. *Brain Research Bulletin*, *71*(6), 610–618. https://doi.org/10.1016/j.brainresbull.2006.12.003

da Cruz, A. B. (2005). Disruption of the MAP1B-related Protein FUTSCH Leads to Changes in the Neuronal Cytoskeleton, Axonal Transport Defects, and Progressive Neurodegeneration in Drosophila. *Molecular Biology of the Cell*. https://doi.org/10.1091/mbc.e04-11-1004

Davis, S. A., Itaman, S., Khalid-Janney, C. M., Sherard, J. A., Dowell, J. A., Cairns, N. J., & Gitcho, M. A. (2018). TDP-43 interacts with mitochondrial proteins critical for mitophagy and mitochondrial dynamics. *Neuroscience Letters*, *678*, 8–15. https://doi.org/10.1016/j.neulet.2018.04.053

De vos, K. J., Chapman, A. L., Tennant, M. E., Manser, C., Tudor, E. L., Lau, K. F., … Grierson, A. J. (2007). Familial amyotrophic lateral sclerosis-linked SOD1 mutants perturb fast axonal transport to reduce axonal mitochondria content. *Human Molecular Genetics*. https://doi.org/10.1093/hmg/ddm226

De Vos, K. J., & Hafezparast, M. (2017). Neurobiology of axonal transport defects in motor neuron diseases: Opportunities for translational research? *Neurobiology of Disease*, *105*, 283–299. https://doi.org/10.1016/j.nbd.2017.02.004

DeJesus-Hernandez, M., Mackenzie, I. R., Boeve, B. F., Boxer, A. L., Baker, M., Rutherford, N. J., … Rademakers, R. (2011). Expanded GGGGCC Hexanucleotide Repeat in Noncoding Region of C9ORF72 Causes Chromosome 9p-Linked FTD and ALS. *Neuron*. https://doi.org/10.1016/j.neuron.2011.09.011

Delgado, R., Maureira, C., Oliva, C., Kidokoro, Y., & Labarca, P. (2000). Size of vesicle pools, rates of mobilization, and recycling at neuromuscular synapses of a Drosophila mutant, shibire. *Neuron*, *28*(3), 941–953. https://doi.org/10.1016/S0896-6273(00)00165-3

Deng, H.-X., Shi, Y., Furukawa, Y., Zhai, H., Fu, R., Liu, E., … Siddique, T. (2006). Conversion to the amyotrophic lateral sclerosis phenotype is associated with intermolecular linked insoluble aggregates of SOD1 in mitochondria. *Proceedings of the National Academy of Sciences*. https://doi.org/10.1073/pnas.0602046103

Deng, H. X., Chen, W., Hong, S. T., Boycott, K. M., Gorrie, G. H., Siddique, N., … Siddique, T. (2011). Mutations in UBQLN2 cause dominant X-linked juvenile and adult-onset ALS and ALS/dementia. *Nature*. https://doi.org/10.1038/nature10353

Deshpande, M., Feiger, Z., Shilton, A. K., Luo, C. C., Silverman, E., & Rodal, A. A. (2016). Role of BMP receptor traffic in synaptic growth defects in an ALS model. *Molecular Biology of the Cell*, *27*(19), 2898–2910. https://doi.org/10.1091/mbc.E16-07-0519

Dey, S., Banker, G., & Ray, K. (2017). Anterograde Transport of Rab4-Associated Vesicles Regulates Synapse Organization in Drosophila. *Cell Reports*, *18*(10), 2452–2463. https://doi.org/10.1016/j.celrep.2017.02.034

Diaper, D. C., Adachi, Y., Sutcliffe, B., Humphrey, D. M., Elliott, C. J. H., Stepto, A., … Hirth, F. (2013). Loss and gain of Drosophila TDP-43 impair synaptic efficacy and motor control leading to age-related neurodegeneration by loss-of-function phenotypes. *Human Molecular Genetics*, *22*(8), 1539–1557. https://doi.org/10.1093/hmg/ddt005

Droppelmann, C. A., Campos-Melo, D., Volkening, K., & Strong, M. J. (2014). The emerging role of guanine nucleotide exchange factors in ALS and other neurodegenerative diseases. *Frontiers in Cellular Neuroscience*. https://doi.org/10.3389/fncel.2014.00282

Dugger, B. N., & Dickson, D. W. (2017). Pathology of neurodegenerative diseases. *Cold Spring Harbor Perspectives in Biology*. https://doi.org/10.1101/cshperspect.a028035

Edens, B. M., Yan, J., Miller, N., Deng, H. X., Siddique, T., & Ma, Y. C. (2017). A novel ALS-associated variant in UBQLN4 regulates motor axon morphogenesis. *ELife*. https://doi.org/10.7554/eLife.25453

Elden, A. C., Kim, H. J., Hart, M. P., Chen-Plotkin, A. S., Johnson, B. S., Fang, X., … Gitler, A. D. (2010). Ataxin-2 intermediate-length polyglutamine expansions are associated with increased risk for ALS. *Nature*. https://doi.org/10.1038/nature09320

Ellis, J. E., Parker, L., Cho, J., & Arora, K. (2010). Activin signaling functions upstream of Gbb to regulate synaptic growth at the Drosophila neuromuscular junction. *Developmental Biology*, *342*, 121–133. https://doi.org/10.1016/j.ydbio.2010.03.012

Estes, P. S., Boehringer, A., Zwick, R., Tang, J. E., Grigsby, B., & Zarnescu, D. C. (2011). Wild-type and A315T mutant TDP-43 exert differential neurotoxicity in a Drosophila model of ALS. *Human Molecular Genetics*. https://doi.org/10.1093/hmg/ddr124

Fallini, C., Bassell, G. J., & Rossoll, W. (2012). The ALS disease protein TDP-43 is actively transported in motor neuron axons and regulates axon outgrowth. *Human Molecular Genetics*. https://doi.org/10.1093/hmg/dds205

Fasshauer, D., Sutton, R. B., Brunger, A. T., & Jahn, R. (1998). Conserved structural features of the synaptic fusion complex: SNARE proteins reclassified as Q- and R-SNAREs. *Proceedings of the National Academy of Sciences*. https://doi.org/10.1073/pnas.95.26.15781

Feiguin, F., Godena, V. K., Romano, G., D'Ambrogio, A., Klima, R., & Baralle, F. E. (2009). Depletion of TDP-43 affects Drosophila motoneurons terminal synapsis and locomotive behavior. *FEBS Letters*, *583*(10), 1586–1592. https://doi.org/10.1016/j.febslet.2009.04.019

Fischer, L. R., Culver, D. G., Tennant, P., Davis, A. A., Wang, M., Castellano-Sanchez, A., … Glass, J. D. (n.d.). *Amyotrophic lateral sclerosis is a distal axonopathy: evidence in mice and man*. https://doi.org/10.1016/j.expneurol.2003.10.004

Frederick, R. L., & Shaw, J. M. (2007). Moving mitochondria: Establishing distribution of an essential organelle. *Traffic*. https://doi.org/10.1111/j.1600-0854.2007.00644.x

Gan, Q., & Watanabe, S. (2018). Synaptic Vesicle Endocytosis in Different Model Systems. *Frontiers in Cellular Neuroscience*. https://doi.org/10.3389/fncel.2018.00171

Godena, V. K., Romano, G., Romano, M., Appocher, C., Klima, R., Buratti, E., … Feiguin, F. (2011). TDP-43 regulates drosophila neuromuscular junctions growth by modulating futsch/MAP1B levels and synaptic microtubules organization. *PLoS ONE*, *6*(3). https://doi.org/10.1371/journal.pone.0017808

Gonzalez-Billault, C., Avila, J., & Cáceres, A. (2001). Evidence for the Role of MAP1B in Axon Formation. In *Molecular Biology of the Cell* (Vol. 12).

Gorczyca, M., Augart, C., & Budnik, V. (1993). Insulin-like receptor and insulin-like peptide are localized at neuromuscular junctions in Drosophila. *The Journal of Neuroscience*. https://doi.org/10.1523/jneurosci.13-09-03692.1993

Gordon, P. (2013). Amyotrophic Lateral Sclerosis: An update for 2013 Clinical Features, Pathophysiology, Management and Therapeutic Trials. *Aging and Disease*. https://doi.org/10.14336/ad.2013.0400295

Halpain, S., & Dehmelt, L. (2006). The MAP1 family of microtubule-associated proteins. *Genome Biology*, *7*(6), 1–7. https://doi.org/10.1186/gb-2006-7-6-224

Highley, J. R., Kirby, J., Jansweijer, J. A., Webb, P. S., Hewamadduma, C. A., Heath, P. R., … Ince, P. G. (2014). Loss of nuclear TDP-43 in amyotrophic lateral sclerosis (ALS) causes altered expression of splicing machinery and widespread dysregulation of RNA splicing in motor neurones. *Neuropathology and Applied Neurobiology*. https://doi.org/10.1111/nan.12148

Hilfiker, S., Pieribone, V. A., Czernik, A. J., Kao, H. T., Augustine, G. J., & Greengard, P. (1999). Synapsins as regulators of neurotransmitter release. *Philosophical Transactions of the Royal Society B: Biological Sciences*, *354*(1381), 269–279. https://doi.org/10.1098/rstb.1999.0378

Hirano, A., Nakano, I., Kurland, L. T., Mulder, D. W., Holley, P. W., & Saccomanno, G. (1984). Fine structural study of neurofibrillary changes in a family with amyotrophic lateral sclerosis. *Journal of Neuropathology and Experimental Neurology*. https://doi.org/10.1097/00005072-198409000-00002

Hirano, M., Quinzii, C. M., Mitsumoto, H., Hays, A. P., Roberts, J. K., Richard, P., & Rowland, L. P. (2011). Senataxin mutations and amyotrophic lateral sclerosis. *Amyotrophic Lateral Sclerosis*. https://doi.org/10.3109/17482968.2010.545952

Hobson, E. V., & McDermott, C. J. (2016). Supportive and symptomatic management of amyotrophic lateral sclerosis. *Nature Reviews Neurology*, *12*(9), 526–538. https://doi.org/10.1038/nrneurol.2016.111

Hoopmann, P., Punge, A., Barysch, S. V., Westphal, V., Buckers, J., Opazo, F., … Rizzoli, S. O. (2010). Endosomal sorting of readily releasable synaptic vesicles. *Proceedings of the National Academy of Sciences*. https://doi.org/10.1073/pnas.1007037107

Hummel, T., Krukkert, K., Roos, J., Davis, G., & Klämbt, C. (2000). Drosophila Futsch/22C10 is a MAP1B-like protein required for dendritic and axonal development. *Neuron*, *26*(2), 357–370. https://doi.org/10.1016/S0896-6273(00)81169-1

Hutton, M., Lendon, C. L., Rizzu, P., Baker, M., Froelich, S., Houlden, H. H., … Heutink, P. (1998). Association of missense and 5’-splice-site mutations in tau with the inherited dementia FTDP-17. *Nature*. https://doi.org/10.1038/31508

Igaz, L. M., Kwong, L. K., Lee, E. B., Chen-Plotkin, A., Swanson, E., Unger, T., … Lee, V. M. Y. (2011). Dysregulation of the ALS-associated gene TDP-43 leads to neuronal death and degeneration in mice. *Journal of Clinical Investigation*. https://doi.org/10.1172/JCI44867

Ikawa, M., Okazawa, H., Tsujikawa, T., Matsunaga, A., Yamamura, O., Mori, T., … Yoneda, M. (2015). Increased oxidative stress is related to disease severity in the ALS motor cortex. *Neurology*. https://doi.org/10.1212/WNL.0000000000001588

Israelson, A., Arbel, N., Da Cruz, S., Ilieva, H., Yamanaka, K., Shoshan-Barmatz, V., & Cleveland, D. W. (2010). Misfolded mutant SOD1 directly

inhibits VDAC1 conductance in a mouse model of inherited ALS. *Neuron*. https://doi.org/10.1016/j.neuron.2010.07.019

Ito-Ishida, A., Miyazaki, T., Miura, E., Matsuda, K., Watanabe, M., Yuzaki, M., & Okabe, S. (2012). Presynaptically Released Cbln1 Induces Dynamic Axonal Structural Changes by Interacting with GluD2 during Cerebellar Synapse Formation. *Neuron*. https://doi.org/10.1016/j.neuron.2012.07.027

Jahn, R., Lang, T., & Sü Dhof, T. C. (2003). Review Membrane Fusion dynamic supramolecular assemblies involving con. In *Cell* (Vol. 112).

Janke, C., & Montagnac, G. (2017). Causes and Consequences of Microtubule Acetylation. *Current Biology*, *27*(23), R1287–R1292. https://doi.org/10.1016/j.cub.2017.10.044

Janssens, J., Wils, H., Kleinberger, G., Joris, G., Cuijt, I., Ceuterick-De Groote, C., … Kumar-Singh, S. (2013). Overexpression of ALS-associated p.M337V human TDP-43 in mice worsens disease features compared to wild-type human TDP-43 mice. *Molecular Neurobiology*. https://doi.org/10.1007/s12035-013-8427-5

Jiang, Z., Wang, W., Perry, G., Zhu, X., & Wang, X. (2015). Mitochondrial dynamic abnormalities in amyotrophic lateral sclerosis. *Translational Neurodegeneration*, *4*(1), 1–6. https://doi.org/10.1186/s40035-015-0037-x

Johnson, G. V. W., & Bailey, C. D. C. (2002). Tau, where are we now? *Journal of Alzheimer's Disease*, *4*(5), 375–398. https://doi.org/10.3233/JAD-2002-4505

Johnson, J. O., Pioro, E. P., Boehringer, A., Chia, R., Feit, H., Renton, A. E., … Pirisi, A. (2014). Mutations in the Matrin 3 gene cause familial amyotrophic lateral sclerosis. *Nature Neuroscience*. https://doi.org/10.1038/nn.3688

Jovičič, A., Mertens, J., Boeynaems, S., Bogaert, E., Chai, N., Yamada, S. B., … Gitler, A. D. (2015). Modifiers of C9orf72 dipeptide repeat toxicity connect nucleocytoplasmic transport defects to FTD/ALS. *Nature Neuroscience*. https://doi.org/10.1038/nn.4085

Kabashi, E., Bercier, V., Lissouba, A., Liao, M., Brustein, E., Rouleau, G. A., & Drapeau, P. (2011). Fus and tardbp but not sod1 interact in genetic models of amyotrophic lateral sclerosis. *PLoS Genetics*. https://doi.org/10.1371/journal.pgen.1002214

Kabashi, E., Lin, L., Tradewell, M. L., Dion, P. A., Bercier, V., Bourgouin, P., … Drapeau, P. (2009). Gain and loss of function of ALS-related mutations of TARDBP (TDP-43) cause motor deficits in vivo. *Human Molecular Genetics*. https://doi.org/10.1093/hmg/ddp534

Kawahara, Y., Ito, K., Sun, H., Aizawa, H., Kanazawa, I., & Kwak, S. (2004). RNA editing and death of motor neurons: There is a glutamate-receptor defect in patients with amyotrophic lateral sclerosis. *Nature*. https://doi.org/10.1038/427801a

Kawamata, H., & Manfredi, G. (2010). Mitochondrial dysfunction and intracellular calcium dysregulation in ALS. *Mechanisms of Ageing and Development*. https://doi.org/10.1016/j.mad.2010.05.003

Kelly, S. M., Elchert, A., & Kahl, M. (2017). Dissection and Immunofluorescent Staining of Mushroom Body and Photoreceptor Neurons in Adult Drosophila melanogaster Brains. *Journal of Visualized Experiments*, *32*(129), 1–13. https://doi.org/10.3791/56174

Keshishian, H. (1996). The Drosophila Neuromuscular Junction: A Model System for Studying Synaptic Development and Function. *Annual Review of Neuroscience*, *19*(1), 545–575. https://doi.org/10.1146/annurev.neuro.19.1.545

Ketschek, A., Jones, S., Spillane, M., Korobova, F., Svitkina, T., & Gallo, G. (2015). Nerve growth factor promotes reorganization of the axonal microtubule array at sites of axon collateral branching. *Developmental Neurobiology*. https://doi.org/10.1002/dneu.22294

Kim, H. J., Raphael, A. R., Ladow, E. S., Mcgurk, L., Weber, R. A., Trojanowski, J. Q., … Bonini, N. M. (2014). Therapeutic modulation of eIF2α phosphorylation rescues TDP-43 toxicity in amyotrophic lateral sclerosis disease models. *Nature Genetics*. https://doi.org/10.1038/ng.2853

King, A. E., Southam, K. A., Dittmann, J., & Vickers, J. C. (2014). Excitotoxin-induced caspase-3 activation and microtubule disintegration

in axons is inhibited by taxol. *Acta Neuropathologica Communications*. https://doi.org/10.1186/2051-5960-1-59

Kiskinis, E., Kralj, J. M., Zou, P., Weinstein, E. N., Zhang, H., Tsioras, K., … Cohen, A. E. (2018). All-Optical Electrophysiology for High-Throughput Functional Characterization of a Human iPSC-Derived Motor Neuron Model of ALS. *Stem Cell Reports*. https://doi.org/10.1016/j.stemcr.2018.04.020

Kleele, T., Marinković, P., Williams, P. R., Stern, S., Weigand, E. E., Engerer, P., … Misgeld, T. (2014). An assay to image neuronal microtubule dynamics in mice. *Nature Communications*. https://doi.org/10.1038/ncomms5827

klima, raffaella, Romano, G., Gbadamos, M., Megighian, A., & Feiguin, F. (2021). Immuno-electrophysiology on Neuromuscular Junctions of Drosophila Third Instar Larva. *BIO-PROTOCOL*, *11*(3). https://doi.org/10.21769/bioprotoc.3913

Kohsaka, H., Okusawa, S., Itakura, Y., Fushiki, A., & Nose, A. (2012). Development of larval motor circuits in Drosophila. *Development, Growth & Differentiation*, *54*(3), 408–419. https://doi.org/10.1111/j.1440-169X.2012.01347.x

Koppers, M., van Blitterswijk, M. M., Vlam, L., Rowicka, P. A., van Vught, P. W. J., Groen, E. J. N., … van den Berg, L. H. (2012). VCP mutations in familial and sporadic amyotrophic lateral sclerosis. *Neurobiology of Aging*. https://doi.org/10.1016/j.neurobiolaging.2011.10.006

Kraemer, B. C., Schuck, T., Wheeler, J. M., Robinson, L. C., Trojanowski, J. Q., Lee, V. M. Y., & Schellenberg, G. D. (2010). Loss of Murine TDP-43 disrupts motor function and plays an essential role in embryogenesis. *Acta Neuropathologica*. https://doi.org/10.1007/s00401-010-0659-0

Kunst, C. B., Mezey, E., Brownstein, M. J., & Patterson, D. (1997). Mutations in SOD1 associated with amyotrophic lateral sclerosis cause novel protein interactions. *Nature Genetics*. https://doi.org/10.1038/ng0197-91

Kuromi, H., & Kidokoro, Y. (1998). Two distinct pools of synaptic vesicles in single presynaptic boutons in a temperature-sensitive Drosophila

mutant, shibire. *Neuron*, *20*(5), 917–925. Retrieved from http://www.ncbi.nlm.nih.gov/pubmed/9620696

Lagier-Tourenne, C., Polymenidou, M., Hutt, K. R., Vu, A. Q., Baughn, M., Huelga, S. C., … Yeo, G. W. (2012). Divergent roles of ALS-linked proteins FUS/TLS and TDP-43 intersect in processing long pre-mRNAs. *Nature Neuroscience*. https://doi.org/10.1038/nn.3230

Laird, A. S., van Hoecke, A., De Muynck, L., Timmers, M., van den Bosch, L., Van Damme, P., & Robberecht, W. (2010). Progranulin is neurotrophic in vivo and protects against a mutant TDP-43 induced axonopathy. *PLoS ONE*. https://doi.org/10.1371/journal.pone.0013368

Lanson, N. A., Maltare, A., King, H., Smith, R., Kim, J. H., Taylor, J. P., … Pandey, U. B. (2011). A Drosophila model of FUS-related neurodegeneration reveals genetic interaction between FUS and TDP-43. *Human Molecular Genetics*. https://doi.org/10.1093/hmg/ddr150

Lepicard, S., Franco, B., de Bock, F., & Parmentier, M.-L. (2014). A Presynaptic Role of Microtubule-Associated Protein 1/Futsch in Drosophila: Regulation of Active Zone Number and Neurotransmitter Release. *Journal of Neuroscience*, *34*(20), 6759–6771. https://doi.org/10.1523/jneurosci.4282-13.2014

Lezi, E., & Swerdlow, R. H. (2012). Mitochondria in neurodegeneration. *Advances in Experimental Medicine and Biology*. https://doi.org/10.1007/978-94-007-2869-1_12

Liachko, N. F., Saxton, A. D., McMillan, P. J., Strovas, T. J., Currey, H. N., Taylor, L. M., … Kraemer, B. C. (2016). The phosphatase calcineurin regulates pathological TDP-43 phosphorylation. *Acta Neuropathologica*. https://doi.org/10.1007/s00401-016-1600-y

Liu, W., Tian, F., Kurata, T., Morimoto, N., & Abe, K. (2012). Dynamic changes of mitochondrial fusion and fission proteins after transient cerebral ischemia in mice. *Journal of Neuroscience Research*, *90*(6), 1183–1189. https://doi.org/10.1002/jnr.23016

M Zerial, & H McBride. (2001). Rab proteins as membrane organizers. *Nature Reviews. Molecular Cell Biology*, *2*(2), 107–117. Retrieved from http://www.nature.com/nrm/journal/v2/n2/pdf/nrm0201_107a.pdf

Magrané, J., Cortez, C., Gan, W. B., & Manfredi, G. (2014). Abnormal mitochondrial transport and morphology are common pathological denominators in SOD1 and TDP43 ALS mouse models. *Human Molecular Genetics*. https://doi.org/10.1093/hmg/ddt528

Marqués, G., Bao, H., Haerry, T. E., Shimell, M. J., Duchek, P., Zhang, B., & O'Connor, M. B. (2002). The Drosophila BMP type II receptor wishful thinking regulates neuromuscular synapse morphology and function. *Neuron*, *33*(4), 529–543. https://doi.org/10.1016/S0896-6273(02)00595-0

Martens, S., & McMahon, H. T. (2008). Mechanisms of membrane fusion: disparate players and common principles. *Nature Reviews. Molecular Cell Biology*, *9*(7), 543–556. https://doi.org/10.1038/nrm2417

Maruyama, H., Morino, H., Ito, H., Izumi, Y., Kato, H., Watanabe, Y., … Kawakami, H. (2010). Mutations of optineurin in amyotrophic lateral sclerosis. *Nature*. https://doi.org/10.1038/nature08971

Matsuyama, S. S., & Jarvik, L. F. (1989). Hypothesis: microtubules, a key to Alzheimer disease. *Proceedings of the National Academy of Sciences*. https://doi.org/10.1073/pnas.86.20.8152

Mattiazzi, M., D'Aurelio, M., Gajewski, C. D., Martushova, K., Kiaei, M., Flint Beal, M., & Manfredi, G. (2002). Mutated human SOD1 causes dysfunction of oxidative phosphorylation in mitochondria of transgenic mice. *Journal of Biological Chemistry*. https://doi.org/10.1074/jbc.M203065200

Matus, S., Medinas, D. B., & Hetz, C. (2014). Common ground: Stem cell approaches find shared pathways underlying ALS. *Cell Stem Cell*. https://doi.org/10.1016/j.stem.2014.05.001

McBride, H. M., Neuspiel, M., & Wasiak, S. (2006). Mitochondria: More Than Just a Powerhouse. *Current Biology*. https://doi.org/10.1016/j.cub.2006.06.054

McCabe, B. D., Marqués, G., Haghighi, A. P., Fetter, R. D., Crotty, M. L., Haerry, T. E., … O'Connor, M. B. (2003). The BMP homolog Gbb provides a retrograde signal that regulates synaptic growth at the Drosophila neuromuscular junction. *Neuron*, *39*(2), 241–254. https://doi.org/10.1016/S0896-6273(03)00426-4

McDonald, K. K., Aulas, A., Destroismaisons, L., Pickles, S., Beleac, E., Camu, W., … Velde, C. Vande. (2011). TAR DNA-binding protein 43 (TDP-43) regulates stress granule dynamics via differential regulation of G3BP and TIA-1. *Human Molecular Genetics*. https://doi.org/10.1093/hmg/ddr021

McGurk, L., Berson, A., & Bonini, N. M. (2015). Drosophila as an in vivo model for human neurodegenerative disease. *Genetics*. https://doi.org/10.1534/genetics.115.179457

McMahon, H. T., & Gallop, J. L. (2005). Membrane curvature and mechanisms of dynamic cell membrane remodelling. *Nature*, *438*(7068), 590–596. https://doi.org/10.1038/nature04396

McMurray, C. T. (2000). Neurodegeneration: Diseases of the cytoskeleton? *Cell Death and Differentiation*. https://doi.org/10.1038/sj.cdd.4400764

Menon, K. P., Carrillo, R. A., & Zinn, K. (2013). Development and plasticity of the Drosophila larval neuromuscular junction. *Wiley Interdisciplinary Reviews. Developmental Biology*. https://doi.org/10.1002/wdev.108

Mizielinska, S., Grönke, S., Niccoli, T., Ridler, C. E., Clayton, E. L., Devoy, A., … Isaacs, A. M. (2014). C9orf72 repeat expansions cause neurodegeneration in Drosophila through arginine-rich proteins. *Science*. https://doi.org/10.1126/science.1256800

Monastirioti, M., Gorczyca, M., Rapus, J., Eckert, M., White, K., & Budnik, V. (1995). Octopamine immunoreactivity in the fruit fly Drosophila melanogaster. *Journal of Comparative Neurology*. https://doi.org/10.1002/cne.903560210

Muller, M., Liu, K. S. Y., Sigrist, S. J., & Davis, G. W. (2012). RIM Controls Homeostatic Plasticity through Modulation of the Readily-Releasable Vesicle Pool. *Journal of Neuroscience*. https://doi.org/10.1523/jneurosci.0981-12.2012

Muqit, M. M. K., & Feany, M. B. (2002). Modelling neurodegenerative diseases in Drosophila: A fruitful approach? *Nature Reviews Neuroscience*. https://doi.org/10.1038/nrn751

Murthy, V. N., & Camilli, P. De. (2003). C <scp>ELL</scp> B <scp>IOLOGY OF THE</scp> P <scp>RESYNAPTIC</scp> T <scp>ERMINAL</scp>. *Annual Review of Neuroscience*. https://doi.org/10.1146/annurev.neuro.26.041002.131445

Mushtaq, Z., Choudhury, S. D., Gangwar, S. K., Orso, G., & Kumar, V. (2016). Human Senataxin Modulates Structural Plasticity of the Neuromuscular Junction in Drosophila through a Neuronally Conserved TGFβ Signalling Pathway. *Neuro-Degenerative Diseases*, *16*(5–6), 324–336. https://doi.org/10.1159/000445435

Nahm, M., Lee, M. J., Parkinson, W., Lee, M., Kim, H., Kim, Y. J., … Lee, S. (2013). Spartin Regulates Synaptic Growth and Neuronal Survival by Inhibiting BMP-Mediated Microtubule Stabilization. *Neuron*, *77*(4), 680–695. https://doi.org/10.1016/j.neuron.2012.12.015

Nakamura, M., Ito, H., Wate, R., Nakano, S., Hirano, A., & Kusaka, H. (2008). Phosphorylated Smad2/3 immunoreactivity in sporadic and familial amyotrophic lateral sclerosis and its mouse model. *Acta Neuropathologica*, *115*(3), 327–334. https://doi.org/10.1007/s00401-007-0337-z

Neumann, M., Sampathu, D. M., Kwong, L. K., Truax, A. C., Micsenyi, M. C., Chou, T. T., … Lee, V. M. Y. (2006). Ubiquitinated TDP-43 in frontotemporal lobar degeneration and amyotrophic lateral sclerosis. *Science*. https://doi.org/10.1126/science.1134108

Nicolas, A., Kenna, K., Renton, A. E., Ticozzi, N., Faghri, F., Chia, R., … Traynor, B. J. (2018). Genome-wide Analyses Identify KIF5A as a Novel ALS Gene. *Neuron*. https://doi.org/10.1016/j.neuron.2018.02.027

Niwa, J. I., Ishigaki, S., Hishikawa, N., Yamamoto, M., Doyu, M., Murata, S., … Sobue, G. (2002). Dorfin ubiquitylates mutant SOD1 and prevents mutant SOD1-mediated neurotoxicity. *Journal of Biological Chemistry*. https://doi.org/10.1074/jbc.M206559200

O'Brien, E. T., Salmon, E. D., & Erickson, H. P. (1997). How calcium causes microtubule depolymerization. *Cell Motility and the Cytoskeleton*, *36*(2), 125–135. https://doi.org/10.1002/(SICI)1097-0169(1997)36:2<125::AID-CM3>3.0.CO;2-8

Oakes, J. A., Davies, M. C., & Collins, M. O. (2017). TBK1: a new player in ALS linking autophagy and neuroinflammation. *Molecular Brain*. https://doi.org/10.1186/s13041-017-0287-x

Palese, F., Sartori, A., Verriello, L., Ros, S., Passadore, P., Manganotti, P., … Pisa, F. E. (2019). Epidemiology of amyotrophic lateral sclerosis in Friuli-Venezia Giulia, North-Eastern Italy, 2002–2014: a retrospective population-based study. *Amyotrophic Lateral Sclerosis and Frontotemporal Degeneration*, *20*(1–2), 90–99. https://doi.org/10.1080/21678421.2018.1511732

Pandey, U. B., & Nichols, C. D. (2011). Human Disease Models in. *Pharmacological Reviews*, *63*(2), 411–436. https://doi.org/10.1124/pr.110.003293.411

Park, K. H. J., Franciosi, S., & Leavitt, B. R. (2013). Postnatal muscle modification by myogenic factors modulates neuropathology and survival in an ALS mouse model. *Nature Communications*. https://doi.org/10.1038/ncomms3906

Patzke, H., & Tsai, L. H. (2002). Cdk5 sinks into ALS. *Trends in Neurosciences*. https://doi.org/10.1016/S0166-2236(00)02000-2

Pérez-Moreno, J. J., & O'Kane, C. J. (2018). GAL4 Drivers Specific for Type Ib and Type Is Motor Neurons in Drosophila . *G3: Genes|Genomes|Genetics*, *9*(February), g3.200809.2018. https://doi.org/10.1534/g3.118.200809

Phillips, J. B., & Westerfield, M. (2014). Zebrafish models in translational research: tipping the scales toward advancements in human health. *Disease Models & Mechanisms*. https://doi.org/10.1242/dmm.015545

Podkowa, M., Zhao, X., Chow, C.-W., Coffey, E. T., Davis, R. J., & Attisano, L. (2010). Microtubule Stabilization by Bone Morphogenetic Protein Receptor-Mediated Scaffolding of c-Jun N-Terminal Kinase Promotes Dendrite Formation † Downloaded from. *MOLECULAR AND CELLULAR BIOLOGY*, *30*(9), 2241–2250. https://doi.org/10.1128/MCB.01166-09

Polymenidou, M., Lagier-Tourenne, C., Hutt, K. R., Huelga, S. C., Moran, J., Liang, T. Y., … Cleveland, D. W. (2011). Long pre-mRNA depletion

and RNA missplicing contribute to neuronal vulnerability from loss of TDP-43. *Nature Neuroscience*. https://doi.org/10.1038/nn.2779

Poskanzer, K. E., Fetter, R. D., & Davis, G. W. (2006). Discrete residues in the c(2)b domain of synaptotagmin I independently specify endocytic rate and synaptic vesicle size. *Neuron*, *50*(1), 49–62. https://doi.org/10.1016/j.neuron.2006.02.021

Poulain, F. E., & Sobel, A. (2010). The microtubule network and neuronal morphogenesis: Dynamic and coordinated orchestration through multiple players. *Molecular and Cellular Neuroscience*, *43*(1), 15–32. https://doi.org/10.1016/j.mcn.2009.07.012

Prasad, A., Bharathi, V., Sivalingam, V., Girdhar, A., & Patel, B. K. (2019). Molecular Mechanisms of TDP-43 Misfolding and Pathology in Amyotrophic Lateral Sclerosis. *Frontiers in Molecular Neuroscience*, *12*(February), 1–36. https://doi.org/10.3389/fnmol.2019.00025

Qi, Y., Zhang, X. J., Renier, N., Wu, Z., Atkin, T., Sun, Z., … Studer, L. (2017). Combined small-molecule inhibition accelerates the derivation of functional cortical neurons from human pluripotent stem cells. *Nature Biotechnology*. https://doi.org/10.1038/nbt.3777

Ramaswami, M., Krishnan, K. S., & Kelly, R. B. (1994). Intermediates in synaptic vesicle recycling revealed by optical imaging of Drosophila neuromuscular junctions. *Neuron*. https://doi.org/10.1016/0896-6273(94)90353-0

Ratnaparkhi, A., Lawless, G. M., Schweizer, F. E., Golshani, P., & Jackson, G. R. (2008). A Drosophila Model of ALS: Human ALS-Associated Mutation in VAP33A Suggests a Dominant Negative Mechanism. *PLoS ONE*, *3*(6), 2334. https://doi.org/10.1371/journal.pone.0002334

Rawson, J. M., Lee, M., Kennedy, E. L., & Selleck, S. B. (2003). Drosophila neuromuscular synapse assembly and function require the TGF-β type I receptor saxophone and the transcription factor Mad. *Journal of Neurobiology*, *55*(2), 134–150. https://doi.org/10.1002/neu.10189

Renton, A. E., Majounie, E., Waite, A., Simón-Sánchez, J., Rollinson, S., Gibbs, J. R., … Traynor, B. J. (2011). A hexanucleotide repeat expansion

in C9ORF72 is the cause of chromosome 9p21-linked ALS-FTD. *Neuron*. https://doi.org/10.1016/j.neuron.2011.09.010

Richmond, J. E., & Broadie, K. S. (2002). The synaptic vesicle cycle: Exocytosis and endocytosis in Drosophila and C. elegans. *Current Opinion in Neurobiology*. https://doi.org/10.1016/S0959-4388(02)00360-4

Robberecht, W., & Philips, T. (2013). The changing scene of amyotrophic lateral sclerosis. *Nature Reviews Neuroscience*. https://doi.org/10.1038/nrn3430

Rodesch, C. K., & Broadie, K. (2000). Genetic studies in Drosophila: vesicle pools and cytoskeleton-based regulation of synaptic transmission. *Neuroreport*, *11*(18), R45-53. https://doi.org/10.1097/00001756-200012180-00002

Romano, G., Holodkov, N., Klima, R., Grilli, F., Guarnaccia, C., Nizzardo, M., … Feiguin, F. (2018). Downregulation of glutamic acid decarboxylase in Drosophila TDP- 43-null brains provokes paralysis by affecting the organization of the neuromuscular synapses. *Scientific Reports*, *8*(1), 1809. https://doi.org/10.1038/s41598-018-19802-3

Romano, G., Klima, R., Buratti, E., Verstreken, P., Baralle, F. E., & Feiguin, F. (2014). Chronological requirements of TDP-43 function in synaptic organization and locomotive control. *Neurobiology of Disease*, *71*, 95–109. https://doi.org/10.1016/j.nbd.2014.07.007

Roos, J., Hummel, T., Ng, N., & Davis, G. W. (2000). Synaptic Microtubule Organization and Is Necessary for Synaptic Growth. *Neuron*, *26*, 371–382.

Roos, J., Hummel, T., Ng, N., Klämbt, C., & Davis, G. W. (2000). Drosophila Futsch regulates synaptic microtubule organization and is necessary for synaptic growth. *Neuron*, *26*(2), 371–382. https://doi.org/10.1016/S0896-6273(00)81170-8

Rothman, J. E. (1994). Mechanisms of intracellular protein transport. *Nature*. https://doi.org/10.1038/372055a0

Rowland, L. P., & Shneider, N. A. (2001). Medical Progress. Amyotrophic Lateral Sclerosis. *The New England Journal of Medicine*. https://doi.org/10.1056/NEJM200105313442207

Saberi, S., Stauffer, J. E., Schulte, D. J., & Ravits, J. (2015). Neuropathology of Amyotrophic Lateral Sclerosis and Its Variants. *Neurologic Clinics*. https://doi.org/10.1016/j.ncl.2015.07.012

Sasaki, S., & Iwata, M. (2007). Mitochondrial alterations in the spinal cord of patients with sporadic amyotrophic lateral sclerosis. *Journal of Neuropathology and Experimental Neurology*. https://doi.org/10.1097/nen.0b013e31802c396b

Sayas, C. L., Tortosa, E., Bollati, F., Ramírez-Ríos, S., Arnal, I., & Avila, J. (2015). Tau regulates the localization and function of End-binding proteins 1 and 3 in developing neuronal cells. *Journal of Neurochemistry*. https://doi.org/10.1111/jnc.13091

Schuster, C. M., Davis, G. W., Fetter, R. D., & Goodman, C. S. (1996). Genetic Dissection of Structural and Functional Components of Synaptic Plasticity. I. Fasciclin II Controls Synaptic Stabilization and Growth. *Neuron*, *17*(4), 641–654. https://doi.org/10.1016/S0896-6273(00)80197-X

Schwarz, T. L. (2013). Mitochondrial Trafficking in Neurons. *Cold Spring Harbor Perspectives in Biology*, *5*(6), a011304–a011304. https://doi.org/10.1101/cshperspect.a011304

Shaw, P., & Eggett, C. J. (2000). Molecular factors underlying selective vulnerability of motor neurons to neurodegeneration in amyotrophic lateral sclerosis. *Journal of Neurology*, *247*(S1), I17–I27. https://doi.org/10.1007/BF03161151

Sheng, Z. H. (2014). Mitochondrial trafficking and anchoring in neurons: New insight and implications. *Journal of Cell Biology*. https://doi.org/10.1083/jcb.201312123

Shi, P., Wei, Y., Zhang, J., Gal, J., & Zhu, H. (2010). Mitochondrial Dysfunction is a Converging Point of Multiple Pathological Pathways in Amyotrophic Lateral Sclerosis. *Journal of Alzheimer's Disease*, *20*, 311–324. https://doi.org/10.3233/JAD-2010-100366

Shiraishi, R., Tamura, T., Sone, M., & Okazawa, H. (2014). Systematic analysis of fly models with multiple drivers reveals different effects of ataxin-1 and huntingtin in neuron subtype-specific expression. *PLoS ONE*, *9*(12). https://doi.org/10.1371/journal.pone.0116567

Si, Y., Cui, X., Kim, S., Wians, R., Sorge, R., Oh, S. J., … King, P. H. (2014). Smads as muscle biomarkers in amyotrophic lateral sclerosis. *Annals of Clinical and Translational Neurology*, *1*(10), 778. https://doi.org/10.1002/ACN3.117

Si, Y., Kim, S., Cui, X., Zheng, L., Oh, S. J., Anderson, T., … King, P. H. (2015). Transforming Growth Factor Beta (TGF-β) Is a Muscle Biomarker of Disease Progression in ALS and Correlates with Smad Expression. *PLOS ONE*, *10*(9), e0138425. https://doi.org/10.1371/JOURNAL.PONE.0138425

Smith, B. N., Ticozzi, N., Fallini, C., Gkazi, A. S., Topp, S., Kenna, K. P., … Bertolin, C. (2014). Exome-wide rare variant analysis identifies TUBA4A mutations associated with familial ALS. *Neuron*. https://doi.org/10.1016/j.neuron.2014.09.027

Song, W., Song, Y., Kincaid, B., Bossy, B., & Bossy-Wetzel, E. (2013). Mutant SOD1G93A triggers mitochondrial fragmentation in spinal cord motor neurons: Neuroprotection by SIRT3 and PGC-1α. *Neurobiology of Disease*. https://doi.org/10.1016/j.nbd.2012.07.004

Sotelo-Silveira, J. R., Lepanto, P., Elizondo, V., Horjales, S., Palacios, F., Martinez-Palma, L., … Barbeito, L. (2009). Axonal Mitochondrial Clusters Containing Mutant SOD1 in Transgenic Models of ALS. *Antioxidants & Redox Signaling*. https://doi.org/10.1089/ars.2009.2614

Spillantini, M. G., & Goedert, M. (1998). Tau protein pathology in neurodegenerative diseases. *Trends in Neurosciences*. https://doi.org/10.1016/S0166-2236(98)01337-X

Staats, K. A., Hernandez, S., Schönefeldt, S., Bento-Abreu, A., Dooley, J., Van Damme, P., … Van Den Bosch, L. (2013). Rapamycin increases survival in ALS mice lacking mature lymphocytes. *Molecular Neurodegeneration*. https://doi.org/10.1186/1750-1326-8-31

Stenmark, H. (n.d.). The ESCRT machinery in endosomal sorting of ubiquitylated membrane proteins Modelling Cancer in Drosophila View project Phagosome Signaling View project. https://doi.org/10.1038/nature07961

Strah, N., Romano, G., Introna, C., Klima, R., Marzullo, M., Ciapponi, L., … Feiguin, F. (2020). TDP-43 promotes the formation of neuromuscular

synapses through the regulation of Disc-large expression in Drosophila skeletal muscles. *BMC Biology*, *18*(1), 34. https://doi.org/10.1186/s12915-020-00767-7

Südhof, T. C. (2004). the Synaptic Vesicle Cycle. *Annual Review of Neuroscience*, *27*(1), 509–547. https://doi.org/10.1146/annurev.neuro.26.041002.131412

Sulkowski, M., Kim, Y. J., & Serpe, M. (2014). Postsynaptic glutamate receptors regulate local BMP signaling at the Drosophila neuromuscular junction. *Development (Cambridge)*, *141*(2), 436–447. https://doi.org/10.1242/dev.097758

Swerdlow, R. H., Parks, J. K., Cassarino, D. S., Trimmer, P. A., Miller, S. W., Maguire, D. J., … Parker, W. D. (1998). Mitochondria in sporadic amyotrophic lateral sclerosis. *Experimental Neurology*, *153*(1), 135–142. https://doi.org/10.1006/exnr.1998.6866

Taes, I., Timmers, M., Hersmus, N., Bento-Abreu, A., Van Den bosch, L., Van damme, P., … Robberecht, W. (2013). Hdac6 deletion delays disease progression in the sod1g93a mouse model of als. *Human Molecular Genetics*. https://doi.org/10.1093/hmg/ddt028

Takayama, S., Dhahbi, J., Roberts, A., Mao, G., Heo, S. J., Pachter, L., … Boffelli, D. (2014). Genome methylation in D. melanogaster is found at specific short motifs and is independent of DNMT2 activity. *Genome Research*. https://doi.org/10.1101/gr.162412.113

Takei, Y., Kondo, S., Harada, A., Inomata, S., Noda, T., & Hirokawa, N. (1997). Delayed development of nervous system in mice homozygous for disrupted microtubule-associated protein 1B (MAP1B) gene. *The Journal of Cell Biology*, *137*(7), 1615–1626. https://doi.org/10.1083/jcb.137.7.1615

Takuma, H., Kwak, S., Yoshizawa, T., & Kanazawa, I. (1999). Reduction of GluR2 RNA editing, a molecular change that increases calcium influx through AMPA receptors, selective in the spinal ventral gray of patients with amyotrophic lateral sclerosis. *Annals of Neurology*. https://doi.org/10.1002/1531-8249(199912)46:6<806::AID-ANA2>3.0.CO;2-S

Tanaka, Y., Nonaka, T., Suzuki, G., Kametani, F., & Hasegawa, M. (2016). Gain-of-function profilin 1 mutations linked to familial amyotrophic lateral sclerosis cause seed-dependent intracellular TDP-43 aggregation. *Human Molecular Genetics*. https://doi.org/10.1093/hmg/ddw024

There, I., & Dna-binding, T. A. R. (2016). Cipolat Mis MS , Brajkovic S , Frattini E , Di Fonzo A , Corti S . Autophagy in motor neuron disease : Key pathogenetic mechanisms and therapeutic targets . Mol Cell Neurosci . 2016 Feb. 1, 84–90. https://doi.org/10.1016/j.mcn.2016.01.012.6

Therrien, M., & Parker, J. A. (2014). Worming forward: Amyotrophic lateral sclerosis toxicity mechanisms and genetic interactions in Caenorhabditis elegans. *Frontiers in Genetics*. https://doi.org/10.3389/fgene.2014.00085

Tischfield, M. A., & Engle, E. C. (2010). Distinct α- and β-tubulin isotypes are required for the positioning, differentiation and survival of neurons: new support for the 'multi-tubulin' hypothesis. *Bioscience Reports*. https://doi.org/10.1042/bsr20100025

Tollervey, J. R., Curk, T., Rogelj, B., Briese, M., Cereda, M., Kayikci, M., … Ule, J. (2011). Characterizing the RNA targets and position-dependent splicing regulation by TDP-43. *Nature Neuroscience*. https://doi.org/10.1038/nn.2778

Tortosa, E., Galjart, N., Avila, J. S., & Sayas, C. L. (2013). MAP1B regulates microtubule dynamics by sequestering EB1/3 in the cytosol of developing neuronal cells. *The EMBO Journal*, *32*, 1293–1306. https://doi.org/10.1038/emboj.2013.76

Tsang, H. T. H., Edwards, T. L., Wang, X., Connell, J. W., Davies, R. J., Durrington, H. J., … Reid, E. (2009). The hereditary spastic paraplegia proteins NIPA1, spastin and spartin are inhibitors of mammalian BMP signalling. *Human Molecular Genetics*, *18*(20), 3805–3821. https://doi.org/10.1093/hmg/ddp324

Tsuda, H., Han, S. M., Yang, Y., Tong, C., Lin, Y. Q., Mohan, K., … Bellen, H. J. (2008). The Amyotrophic Lateral Sclerosis 8 Protein VAPB Is Cleaved, Secreted, and Acts as a Ligand for Eph Receptors. *Cell*. https://doi.org/10.1016/j.cell.2008.04.039

Tymanskyj, S. R., Scales, T. M. E., & Gordon-Weeks, P. R. (2012). MAP1B enhances microtubule assembly rates and axon extension rates

in developing neurons. *Molecular and Cellular Neuroscience*. https://doi.org/10.1016/j.mcn.2011.10.003

Ugur, B., Chen, K., & Bellen, H. J. (2016). Drosophila tools and assays for the study of human diseases . *Disease Models & Mechanisms*. https://doi.org/10.1242/dmm.023762

Van Damme, P., Robberecht, W., & Van Den Bosch, L. (2017). Modelling amyotrophic lateral sclerosis: progress and possibilities. *Disease Models & Mechanisms*, *10*(5), 537–549. https://doi.org/10.1242/dmm.029058

Van Damme, P., Van Hoecke, A., Lambrechts, D., Vanacker, P., Bogaert, E., Van Swieten, J., … Robberecht, W. (2008). Progranulin functions as a neurotrophic factor to regulate neurite outgrowth and enhance neuronal survival. *Journal of Cell Biology*. https://doi.org/10.1083/jcb.200712039

Vance, C., Rogelj, B., Hortobágyi, T., De Vos, K. J., Nishimura, A. L., Sreedharan, J., … Shaw, C. E. (2009). Mutations in FUS, an RNA processing protein, cause familial amyotrophic lateral sclerosis type 6. *Science*. https://doi.org/10.1126/science.1165942

Vande Velde, C., McDonald, K. K., Boukhedimi, Y., McAlonis-Downes, M., Lobsiger, C. S., Hadj, S. B., … Cleveland, D. W. (2011). Misfolded SOD1 associated with motor neuron mitochondria alters mitochondrial shape and distribution prior to clinical onset. *PLoS ONE*. https://doi.org/10.1371/journal.pone.0022031

Vanden Broeck, L., Naval-Sánchez, M., Adachi, Y., Diaper, D., Dourlen, P., Chapuis, J., … Dermaut, B. (2013). TDP-43 Loss-of-Function Causes Neuronal Loss Due to Defective Steroid Receptor-Mediated Gene Program Switching In Drosophila. *Cell Reports*. https://doi.org/10.1016/j.celrep.2012.12.014

Verstreken, P., Kjaerulff, O., Lloyd, T. E., Atkinson, R., Zhou, Y., Meinertzhagen, I. A., & Bellen, H. J. (2002). Endophilin mutations block clathrin-mediated endocytosis but not neurotransmitter release. *Cell*. https://doi.org/10.1016/S0092-8674(02)00688-8

Verstreken, P., Koh, T. W., Schulze, K. L., Zhai, R. G., Hiesinger, P. R., Zhou, Y., … Bellen, H. J. (2003). Synaptojanin is recruited by endophilin to promote synaptic vesicle uncoating. *Neuron*. https://doi.org/10.1016/S0896-6273(03)00644-5

Verstreken, P., Ohyama, T., & Bellen, H. J. (2008). FM 1–43 Labeling of Synaptic Vesicle Pools at the. *Methods*, *43*, 349–369.

Villarroel-Campos, D., & Gonzalez-Billault, C. (2014). The MAP1B case: An old MAP that is new again. *Developmental Neurobiology*. https://doi.org/10.1002/dneu.22178

Vinsant, S., Mansfield, C., Jimenez-Moreno, R., Moore, V. D. G., Yoshikawa, M., Hampton, T. G., … Milligan, C. (2013). Characterization of early pathogenesis in the SOD1G93A mouse model of ALS: Part II, results and discussion. *Brain and Behavior*. https://doi.org/10.1002/brb3.142

Wang, P., Deng, J., Dong, J., Liu, J., Bigio, E. H., Mesulam, M., … Wu, J. Y. (2019). TDP-43 induces mitochondrial damage and activates the mitochondrial unfolded protein response. *PLoS Genetics*, *15*(5), e1007947. https://doi.org/10.1371/journal.pgen.1007947

Wang, W., Li, L., Lin, W. L., Dickson, D. W., Petrucelli, L., Zhang, T., & Wang, X. (2013). The ALS disease-associated mutant TDP-43 impairs mitochondrial dynamics and function in motor neurons. *Human Molecular Genetics*. https://doi.org/10.1093/hmg/ddt319

Wang, W., Wang, L., Lu, J., Siedlak, S. L., Fujioka, H., Liang, J., … Wang, X. (2016). The inhibition of TDP-43 mitochondrial localization blocks its neuronal toxicity. *Nature Medicine*. https://doi.org/10.1038/nm.4130

Wang, X., Shaw, W. R., Tsang, H. T. H., Reid, E., & O'Kane, C. J. (2007). Drosophila spichthyin inhibits BMP signaling and regulates synaptic growth and axonal microtubules. *Nature Neuroscience*, *10*(2), 177–185. https://doi.org/10.1038/nn1841

Watson, M. R., Lagow, R. D., Xu, K., Zhang, B., & Bonini, N. M. (2008). A Drosophila model for amyotrophic lateral sclerosis reveals motor neuron damage by human SOD1. *Journal of Biological Chemistry*. https://doi.org/10.1074/jbc.M804817200

Webster, C. P., Smith, E. F., Bauer, C. S., Moller, A., Hautbergue, G. M., Ferraiuolo, L., … De Vos, K. J. (2016). The C9orf72 protein interacts with Rab1a and the ULK1 complex to regulate initiation of autophagy. *The EMBO Journal*, *35*, 1656–1676. https://doi.org/10.15252/embj.201694401

Wiedemann, F. R., Manfredi, G., Mawrin, C., Flint Beal, M., & Schon, E. A. (2002). Mitochondrial DNA and respiratory chain function in spinal cords of ALS patients. *Journal of Neurochemistry*. https://doi.org/10.1046/j.0022-3042.2001.00731.x

Winther, A. M. E., Vorontsova, O., Rees, K. A., Nareoja, T., Sopova, E., Jiao, W., & Shupliakov, O. (2015). An Endocytic Scaffolding Protein together with Synapsin Regulates Synaptic Vesicle Clustering in the Drosophila Neuromuscular Junction. *Journal of Neuroscience*, *35*(44), 14756–14770. https://doi.org/10.1523/jneurosci.1675-15.2015

Withers, G. S., Higgins, D., Charette, M., & Banker, G. (n.d.). Bone morphogenetic protein-7 enhances dendritic growth and receptivity to innervation in cultured hippocampal neurons.

Xu, Z., Poidevin, M., Li, X., Li, Y., Shu, L., Nelson, D. L., … Jin, P. (2013). Expanded GGGGCC repeat RNA associated with amyotrophic lateral sclerosis and frontotemporal dementia causes neurodegeneration. *Proceedings of the National Academy of Sciences*. https://doi.org/10.1073/pnas.1219643110

Yang, C., Wang, H., Qiao, T., Yang, B., Aliaga, L., Qiu, L., … Xu, Z. (2014). Partial loss of TDP-43 function causes phenotypes of amyotrophic lateral sclerosis. *Proceedings of the National Academy of Sciences*. https://doi.org/10.1073/pnas.1322641111

Yau, K. W., Schatzle, P., Tortosa, E., Pages, S., Holtmaat, A., Kapitein, L. C., & Hoogenraad, C. C. (2016). Dendrites In Vitro and In Vivo Contain Microtubules of Opposite Polarity and Axon Formation Correlates with Uniform Plus-End-Out Microtubule Orientation. *Journal of Neuroscience*. https://doi.org/10.1523/jneurosci.2430-15.2016

Zhang, H., Xue, C., Shah, R., Bermingham, K., Hinkle, C. C., Li, W., … Reilly, M. P. (2015). Functional Analysis and Transcriptomic Profiling of iPSC-Derived Macrophages and Their Application in Modeling Mendelian Disease. *Circulation Research*. https://doi.org/10.1161/CIRCRESAHA.117.305860

Zhang, K., Coyne, A. N., & Lloyd, T. E. (2018). Drosophila models of amyotrophic lateral sclerosis with defects in RNA metabolism. *Brain*

Research, *1693*(April), 109–120. https://doi.org/10.1016/j.brainres.2018.04.043

Zhang, Y., Li, N., Caron, C., Matthias, G., Hess, D., Khochbin, S., & Matthias, P. (2003). HDAC-6 interacts with and deacetylates tubulin and microtubules in vivo. *EMBO Journal*. https://doi.org/10.1093/emboj/cdg115

Zhang, Y. Q., Bailey, A. M., Matthies, H. J. G., Renden, R. B., Smith, M. A., Speese, S. D., … Broadie, K. (2001). Drosophila fragile x-related gene regulates the MAP1B homolog Futsch to control synaptic structure and function. *Cell*, *107*(5), 591–603. https://doi.org/10.1016/S0092-8674(01)00589-X